IOWA STATE UNIVERSITY
Digital Repository

2015

Studies on electric power markets: preparing for the penetration of renewable resources

Deung-Yong Yong Heo
Iowa State University

Studies on electric power markets: Preparing for the penetration of renewable resources

by

Deung-Yong Heo

A dissertation submitted to the graduate faculty

in partial fulfillment of the requirements for the degree of

DOCTOR OF PHILOSOPHY

Major: Economics

Program of Study Committee:

Leigh S. Tesfatsion, Major Professor

John R. Schroeter

Sergio H. Lence

Gray Calhoun

Steve Kautz

Iowa State University

Ames, Iowa

2015

DEDICATION

I would like to dedicate this thesis to my wife, to my daughter and son, to my parents, to my grand parents in heaven, and to my brothers without whose support I would not have been able to complete this work. I would also like to thank my friends and family for their loving guidance. I would specially like to thank Iowas state university department of economics for its financial assistance during the writing of this work.

TABLE OF CONTENTS

LIST OF TABLES

LIST OF FIGURES

ACKNOWLEDGEMENTS

I would like to take this opportunity to express my thanks to those who helped me with various aspects of conducting research and the writing of this thesis. First and foremost, I am greatly in debt to my major professor Dr. Leigh S. Tesfatsion for her guidance, patience, and support throughout this research and the writing of this thesis. Her insights and words of encouragement have inspired me and kept me motivated to finish my thesis. Without her direction, I could not achieve my Ph.D. degree and job position. I shall never forget her kindness.

I would also like to thank my committee members for their efforts and contributions to this work: Dr. John R. Schroeter, Dr. Sergio H. Lence, Dr. Gray Calhoun, and Dr. Steve Kautz.

I would additionally like to thank Dr. Abhishek Somani for his guidance on my Ph.D. internship at Pacific Northwest National Laboratory. Finally, I would like to thank Dr. Oh Sang Kwon for his guidance throughout the initial stages of my graduate career at Seoul National University.

ABSTRACT

This thesis investigates the implication of empirical grounded electric power market facts using multiple methodologies, including market and contract design, analytic method, statistical method, and agent-based simulation method. Basically, this thesis focuses on centrally-managed electric power markets.

European and U.S. electricity sectors have undergone substantial restructuring over the past twenty years. They have devolved from highly regulated systems operated by vertically integrated utilities to relatively decentralized systems based more fully on market valuation and allocation mechanisms.

These restructuring efforts have been driven by a desire to ensure efficient energy production and utilization, reliable energy supplies, affordable energy prices, and effective rules and regulations for environmental protection. In keeping with the latter goal, a dramatic change is taking place in energy mixes: namely, a rapid penetration of variable energy resources combined with a movement away from traditional thermal generation.

Variable energy resources (VERs) are renewable energy resources, such as wind and solar power, whose generation cannot be closely controlled to match changes in load or to meet other system requirements. Consequently, the integration of VERs tends to increase the volatility of net load (ie, load minus as-available generation) as well as the frequency of strong ramp events. Flexibility in service provision by other types of resources then becomes increasingly important to maintain the reliability and efficiency of power system operations.

To accommodate increased VER penetration, TSOs and ISOs have introduced major changes in their market rules and operational procedures. These changes have included

new product definitions to enhance load-following capability (eg, ramping products), revised market eligibility requirements to encourage greater VER participation, and the introduction of capacity markets in an attempt to ensure sufficient thermal generation as a backstop for the intermittency of VER generation.

Also, CO_2 emission issues are increasing important in electric power markets. In the U.S., the largest source of CO_2 emissions is the electricity sector, which was responsible for 32% of total emissions in 2012. The Obama Administration proposed a Clean Power Plan in June 2014; nationwide, by 2030, this plan would achieve approximately 30 percent of CO_2 emission reduction relative to 2005 CO_2 emission levels in the power sector. There are several important issues arising from carbon mitigation options such as a carbon tax imposition and increase penetration of VERs need to be resolved.

Chapter 2 introduces standardized energy and reserve contracts with swing (flexibility) in their contractual terms to resolve key issues that have arisen for centrally-managed wholesale electric power markets with increased penetration of renewable energy resources. Concrete examples are used to demonstrate how the trading of these standardized contracts can be supported by linked forward markets in a manner that permits efficient real-time balancing of net load subject to system and reserve-requirement constraints. Comparisons with existing wholesale electric power markets are given, and key policy implications are highlighted.

Chapter 3 extends the system pattern short-term forecasting method for power systems to incorporate non-dispatchable renewable energy, thus permitting the forecasting of CO_2 emissions along with the forecasting of prices, line congestion, and other system variables. It also develops an empirically-based system pattern transition matrix permitting a dynamic extension of the method. The practical usefulness of the resulting extended forecasting method is illustrated by means of a 5-bus test system based on data from the Midcontinent Independent System Operator (MISO).

Chapter 4 develops a 9-zone test system based on MISO data for application in electric power market studies. This 9-zone test system models MISO's original seven midwestern zones together with two recently-incorporated southern zones operating over a 15-line AC transmission grid. Generators with different fuel types and capacities submit hourly supply offers in a day-ahead market (DAM). Load-serving entities submit hourly demand bids into a day-ahead market in the form of a 24-hour regional load profile. This 9-zone test system allows a wide range of sensitivity studies. To illustrate the capabilities of the 9-zone test system, this study undertakes a comparative study of DAM Locational Marginal Price (LMP) outcomes for MISO prior to and after the integration of the two southern zones by conducting test-bed simulations for 7-zone and 9-zone test cases based on MISO data.

Chapter 5 analyzes how the imposition of a carbon tax and the increased penetration of wind power in such markets could impact CO_2 emissions and other key outcomes, such as energy dispatch, energy prices, market participant profits (by fuel type), and government tax revenues. Another innovation of this part is that the effects of increases in a carbon tax and wind power penetration are studied jointly. It is shown, for example, that CO_2 emissions decrease from 0.23% to 6.17% as the carbon tax and the degree of wind penetration are systematically varied from a base case of zero tax and zero wind. The profits of coal- and oil-fired generation systematically decrease with increases in the carbon tax and/or increases in wind penetration, but the profits of other types of generation exhibit a more complex response. Comparisons with current MISO conditions are also given, and key policy implications are discussed.

CHAPTER 1. GENERAL INTRODUCTION

1.1 Introduction

This thesis investigates the implication of empirical grounded electric power market facts using multiple methodologies, including market and contract design, analytic method, statistical method, and agent-based simulation method. Basically, this thesis focuses on centrally-managed electric power markets.

European and U.S. electricity sectors have undergone substantial restructuring over the past twenty years. They have devolved from highly regulated systems operated by vertically integrated utilities to relatively decentralized systems based more fully on market valuation and allocation mechanisms.

As part of this restructuring, oversight agencies have been established at several different levels to encourage cooperation and coordination. The European Network of Transmission System Operators for Electricity (ENTSO-E), founded in 2008, currently consists of forty-one Transmission System Operators (TSOs) from thirty-four European countries; its primary task is to promote the coordinated management of the European power grid. The U.S. Federal Energy Regulatory Commission (FERC) oversees the activities of seven Independent System Operators (ISOs), established since the mid-1990s, that are tasked with managing power system operations in seven U.S. electric energy regions comprising over 60% of U.S. generating capacity.

These restructuring efforts have been driven by a desire to ensure efficient energy production and utilization, reliable energy supplies, affordable energy prices, and effective

rules and regulations for environmental protection. In keeping with the latter goal, a dramatic change is taking place in energy mixes: namely, a rapid penetration of variable energy resources combined with a movement away from traditional thermal generation.

Variable energy resources (VERs) are renewable energy resources, such as wind and solar power, whose generation cannot be closely controlled to match changes in load or to meet other system requirements. Consequently, the integration of VERs tends to increase the volatility of net load (ie, load minus as-available generation) as well as the frequency of strong ramp events. Flexibility in service provision by other types of resources then becomes increasingly important to maintain the reliability and efficiency of power system operations.

To accommodate increased VER penetration, TSOs and ISOs have introduced major changes in their market rules and operational procedures. These changes have included new product definitions to enhance load-following capability (eg, ramping products), revised market eligibility requirements to encourage greater VER participation, and the introduction of capacity markets in an attempt to ensure sufficient thermal generation as a backstop for the intermittency of VER generation.

Also, CO_2 emission issues are increasing important in electric power markets. In the U.S., the largest source of CO_2 emissions is the electricity sector, which was responsible for 32% of total emissions in 2012. The Obama Administration proposed a Clean Power Plan in June 2014; nationwide, by 2030, this plan would achieve approximately 30 percent of CO_2 emission reduction relative to 2005 CO_2 emission levels in the power sector. There are several important issues arising from carbon mitigation options such as a carbon tax imposition and increase penetration of VERs need to be resolved.

First, current electric power markets need appropriate compensation for flexibility in service provision. TSO/ISO product definitions are specified in broad rigid terms (eg, capacity, energy, ramp-rate, regulation, non-spinning reserve) that do not permit resources to be further differentiated and compensated on the basis of additional valuable

flexibility in service provision, such as an ability to ramp up and down between minimum and maximum values over very short time intervals. Second, VERs increase volatility and uncertainty in electric power markets because VERs are non-dispatchable. When the penetration of renewable energy reaches relatively high levels, characteristics and operations of the current power system will be significantly changed and additional costs will be incurred in order to ensure sufficient resources for system reliability. Third, carbon tax imposition can change relative generation costs of generators based on carbon intensities implied by fuel type. This can lead fuel mix changes in current power markets and affects market participants' profits. Thus a thorough studies are necessary to resolve these key issues in electric power markets.

This thesis proposes new contract and market design to attain flexible energy and service provisions. Also, this thesis develops an improved short term forecasting method for power market system variables such as dispatch levels, power flows in transmission lines, and electricity prices with increased penetration of VERs. A 5-bus test case is used to test the verification of the method. An empirically-based test system is developed based on data from the Midcontinent Independent System Operator (MISO) for application in electric power market studies. This test system embed MISO's rules of operation and physical attributes such as generation technology, transmission line limits, and capacity proportions by fuel type. Using this test system, this thesis systematically analyzes the effects of CO_2 reduction options on electric power market key outcomes.

1.2 Organization of the Thesis

The remainder of this thesis is organized as follows:

Chapter 2 introduces standardized energy and reserve contracts with swing (flexibility) in their contractual terms to resolve key issues that have arisen for centrally-managed wholesale electric power markets with increased penetration of renewable en-

ergy resources. Concrete examples are used to demonstrate how the trading of these standardized contracts can be supported by linked forward markets in a manner that permits efficient real-time balancing of net load (conventional load - as-available generation) subject to system and reserve-requirement constraints.

Based on the basic system pattern method, Chapter 3 develops an extended system pattern method for short-term forecasting of power market performance that: incorporates non-dispatchable renewable energy and investigates its effects on electric power markets, broadens the scope of the basic system pattern method to permit short-term forecasting of CO2 emissions as well as other power system variables and investigate its applicability for a scenario reduction method, and introduces the concept of empirically-based system pattern transition matrix and its applicability for status forecasting of power system variables.

Chapter 4 develops an empirically-based test system based on data from the Midcontinent Independent System Operator (MISO) for application in electric power market studies. This test system embeds MISO's rules of operation, physical attributes of market generation technology and capacity, transmission constraints, and capacity proportion by fuel type.

Using the test system developed in Chapter 4, Chapter 5 systematically analyzes the effects of two treatment factors for CO_2 reduction options, a carbon tax imposition and wind power penetration, on electric power market key outcomes such as CO_2 emissions, generator dispatch levels, costs, revenues and profits, and carbon tax revenues.

Chapter 6 concludes the whole thesis. Key findings and interesting extensions of each research topic are summarized to illustrate the main contributions of this thesis to academic literature and practical studies.

CHAPTER 2. STANDARDIZED CONTRACTS WITH SWING FOR THE MARKET SUPPORTED PROCUREMENT OF ENERGY AND RESERVE: ILLUSTRATIVE EXAMPLES

2.1 Introduction

European and U.S. electricity sectors have undergone substantial restructuring over the past twenty years. They have devolved from highly regulated systems operated by vertically integrated utilities to relatively decentralized systems based more fully on market valuation and allocation mechanisms.

As part of this restructuring, oversight agencies have been established at several different levels to encourage cooperation and coordination. The European Network of Transmission System Operators for Electricity (ENTSO-E), founded in 2008, currently consists of forty-one Transmission System Operators (TSOs) from thirty-four European countries; its primary task is to promote the coordinated management of the European power grid [32]. The U.S. Federal Energy Regulatory Commission (FERC) oversees the activities of seven Independent System Operators (ISOs), established since the mid-1990s, that are tasked with managing power system operations in seven U.S. electric energy regions comprising over 60% of U.S. generating capacity [28].

These restructuring efforts have been driven by a desire to ensure efficient energy production and utilization, reliable energy supplies, affordable energy prices, and effective

rules and regulations for environmental protection. In keeping with the latter goal, a dramatic change is taking place in energy mixes: namely, a rapid penetration of variable energy resources combined with a movement away from traditional thermal generation.

Variable energy resources (VERs) are renewable energy resources, such as wind and solar power, whose generation cannot be closely controlled to match changes in load or to meet other system requirements. Consequently, the integration of VERs tends to increase the volatility of net load (ie, load minus as-available generation) as well as the frequency of strong ramp events. Flexibility in service provision by other types of resources then becomes increasingly important to maintain the reliability and efficiency of power system operations.

To accommodate increased VER penetration, TSOs and ISOs have introduced major changes in their market rules and operational procedures [31, 47, 29, 74]. These changes have included new product definitions to enhance load-following capability (eg, ramping products), revised market eligibility requirements to encourage greater VER participation, and the introduction of capacity markets in an attempt to ensure sufficient thermal generation as a backstop for the intermittency of VER generation.

Nevertheless, several important issues arising from increased VER penetration still need to be resolved. One key issue is that energy and reserve products are variously defined and compensated across the different energy regions; see, eg, Ellison et al. [30]. This makes it difficult to compare and evaluate the efficiency and fairness of system operations across these regions.

A second key issue is appropriate compensation for flexibility in service provision. TSO/ISO product definitions are specified in broad rigid terms (eg, capacity, energy, ramp-rate, regulation, non-spinning reserve) that do not permit resources to be further differentiated and compensated on the basis of additional valuable flexibility in service provision, such as an ability to ramp up and down between minimum and maximum values over very short time intervals.

A third key issue is that attempts to accommodate new products have led to the introduction of out-of-market (OOM) compensation processes. In 2011 FERC issued Order 755 to address OOM payment problems for one particular product category in U.S. ISO-managed wholesale power markets: namely, regulation with different abilities to follow electronic dispatch signals with high accuracy [38]. However, given its limited scope, Order 755 does not fully eliminate the need in these markets to resort to OOM processes. As stressed by Bushnell [14], the additional complexity resulting from OOM compensation processes provides increased opportunities for market participants to gain unfair profit advantages through strategic behaviors.

In response to these issues, a group of researchers sponsored by Sandia National Laboratories prepared a report [86] recommending that energy and reserve contracts be standardized in firm and option forms permitting separate pricing for service availability and for real-time service performance, and that the trading of these contracts be supported by a linked sequence of forward markets whose design is also standardized. This report builds on important earlier work by Bidwell [8], Bunn [13], Chao and Wilson [18], and Oren [76], who stress the relevance of options and two-part pricing for electricity markets.

The current study uses concrete numerical examples to explore the policy implications of the recommendations in Tesfatsion et al. [86]. In Section 2.2 we present a general template for a *Standardized Contract (SC)* with swing (flexibility) in its contractual terms, together with an illustrative SC example. We also outline in broad terms how the trading of SCs can be supported by linked centrally-managed day-ahead and real-time markets. In Section 2.3 and Section 2.4 we present our main results: namely, examples demonstrating how our proposed SC system, implemented via linked day-ahead and real-time markets, permits efficient real-time balancing of net load subject to system and reserve-requirement constraints.

Comparisons of our proposed SC system with existing European and U.S. wholesale power market operations, standardized power contracts, pricing mechanisms, and VER initiatives are provided in Sections 2.5.1-2.5.4. In Section 2.5.5 we discuss how our SC system provides a robust-control approach to the handling of uncertain net load that avoids the need to specify detailed scenarios with associated probabilities, a common requirement of standard stochastic control approaches. In Section 2.5.6 we conjecture how our proposed SC system, extended to longer-term forward markets, could help to provide better incentives for thermal generation capacity investment as a backstop for the intermittency of VER generation by facilitating the resolution of merit-order and missing-money problems.

Throughout Sections 2.2-2.5 the following key policy implications of our proposed SC system are highlighted:

- permits full market-based compensation for availability and performance

- facilitates a level playing field for market participation

- facilitates co-optimization of energy and reserve markets

- supports forward-market trading of energy and reserve

- permits resource providers to offer flexible service availability

- provides system operators with real-time flexibility in service usage

- facilitates accurate load forecasting and following of dispatch signals

- permits resources to internally manage UC and capacity constraints

- permits the robust-control management of uncertain net load

- eliminates the need for OOM payment adjustments

- reduces the complexity of market rules

The concluding Section 2.6 provides a concise summary discussion of each of these policy implications.

2.2   Proposed Standardized Contract System

2.2.1   General Form of a Standardized Contract

Energy refers to the actual generation of electrical energy, whereas reserve refers to generation-capacity availability. Four standardized contracts are proposed in Tesfatsion et al. [86] to facilitate energy and reserve trading: namely, *firm contracts (FCs)* and *option contracts (OCs)* taking either fixed or swing form.

An FC is a non-contingent contract that requires specific performance from both counterparties. It obligates the holder to procure services from the issuer, and the issuer to deliver these services, under the contractually specified terms of the FC. In contrast, an OC gives the holder the right, but not the obligation, to procure services from the issuer under contractually specified terms. The right can be activated by exercise of the OC at a contractually permitted exercise time. Once exercised, an OC imposes specific performance obligations on both counterparties. That is, as for an FC, an exercised OC obligates the holder to procure services from the issuer, and the issuer to deliver these services, under the contractually specified terms of the OC.

An FC or OC is a *fixed* contract if each of its contractual terms is designated as a single possible value. An FC or OC is a *swing* contract if at least one of its contractual terms is designated as a set of possible values, thus permitting some degree of flexibility in its implementation. A fixed FC is a *block-energy* contract if its contractual terms obligate the issuer to maintain a specified constant power level during a specified time interval.

As depicted in Fig. 2.1, fixed/swing OCs, fixed/swing FCs, and block-energy contracts are all special cases of swing OCs. A swing OC reduces to a fixed OC if each of its

contractual terms is a single point value. A swing OC reduces to a swing FC if its permitted exercise times consist of a single time point that coincides with the contract procurement time. A swing FC reduces to a fixed FC if each of its contractual terms is a single point value.
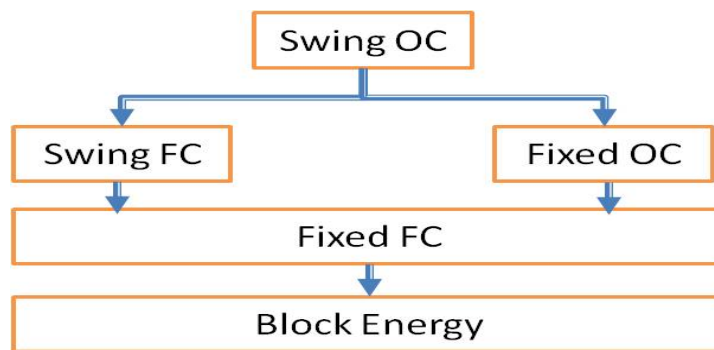
Figure 2.1: Hierarchical structure of contracts

Hereafter, this study focuses on *Standardized Contracts (SCs)* in swing-OC form for the flexible provision of energy and reserve services. For concreteness, we next present a template for an SC that provides seven basic types of services for a particular operating hour: delivery location; down/up direction; exercise time; power-begin time; power-end time; down/up ramp rate; and power level. We illustrate swing in five of these service types by depicting their sets of possible values as intervals.[1]

---

[1]SCs can take much more general forms than illustrated in the current study. For example, SCs can include other types of services such as voltage control, reactive power support, and energy storage capacity; swing can be present in any of these services; swing possible value sets do not need to be in interval form; and the operating period does not need to be an hour.

Template for a Standardized Contract (SC):

$$\text{SC} = [k, d, T_{ex}, T_{pb}, T_{pe}, R_C, P_C, \phi] \tag{2.1}$$

k = Location where service delivery is to occur

d = Direction (down or up)

$T_{ex} = [t_{ex}^{min}, t_{ex}^{max}]$ = Range of possible exercise times t_{ex}

$T_{pb} = [t_{pb}^{min}, t_{pb}^{max}]$ = Range of possible power-begin times t_{pb}

$T_{pe} = [t_{pe}^{min}, t_{pe}^{max}]$ = Range of possible power-end times t_{pe}

$R_C = [-r^D, r^U]$ = Range of possible down/up ramp rates r

$P_C = [p^{min}, p^{max}]$ = Range of possible power levels p

ϕ = Performance payment method for real-time service performance

The down/up limits $-r^D$ and r^U for the ramp-rates r (MW/min) are assumed to satisfy $-r^D \leq 0 \leq r^U$. The lower bound p^{min} for the power levels p (MW) is assumed to be non-negative. The direction (down or up) of an SC determines whether these power levels describe power curtailments or absorptions (down) or power injections (up). The time points t_{ex}, t_{pb}, and t_{pe} denote specific calendar times expressed at the granularity of minutes.

The presence of swing in the contractual terms of an SC permits this SC to function as both an energy and a reserve product. Actual real-time service performance under such an SC cannot be determined until after the end of the operating hour H even if the SC is a firm (non-optional) contract. Consequently, the contractual terms of an SC include a performance payment method ϕ to be used to determine the ex-post payment to the SC issuer for real-time service performance (if any).

The performance payment method ϕ can take a wide variety of forms. For example, as illustrated in Section 2.3, ϕ might denote a pre-specified price (\$/MWh) for delivered down/up energy. More generally, ϕ could denote a contingent price for delivered down/up energy that depends on market conditions (eg, fuel prices) at the time of the delivery.

Alternatively, ϕ could provide for the compensation of delivered power measured as *mileage*, ie, as the sum of absolute-value up and down power movements over the real-time dispatch interval, a metric now being used for regulation service performance in many energy markets to meet the requirements of FERC Order 755 [7].

In order for an SC to be implementable, its contractual terms must satisfy certain basic requirements. For example, t_{pb}^{min} cannot exceed t_{pe}^{max}. In this study it is presumed that an SC issuer is responsible for ensuring that it can feasibly implement the terms of any SC it offers. Realistically, however, penalties and eligibility requirements might need to be introduced to help ensure that the issuers of cleared SCs accurately follow real-time dispatch instructions, and that these instructions are in accordance with the contractual terms of the cleared SCs. These contract enforcement mechanisms could constitute part of the performance payment method ϕ included within each SC, or they could be instituted at the level of the power system as a whole.

2.2.2   Illustrative Example of a Standardized Contract

The illustrative up-energy SC depicted in Fig. 2.2 provides a combination of fixed and swing attributes. The delivery location (bus k) and direction (up) are specified as single values, as are the exercise time t_{ex}, the power-begin time t_{pb}, and the power-end time t_{pe}. On the other hand, the down/up ramp rate r and the power level p are swing attributes that can be varied over a range of values.

The darker (green) area within the resulting corridor of contractually-admissible power dispatch paths depicted in Fig. 2.2 is the up-energy injection that results from one such path. Any actual up-energy injection is compensated ex post in accordance with the performance payment method ϕ included among the SC's contractual terms. An example of a down-energy SC can be obtained from Fig. 2.2 by considering a 180° rotation of the depicted figure around the time axis.

Figure 2.2: Example of an SC for up-energy with ramp-rate and power-level swing that is offered at bus k by a generator with a maximum capacity of 70MW

The SC depicted in Fig. 2.2 can be more concretely interpreted as an up-energy SC offered by a Demand Response Resource (DRR) into an ISO-managed day-ahead market (DAM) on day D-1 for a particular operating hour H on day D, as follows. Consider a Load Serving Entity (LSE) functioning as a load aggregator for a large distribution feeder connected to the transmission grid at a particular bus k. Residential households on this feeder have smart meters for their HVAC loads in wireless communication with the LSE that permits the LSE to make adjustments to these loads. The LSE has permission from each of these households to make small adjustments in their HVAC energy usage in return for an agreed-upon monthly lump-sum compensation. The LSE can participate in a DAM as a DRR either by offering up-energy implemented via HVAC load reductions or by offering down-energy implemented via HVAC load increases.

Suppose the LSE participates in the DAM on day D-1 as a DRR by offering the following up-energy SC at some offer price v for hour H of day D, where hour H is the time interval between 1300EST and 1400EST:

- Delivery location = Bus k

- Direction = Up

- T_{ex} = Exercise time t_{ex} = 0900EST on day D

- T_{pb} = Power-begin time t_{pb} = 1300EST on day D

- T_{pe} = Power-end time t_{pe} = 1400EST on day D

- $R_C = [-1.3\text{MW/min}, +1.4\text{MW/Min}]$ = Range of possible down/up ramp rates r

- $P_C = [10\text{MW}, 50\text{MW}]$ = Range of possible power levels p

- ϕ = Payment method for compensation of delivered power mileage, including a penalty payment adjustment for deviations between instructed and actual power mileage

Suppose, also, that this SC is cleared by the ISO. The ISO is then obligated to ensure that the DRR receives in compensation its offer price v as payment for making available for hour-H operations on day D the services included in this SC. In turn, the ISO has the right, but not the obligation, to exercise this SC at 0900EST on day D.

If the SC is exercised, the DRR must be ready to follow any electronic dispatch signal on day D, starting at time t_{pb} = 1300EST and ending at time t_{pe} = 1400EST, that calls for the DRR to provide a path of power injections lying within its offered range P_C of power levels that can feasibly be achieved without violating the DRR's offered range R_C of down/up ramp rates. In turn, the ISO is obligated to ensure that the DRR is compensated for the mileage of this controlled power path in accordance with the terms of the performance payment method ϕ.

2.2.3   Support of SC Trading via Linked Forward Markets

As in Tesfatsion et al. [86], we propose that SC trading be supported by a sequence of linked centrally-managed forward markets whose planning horizons can range from minutes to years. For concreteness, however, we focus in this study on the support of SC trading by means of linked day-ahead and real-time markets that are centrally managed by a non-profit *Independent System Operator (ISO)*; see Fig. 2.3.

Market Type	Participants	Contracts	Decision Variables	ISO Optimization Method
Day-Ahead Market (DAM)	LSEs	SC Block-Energy Bids	LSE SC Bids; Disp. GenCo / DRR / ESD SC Offers; ISO SC Bids	Security-Constrained Unit Commitment (SCUC) & Security-Constrained Economic Dispatch (SCED)
	Disp. GenCos, DRRs, and ESDs	SC Offers		
	Non-Disp. VERs	—		
	ISO	SC Bids		
Real-Time Market (RTM)	Disp. GenCos, DRRs, and ESDs	SC Offers	Disp. GenCo / DRR / ESD SC Offers; ISO SC Bids	SCED
	Non-Disp. VERs	—		
	ISO	SC Bids		

Figure 2.3: Proposed ISO-managed day-ahead and real-time markets

The non-ISO participants in our proposed day-ahead market (DAM) and real-time market (RTM) include: (i) *Load-Serving Entities (LSEs)* who submit SC demand bids in the form of block energy contracts on behalf of retail energy customers; (ii) dispatchable *Generation Companies (GenCos)*, *Demand Response Resources (DRRs)*, and *Energy Storage Devices (ESDs)* who submit SC supply offers; and (iii) non-dispatchable VERs whose as-available generation is treated as negative load.[2] The requirement that LSE SC

___

[2]As discussed in Section 2.5.4, our proposed SC system could be generalized to allow designated types of VERs to offer their generation as "dispatchable intermittent resources" in DAM/RTM operations, as is now being permitted in MISO [64]. However, this would raise a number of issues best left for

demand bids be in block-energy form avoids the need for LSEs to exercise load-balancing discretion in the implementation of SCs with swing or option exercise times.

Participation in our proposed DAM/RTM processes is not meant to preclude electricity traders from procuring physical and financial instruments in power exchanges and over-the-counter power markets to hedge their price and volume risks. However, physical instruments whose terms require the use of transmission line facilities must be self-scheduled and cleared in the DAM or RTM to ensure transmission availability and overall system reliability.

The ISO managing the DAM undertakes *Security-Constrained Unit Commitment (SCUC)* and *Security-Constrained Economic Dispatch (SCED)* conditional on LSE SC demand bids, ISO SC demand bids (for reserve procurement only), and SC supply offers from dispatchable GenCos, DRRs, and ESDs. To retain the ISO's non-profit status, all costs incurred by the ISO for SC procurement must be passed through to market participants.

This cost pass-through could simply require all procurement costs to be allocated to the LSEs in proportion to their share of real-time loads. However, the presence of performance payment methods ϕ in SC bids/offers permits more sophisticated arrangements. For example, an LSE's cost allocation could be based in part on its forecasting performance, measured ex post by comparing its cleared SC demand bids against the actual real-time loads of its customers; and an SC supplier's cost allocation could be based in part on the accuracy of its service performance, measured ex-post by examining how well it was able to follow real-time dispatch instructions.

The ISO's DAM SCUC/SCED objective is to minimize the expected total net cost of ensuring that sufficient generation is available to balance next-day forecasted net loads with suitable local and system-wide reserve buffers. Dispatchable generation availability is determined from dispatchable GenCo, DRR, and/or ESD supply offers. Next-day net

---

future studies, eg, should VERs be charged or penalized the same as ordinary dispatchable generation for deviations from their cleared dispatch offers?

load forecasts for power-balance purposes are determined from LSE SC demand bids and forecasted VER generation. Reserve buffers are ensured by ISO SC demand bids.

As usual, the DAM SCUC/SCED is subject to unit commitment (UC) conditions, generation-capacity limits, power-balance constraints, transmission-line limits, and both local and system-wide reserve-requirement constraints. However, the imposition of the UC conditions and generation-capacity limits occurs through the contractual terms of the DAM SC supply offers rather than through ISO-imposed constraints.

We also propose an ISO-managed RTM that runs a SCED every five minutes. Dispatchable GenCos, DRRs, and ESDs can offer SCs into the RTM. Only the ISO is permitted to procure these SCs, for balancing and reserve procurement purposes; and all ISO RTM procurement costs must be passed through to market participants in order to preserve the non-profit status of the ISO.

The ISO's RTM SCED objective is to minimize the expected total cost of ensuring that adequate generation is available to balance ISO-forecasted real-time net loads with suitable local and system-wide reserve buffers, given the existing inventory of previously-cleared SCs. This RTM SCED is subject to generation-capacity limits, power-balance constraints, transmission-line limits, and both local and system-wide reserve-requirement constraints. The imposition of the generation-capacity limits occurs through the contractual terms of the RTM SC supply offers rather than through ISO-imposed constraints.

SCs can provide a wide diversity of services through their contractual terms. As discussed in greater detail in Section 2.5.3, appropriate compensation for these diverse services requires a flexible pricing mechanism. Our DAM and RTM are therefore formulated as discriminatory-price auctions in which participants pay (or are paid) their bid/offer prices for cleared SCs. These bid/offer price payments are compensations for service availability. Any real-time service performance rendered through these cleared SCs is compensated ex post in accordance with the performance payment methods appearing among the contractual terms of the cleared SCs.

Finally, SCs with swing in their contractual terms can function as both energy and reserve, and SCs in option form can also function as reserve even if their contractual terms are fixed. Consequently, our proposed DAM and RTM intrinsically involve a co-optimization of energy and reserve.

The next two sections use concrete examples to demonstrate how SC trading can be supported by means of our proposed linked DAM and RTM processes in a way that ensures optimal balancing of real-time net loads subject to system and reserve-requirement constraints.

2.3 RTM Illustrative Example

2.3.1 Overview

Sections 2.3.2 through 2.3.7 present a numerical example illustrating how SC trading can be supported by means of an RTM in the absence of transmission congestion and without consideration of linkages to earlier DAM processes. The handling of RTM transmission congestion is addressed in Section 2.3.8, and linkages with earlier DAM processes are considered in Section 2.4.

2.3.2 Basic Assumptions

Suppose an RTM takes place immediately prior to a particular operating period for which no congestion is anticipated. For concreteness, we assume this operating period is a particular hour H on a particular day D, expressed at the granularity of minutes.

LSE demand bids for hour H are assumed to take the form of constant non-price-responsive power levels, a simple block-energy form that greatly eases graphical exposition.[3] VER as-available generation exhibiting stochastic variation over hour H is treated as negative load.

Net load for hour H is then defined to be aggregate LSE demand bids for hour H minus aggregate VER as-available generation for hour H. The ISO-forecasted net load profile for hour H of day D at the start of this RTM is assumed to take the form given in Fig. 2.4. The objective of the ISO managing the RTM is to ensure that this forecasted net load profile is balanced by generation with an appropriate reserve buffer, keeping costs to a minimum. The ISO attempts to achieve this objective by procuring a suitable combination of SCs from dispatchable generation suppliers participating in the RTM.
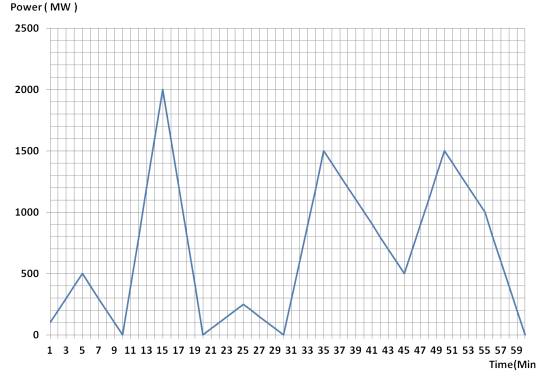
Figure 2.4: ISO-forecasted net load profile for hour H of day D at start of RTM

These participant suppliers are assumed to consist of three GenCos with the following ramp-rate and generation-capacity attributes, expressed in Section 2.2.1 notation:

$$\text{G1}: \ r_1^D = r_1^U = 120\text{MW/min}, \text{Cap}_1^{min} = 0\text{MW}, \ \text{Cap}_1^{max} = 600\text{MW}$$

$$\text{G2}: \ r_2^D = r_2^U = 200\text{MW/min}, \text{Cap}_2^{min} = 0\text{MW}, \ \text{Cap}_2^{max} = 700\text{MW}$$

$$\text{G3}: \ r_3^D = r_3^U = 300\text{MW/min}, \text{Cap}_3^{min} = 0\text{MW}, \ \text{Cap}_3^{max} = 900\text{MW}$$

---

[3]Two-part LSE demand bids including both price-responsive and non-price-responsive portions, as in actual U.S. ISO-managed wholesale power markets, can be modeled by allowing each LSE to actively bid for multiple block-energy contracts at differing bid prices in addition to submitting a non-price-responsive block energy contract.

Each of these GenCo offers into the RTM a collection of portfolios, called *GenPorts*, together with associated GenPort offer prices. A GenPort consists of one or more SCs whose terms the GenCo could simultaneously fulfill during hour H if called upon to do so by the ISO. The ISO can clear at most one GenPort from each GenCo in the RTM.

The offer price $v_{i,j}$ for GenPort$_{i,j}$ is the payment requested by Gi for guaranteeing it will be available in hour H to fulfill the terms of the SCs included in GenPort$_{i,j}$ if signalled to do so. Thus, $v_{i,j}$ compensates Gi for service availability costs, such as fixed avoidable costs and lost opportunity costs. In addition, assuming GenPort$_{i,j}$ is cleared by the ISO, Gi will also receive performance payments for any services it renders during hour H under the contractual terms of the SCs in GenPort$_{i,j}$. Any such performance payments will be determined in accordance with the performance payment methods ϕ included among the contractual terms of the SCs in GenPort$_{i,j}$. For the example at hand, each of these performance payment methods ϕ is assumed to take the form of a pre-specified price ($/MWh) for delivered down/up energy.[4]

As clarified in subsequent sections, this two-part pricing scheme permits the GenCos to ensure the recovery of their expected total costs through a market process, taking into account their local attributes and conditions. It also permits the ISO to closely tailor the cleared RTM GenPorts to real-time needs for net load balancing subject to system and reserve-requirement constraints.

The ISO is permitted to clear at most one GenPort from each GenCo in the RTM. The resulting cleared GenPorts can thus be represented in the following *ISO Portfolio (ISOPort)* form:

$$\text{ISOPort} = \{\text{GenPort}_1, \text{GenPort}_2, \text{GenPort}_3\}, \tag{2.2}$$

where no procurement from a GenCo Gi (GenPort$_i$=None) is possible.

---

[4]For example, each SC$_{i,j,m}$ in GenPort$_{i,j}$ could correspond to a distinct generation unit m owned by Gi, and the performance payment method $\phi_{i,j,m}$ for SC$_{i,j,m}$ could be a down/up energy price ($/MWh) given by the expected next-day marginal dispatch cost for unit m.

2.3.3 RTM Supply Offer Specifications

A GenCo's RTM supply offer is a collection of GenPorts together with associated GenPort offer prices. Suppose each GenCo offers up-energy in firm contract form, ie, exercise time $t_{ex} = t_{ex}^{min} = t_{ex}^{max} = $ RTM end-time. Suppressing location (k), direction (up), exercise time t_{ex}, and measurement units from SC representations for ease of exposition, the RTM supply offers of GenCos G1, G2, and G3 are assumed to take the following form:

G1's supply offer consists of two GenPorts, each with one SC:

$$\text{GenPort}_{1,1} = \{\text{SC}_{1,1}\} \text{ at offer price } v_{1,1}, \tag{2.3}$$

$$\text{SC}_{1,1} = [t_{pb} = 0, \ t_{pe} = 60, \ |r| \le 100, \ 0 \le p \le 500, \ \phi = 100]$$

$$\text{GenPort}_{1,2} = \{\text{SC}_{1,2}\} \text{ at offer price } v_{1,2}, \tag{2.4}$$

$$\text{SC}_{1,2} = [t_{pb} = 0, \ t_{pe} = 60, \ |r| \le 120, \ 0 \le p \le 500, \ \phi = 105].$$

G2's supply offer consists of three GenPorts with multiple SCs:

$$\text{GenPort}_{2,1} = \{\text{SC}_{2,1,1}, \text{SC}_{2,1,2}\} \text{ at offer price } v_{2,1}, \tag{2.5}$$

$$\text{SC}_{2,1,1} = [t_{pb} = 10, \ t_{pe} = 20, \ |r| \le 200, \ 0 \le p \le 600, \ \phi = 135]$$

$$\text{SC}_{2,1,2} = [t_{pb} = 30, \ t_{pe} = 60, \ |r| \le 200, \ 0 \le p \le 600, \ \phi = 130]$$

$$\text{GenPort}_{2,2} = \{\text{SC}_{2,2,1}, \text{SC}_{2,2,2}, \text{SC}_{2,2,3}\} \text{ at offer price } v_{2,2}, \tag{2.6}$$

$$\text{SC}_{2,2,1} = [t_{pb} = 0, \ \ t_{pe} = 10, \ |r| \le 100, \ 0 \le p \le 100, \phi = 105]$$

$$\text{SC}_{2,2,2} = [t_{pb} = 10, \ t_{pe} = 20, \ |r| \le 200, \ 0 \le p \le 600, \phi = 135]$$

$$\text{SC}_{2,2,3} = [t_{pb} = 30, \ t_{pe} = 60, \ |r| \le 200, \ 0 \le p \le 600, \phi = 130]$$

$$\text{GenPort}_{2,3} = \{\text{SC}_{2,3,1}, \text{SC}_{2,3,2}, \text{SC}_{2,3,3}\} \text{ at offer price } v_{2,3}, \tag{2.7}$$

$$\text{SC}_{2,3,1} = [t_{pb} = 0, \ t_{pe} = 10, \ |r| \le 100, \ 0 \le p \le 100, \ \phi = 105]$$

$$\text{SC}_{2,3,2} = [t_{pb} = 10, \ t_{pe} = 20, \ |r| \le 200, \ 0 \le p \le 700, \ \phi = 140]$$

$$\text{SC}_{2,3,3} = [t_{pb} = 30, \ t_{pe} = 60, \ |r| \le 200, \ 0 \le p \le 700, \ \phi = 135]$$

G3's supply offer consists of two GenPorts with multiple SCs:

$$\text{GenPort}_{3,1} = \{\text{SC}_{3,1,1}, \text{SC}_{3,1,2}, \text{SC}_{3,1,3}\} \text{ at offer price } v_{3,1}, \qquad (2.8)$$

$$\text{SC}_{3,1,1} = [t_{pb} = 10, \ t_{pe} = 20, \ |r| \leq 300, \ 0 \leq p \leq 900, \ \phi = 175]$$

$$\text{SC}_{3,1,2} = [t_{pb} = 33, \ t_{pe} = 39, \ |r| \leq 200, \ 0 \leq p \leq 400, \ \phi = 155]$$

$$\text{SC}_{3,1,3} = [t_{pb} = 48, \ t_{pe} = 54, \ |r| \leq 200, \ 0 \leq p \leq 400, \ \phi = 155]$$

$$\text{GenPort}_{3,2} = \{\text{SC}_{3,2,1}, \text{SC}_{3,2,2}, \text{SC}_{3,2,3}\} \text{ at offer price } v_{3,2}, \qquad (2.9)$$

$$\text{SC}_{3,2,1} = [t_{pb} = 10, \ t_{pe} = 20, \ |r| \leq 300, \ 0 \leq p \leq 900, \ \phi = 175]$$

$$\text{SC}_{3,2,2} = [t_{pb} = 30, \ t_{pe} = 39, \ |r| \leq 200, \ 0 \leq p \leq 400, \ \phi = 150]$$

$$\text{SC}_{3,2,3} = [t_{pb} = 44, \ t_{pe} = 54, \ |r| \leq 200, \ 0 \leq p \leq 400, \ \phi = 150]$$

2.3.4 Power-Balance Constraints for ISOPorts

Any ISOPort cleared by the ISO in the RTM must permit the achievement of a *Zero Balance Gap (ZBG)*, i.e., an exact balancing of RTM-cleared generation against the ISO's forecasted hour-H load profile in Fig. 2.4. For example, Figs. 2.5-2.7 show how each of the following ISOPorts enables the achievement of a ZBG:

$$\text{ISOPort}_1 = \{\text{GenPort}_{1,1}, \text{GenPort}_{2,2}, \text{GenPort}_{3,1}\} \qquad (2.10)$$

$$\text{ISOPort}_2 = \{\text{GenPort}_{1,1}, \text{GenPort}_{2,3}, \text{GenPort}_{3,1}\} \qquad (2.11)$$

$$\text{ISOPort}_3 = \{\text{GenPort}_{1,2}, \text{GenPort}_{2,3}, \text{GenPort}_{3,2}\} \qquad (2.12)$$

Each color in these figures indicates the dispatch of generation from a particular GenPort for a particular GenCo, and different shades of the same color indicate the dispatch of generation from distinct SCs within a particular GenPort.

Consider, in particular, Fig. 2.6 for ISOPort$_2$ in (2.11). The yellow areas correspond to GenPort$_{1,1}$ in (2.3), and the single shade of yellow represents energy dispatched via this GenPort's single SC constituent, SC$_{1,1}$. The green areas correspond to GenPort$_{2,3}$
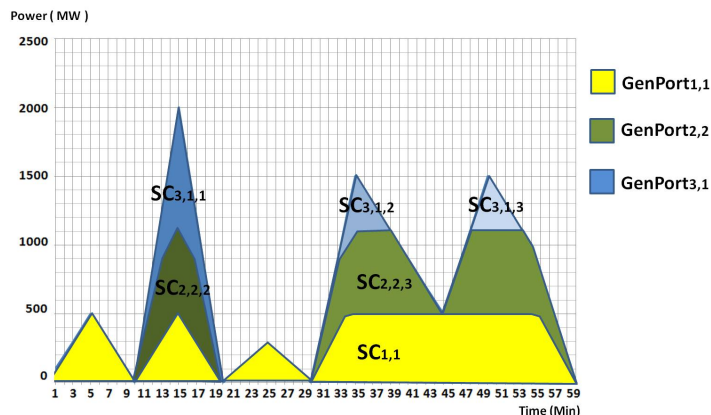
Figure 2.5: Zero balance gap achieved by $ISOPort_1$ for hour H of day D
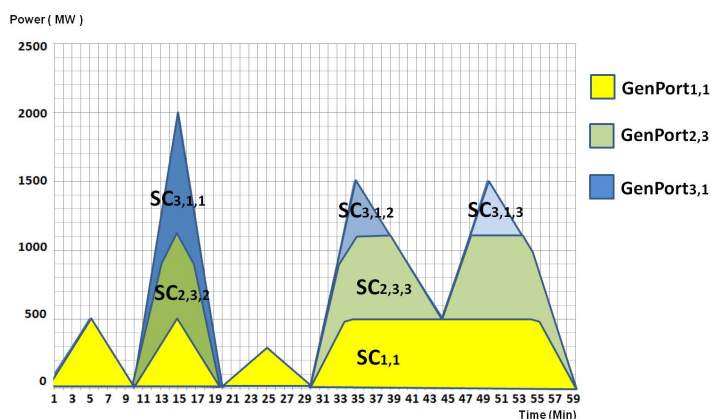
Figure 2.6: Zero balance gap achieved by $ISOPort_2$ for hour H of day D

in (2.7), and the two areas with different shades of green represent the energy dispatched via two of this GenPort's three SC constituents, $SC_{2,3,2}$ and $SC_{2,3,3}$. Finally, the blue areas correspond to $GenPort_{3,1}$ in (2.8), and the three areas with different shades of blue represent the energy dispatched via this GenPort's three SC constituents, $SC_{3,1,1}$, $SC_{3,1,2}$, and $SC_{3,1,3}$.

2.3.5 Expected Total Cost of a Power-Balanced ISOPort

Consider any $ISOPort=(GenPort_1, GenPort_2, GenPort_3)$ that achieves a ZBG for hour H. The expected total cost of this ISOPort is the sum of payments arising from two sources: (i) the portfolio offer prices $\{v_1, v_2, v_3\}$ that must be paid to GenCos G1, G2,
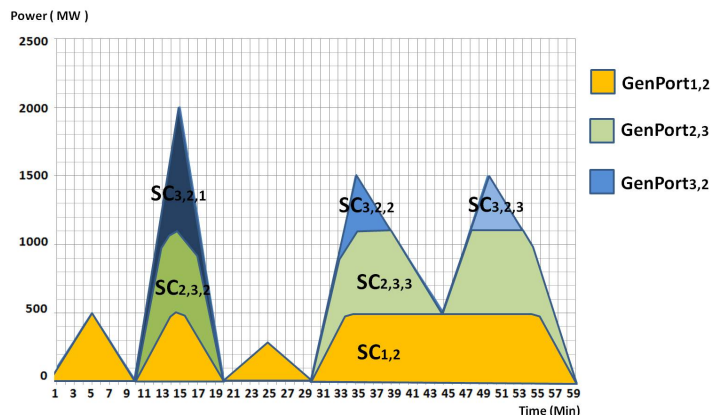
Figure 2.7: Zero balance gap achieved by ISOPort_3 for hour H of day D

and G3 for the procurement of GenPort_1, GenPort_2, and GenPort_3; and (ii) the total performance payments the ISO expects it will have to make to G1, G2, and G3 for down/up energy delivery during hour H under the contractual terms of these constituent GenPorts in order to achieve the ZBG.

For example, to calculate the expected total performance payments (ii) implied by the depicted ZBG implementation of ISOPort_2 depicted in Fig. 2.6, first measure the energy (MWh) for each of the areas in Fig. 2.6 with a distinct color shading; each such area corresponds to a distinct SC implementation. Next, multiply each of these energy amounts by the performance price ϕ ($/MWh) included among the contractual terms of the corresponding SC. Finally, add up all of these amounts.

2.3.6 Reserve Inherent in a Power-Balanced ISOPort

The achievement of a ZBG by an ISOPort implies that the generation available through this ISOPort is capable of balancing the ISO's *forecasted* hour-H load profile. However, if the SCs constituting this ISOPort include swing, then the ISOPort can also achieve a ZBG for a range of hour-H load profiles that deviate from the ISO's forecasted hour-H load profile. Hereafter, this range will be referred to as the *Reserve Range (RR)* of the ZBG ISOPort.

The RR of a ZBG ISOPort with swing functions as a robust-control device for load-balancing, reducing the need to consider detailed load scenarios and load-scenario probabilities. However, its exact form depends in a complicated manner on the particular attribute specifications of the SCs that constitute the ISOPort as well as on the minute-by-minute operating state of the *GenCo suppliers*, i.e., the GenCos that have offered these SCs. Consequently, in any practical application, the RR will have to be approximated.

For example, Figs. 2.8 through 2.10 plot approximate RRs for ISOPorts 1, 2, and 3 in (2.10) through (2.12) by assuming that the GenCo suppliers at the start of each minute M are at their ZBG-generation levels. The depicted approximate RRs are conditional on the ISO's forecasted hour-H load profile shown in Fig. 2.4 and on the ISO's hour-H ZBG implementations for ISOPorts 1, 2, and 3 shown in Figs. 2.5 through 2.7.
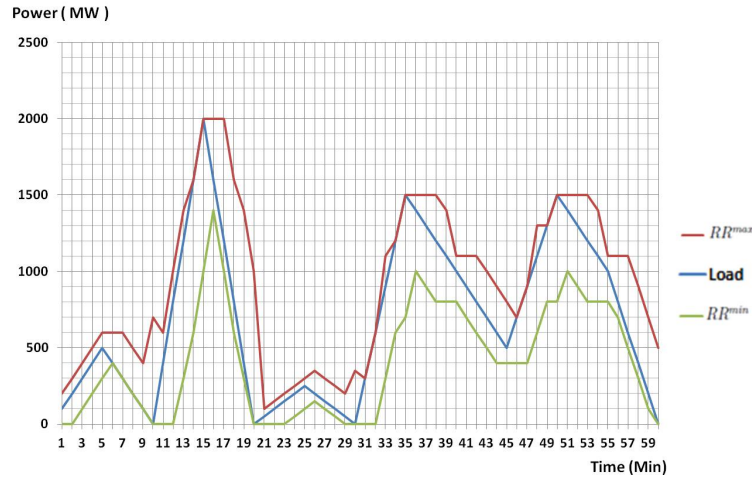
Figure 2.8: Reserve range RR for ISOPort$_1$ during hour H of day D

In particular, the approximate RR depicted in Fig. 2.9 for ISOPort$_2$ was derived by means of the following steps, applicable for any ZBG ISOPort. At the start of each minute M of hour H, calculate the minimum and maximum power levels RR_M^{min} and RR_M^{max} that could be attained at the end of minute M. These minimum and maximum power levels depend on: (a) the contractual terms of the SCs constituting ISOPort$_2$; (b)
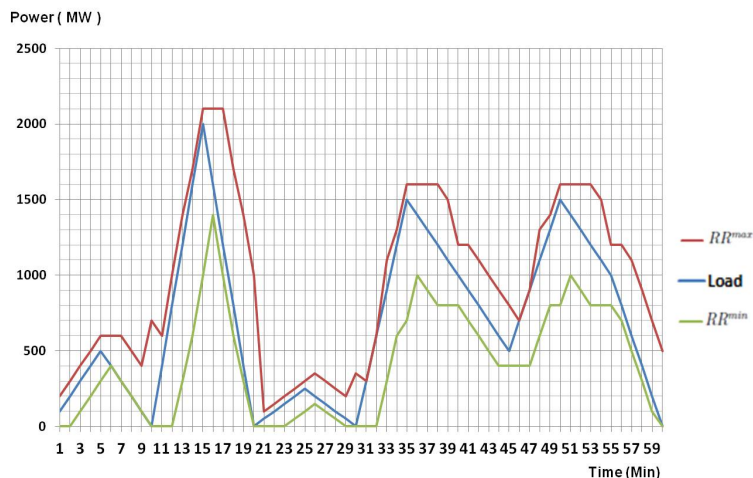
Figure 2.9: Reserve range RR for ISOPort_2 during hour H of day D
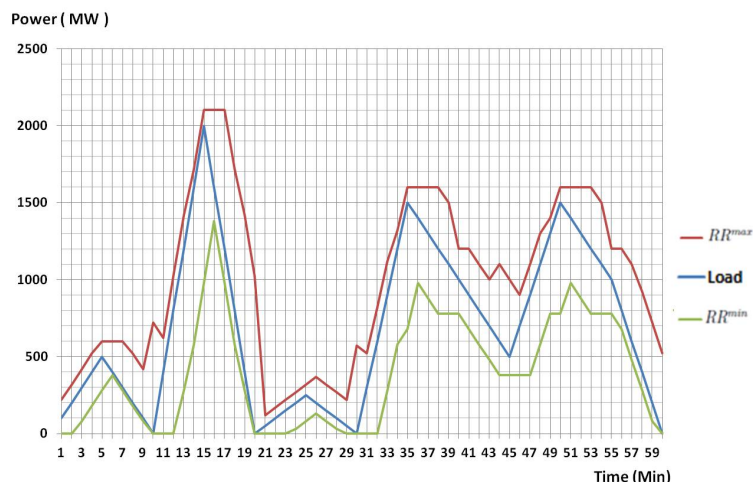
Figure 2.10: Reserve range RR for ISOPort_3 during hour H of day D

the particular ZBG implementation of ISOPort_2 for hour H; and (c) the ZBG operating state of each GenCo supplier for ISOPort_2 at the start of each minute M of hour H.

Specifically, for each GenCo supplier Gi, and for each minute M during the operating hour H, let $\text{Gen}_{i,M}$ denote the ZBG generation level (MW) of Gi at the start of M. Also, let $r_{i,M}^D$ / $r_{i,M}^U$ denote the down/up ramp-rate limits (MW/min) for Gi during M, and let $p_{i,M}^{min}$ / $p_{i,M}^{max}$ denote the min/max power limits (MW) for Gi at the end of M. Then the lower and upper bounds on the power levels that could be delivered by Gi at the end of

M, conditional on its ZBG state at the start of M, are given by

$$\mathrm{PI}^L_{i,M} = \max\left\{\mathrm{Gen}_{i,M} - r^D_{i,M},\ p^{min}_{i,M}\right\} \ \geq\ p^{min}_{i,M} \tag{2.13}$$

$$\mathrm{PI}^U_{i,M} = \min\left\{\mathrm{Gen}_{i,M} + r^U_{i,M},\ p^{max}_{i,M}\right\} \ \leq\ p^{max}_{i,M} \tag{2.14}$$

The minimum power level RR^{min}_M attainable for the system as a whole at the end of minute M can be approximated by summing the lower power bounds (2.13) across the set G_H of GenCo suppliers Gi. Similarly, the maximum power level RR^{max}_M attainable for the system as a whole at the end of minute M can be approximated by summing the upper power bounds (2.14) across the set G_H of GenCo suppliers Gi. The reserve range RR_M at the end of minute M is then approximately given by the power-level interval between these summed lower and upper bounds:

$$\mathrm{RR}_M = [\mathrm{RR}^{min}_M,\ \mathrm{RR}^{max}_M] = \left[\ \sum_{i\in\mathrm{G}_H}\mathrm{PI}^L_{i,M},\ \sum_{i\in\mathrm{G}_H}\mathrm{PI}^U_{i,M}\ \right] \tag{2.15}$$

and the RR over the entire hour H, expressed at the granularity of minutes, is approximately given by

$$\mathrm{RR}\ =\ \{\mathrm{RR}_M \mid M \in H\} \tag{2.16}$$

To illustrate in more concrete terms the determination of the RR for any given hour H, consider the following simple example. Let the load profile for some operating hour H be as depicted in Fig. 2.4. Suppose the ISO is planning to achieve a ZBG for this load profile by implementation of ISOPort$_2$ in (2.11) with GenCo suppliers G1, G2, and G3, where the dispatch levels for these GenCo suppliers are as depicted in Fig. 2.6.

Suppose the system is at the start of minute M=35 (or equivalently, at the end of minute M=34). The ZBG generation levels for G1, G2, and G3 are 400MW, 600MW, and 200MW, respectively. The down/up ramp-rate limits for G1 are $r^D_{1,35} = r^U_{1,35} = 100\mathrm{MW/min}$, and the min/max power limits for G1 are $p^{min}_{1,35} = 0\mathrm{MW}$ and $p^{max}_{1,35} = 500\mathrm{MW}$. The down/up ramp-rate limits for G2 are $r^D_{2,35} = r^U_{2,35} = 200\mathrm{MW/min}$ and the min/max

power limits for G2 are $p_{2,35}^{min} = 0$MW and $p_{2,35}^{max} = 700$MW. Finally, the down/up ramp-rate limits for G3 are $r_{3,35}^{D} = r_{3,35}^{U} = 200$MW/min and the min/max power limits for G3 are $p_{3,35}^{min} = 0$MW and $p_{3,35}^{max} = 400$MW.

Given these conditions at the start of M=35, the lower and upper power bounds attainable by each GenCo supplier at the end of minute M=35 can be calculated using (2.13) and (2.14), as follows:

$$\mathrm{PI}_{1,35}^{L} = \max\left\{400MW - 100MW,\ 0MW\right\} = 300MW$$

$$\mathrm{PI}_{1,35}^{U} = \min\left\{400MW + 100MW,\ 500MW\right\} = 500MW$$

$$\mathrm{PI}_{2,35}^{L} = \max\left\{600MW - 200MW,\ 0MW\right\} = 400MW$$

$$\mathrm{PI}_{2,35}^{U} = \min\left\{600MW + 200MW,\ 700MW\right\} = 700MW$$

$$\mathrm{PI}_{3,35}^{L} = \max\left\{200MW - 200MW,\ 0MW\right\} = 0MW$$

$$\mathrm{PI}_{3,35}^{U} = \min\left\{200MW + 200MW,\ 400MW\right\} = 400MW$$

Consequently, the reserve range RR_{35} at the end of minute M=35 can be approximated using (2.15), as follows:

$$\mathrm{RR}_{35} = [300MW + 400MW + 0MW,\ 500MW + 700MW + 400MW]$$

$$= [700MW,\ 1{,}600MW] \tag{2.17}$$

The above method is used to derive the plots in Figs. 2.8-2.10 for the complete hour-H RRs for ISOPorts 1, 2, and 3 described in (2.10) through (2.12).

The GenCos can seek compensation for the RR characteristics of their RTM-offered GenPorts through their GenPort offer prices. In addition, GenCos with cleared GenPorts will be compensated ex post for any actual down/up energy they deliver during hour H, using the performance prices ϕ appearing among the contractual terms of these cleared GenPorts. This includes, in particular, compensation for any down/up energy needed to balance deviations between actual and ISO-forecasted real-time loads.

2.3.7   Practical Determination of Optimal ISOPorts

Let $\{L_M \mid 1 \leq M \leq 60\}$ denote the ISO-forecasted load profile for hour H. Suppose the ISO's requirements for down/up reserve during H can be expressed in terms of the following restrictions on the reserve range (2.16) for this load profile for some given $\boldsymbol{\alpha}^* = (\alpha^{D*}, \alpha^{U*}) \geq 0$: For each minute M of hour H, the lower and upper bounds of RR_M in (2.16) must satisfy

$$RR_M^{min} \leq [1 - \alpha^{D*}]L_M \leq [1 + \alpha^{U*}]L_M \leq RR_M^{max} \tag{2.18}$$

Suppose at least one feasible ISOPort achieves a ZBG for H. Then the ISO can formulate its RTM optimization problem as a multi-criteria optimization problem with three lexicographically-ordered objectives: (i) ensure a ZBG; (ii) ensure RR reliability at level $\boldsymbol{\alpha}^*$, i.e., satisfy condition (2.18); and (iii) minimize the expected total cost of ensuring (i) and (ii).

More precisely, as schematically depicted in Fig. 2.11(a), the ISO can undertake the following three steps in sequence. First, determine the set $\mathcal{I}^{\mathcal{Z}}$ of all feasible ISOPorts that achieve a ZBG. Second, determine the (possibly empty) subset $\mathcal{I}^{\mathcal{Z}}_{\alpha^*}$ of $\mathcal{I}^{\mathcal{Z}}$ for which the RR requirement (2.18) is satisfied. Third, determine the subset $\mathcal{I}^{\mathcal{Z},\mathcal{MTC}}_{\alpha^*}$ of $\mathcal{I}^{\mathcal{Z}}_{\alpha^*}$ entailing minimum expected total cost, where this expected total cost consists of both GenPort procurement costs and expected ex-post GenPort performance costs for ensuring a ZBG that satisfies RR requirement (2.18). Any element of $\mathcal{I}^{\mathcal{Z},\mathcal{MTC}}_{\alpha^*}$ constitutes an optimal ISOPort selection for the RTM.

Relatively small values for $(\alpha^{D*}, \alpha^{U*})$ in (2.18) might be needed to ensure the non-emptiness of $\mathcal{I}^{\mathcal{Z}}_{\alpha^*}$. For example, as depicted in Figs. 2.8-2.10, ISOPort$_1$, ISOPort$_2$ and ISOPort$_3$ can each achieve a ZBG that satisfies the RR_{α^*} constraint (2.18) when $\alpha^{D*} = \alpha^{U*} = 0$. However, only ISOPort$_3$ can achieve a ZBG that satisfies the RR_{α^*} constraint (2.18) when $\alpha^{D*} = \alpha^{U*} = 0.5$. Smaller values for α^{D*} and α^{U*} should also entail lower minimum total costs due to less need for swing in the cleared SCs. On the other hand,
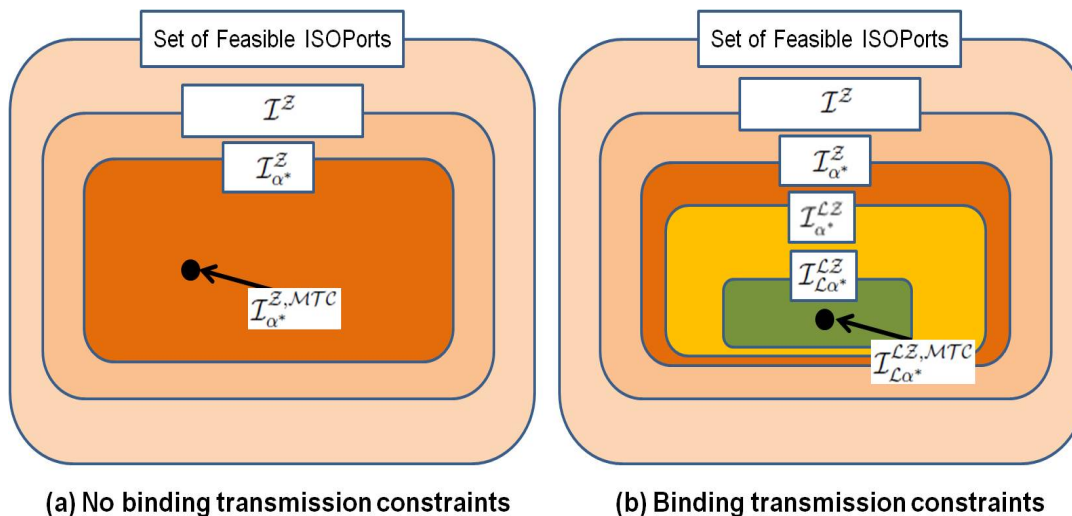
Figure 2.11: Depiction of the subsets $\mathcal{I}_{\alpha^*}^{\mathcal{Z},\mathcal{MTC}}$ and $\mathcal{I}_{\mathcal{L}\alpha^*}^{\mathcal{LZ},\mathcal{MTC}}$ of optimal (minimum total expected cost) ISOPorts subject to (a) system-wide ZBG and RR constraints in the absence of binding transmission constraints and (b) local ZBG and RR constraints in the presence of binding transmission constraints.

setting these values too small could jeopardize grid reliability if actual real-time loads differ significantly from their forecasted levels.

2.3.8 Incorporation of Transmission-Line Limits

Until now, our RTM illustrative example has assumed an absence of transmission congestion. This simplification has permitted us to focus solely on the economic dispatch problem of ensuring a balance between total dispatched generation and ISO-forecasted total system load, subject to a system-wide RR_{α^*} constraint (2.18).

Consider, now, an RTM for which the flow of power on each transmission line is subject to a potentially binding limit. In this case it is not sufficient to consider power and ramp-rate availability on a system-wide basis alone, since transmission congestion could limit the ability to move power from one bus to another. Rather, to ensure reliability, an ISO will need to impose a ZBG constraint at each bus, hereafter this constraint is referred to as a *local* ZBG constraint.[5] Moreover, the ISO will also presumably wish to

---

[5]Ignoring losses, the local ZBG constraint at each bus k is an equation ensuring that the total power

impose an $\mathrm{RR}_{\alpha*}$ constraint (2.18) at each bus, hereafter this constraint is referred to as a *local* $\mathrm{RR}_{\alpha*}$ constraint.[6]

Note that a ZBG ISOPort satisfying a local $\mathrm{RR}_{\alpha*}$ constraint at each bus automatically satisfies a system-wide $\mathrm{RR}_{\alpha*}$ constraint. Consequently, as depicted in Fig. 2.11(b), the following nested relationships hold. The set $\mathcal{I}_{\alpha*}^{\mathcal{LZ}}$ consisting of all feasible ISOPorts satisfying a local ZBG constraint at each bus and a system-wide $\mathrm{RR}_{\alpha*}$ constraint is a subset of $\mathcal{I}_{\alpha*}^{\mathcal{Z}}$. Moreover, the set $\mathcal{I}_{\mathcal{L}\alpha*}^{\mathcal{LZ}}$ consisting of all feasible ISOPort selections satisfying local ZBG and $\mathrm{RR}_{\alpha*}$ constraints at each bus is a subset of $\mathcal{I}_{\alpha*}^{\mathcal{LZ}}$. Finally, the set $\mathcal{I}_{\mathcal{L}\alpha*}^{\mathcal{LZ},\mathcal{MTC}}$ consisting of all optimal (minimum expected total cost) ISOPort selections for the RTM SCED optimization augmented with local ZBG and $\mathrm{RR}_{\alpha*}$ constraints at each bus is a subset of $\mathcal{I}_{\mathcal{L}\alpha*}^{\mathcal{LZ}}$.

For example, as in Section 2.3.2, consider an RTM with three GenCo participants G1, G2, and G3 that takes place immediately before an operating hour H on some day D. Assume, now, that this RTM is operating over a 2-bus transmission grid with buses A and B, where G1 is located at bus A and G2 and G3 are located at bus B, and that the transmission line connecting buses A and B has a capacity limit of 1,100MW. As depicted in Fig. 2.4, the ISO-forecasted load at the end of minute M=15 for hour H is L_{15}=2,000MW. Assume the ISO has forecasted that L_{15} will be divided into a load LA=1,500MW at bus A, and a load LB=500MW at bus B.

Suppose the ISO secures ISOPort$_3$ in the RTM in an attempt to ensure a ZBG for hour H, where ISOPort$_3$ is given by (2.12). The GenCo suppliers for ISOPort$_3$ are G1, G2, and G3. Suppose the generation levels for G1, G2, and G3 at the start of minute M=15 are given by 400MW, 600MW and 600MW, respectively. Using the contractual

---

injected at bus k equals the total power withdrawn at bus k plus the total power flowing out from bus k to other buses.

[6]In practice, local reserve requirements are imposed at the level of reserve zones. Roughly defined, a reserve zone is a grid region (buses plus connecting transmission lines) with normally negligible internal congestion that can on occasion operate as a load pocket because the transmission lines linking this region to other grid regions become congested. Load pockets can cause reliability problems if the generation capacity internal to the pocket is not sufficient to meet internal load. In this subsection, reserve zones are assumed to consist of singleton buses for ease of exposition.

terms of the SCs in ISOPort$_3$, it can then be shown that the feasible power intervals for G1, G2, and G3 at the end of minute M=15 are as follows:[7] [280MW,500MW] for G1; [400MW,700MW] for G2; and [300MW,900MW] for G3.
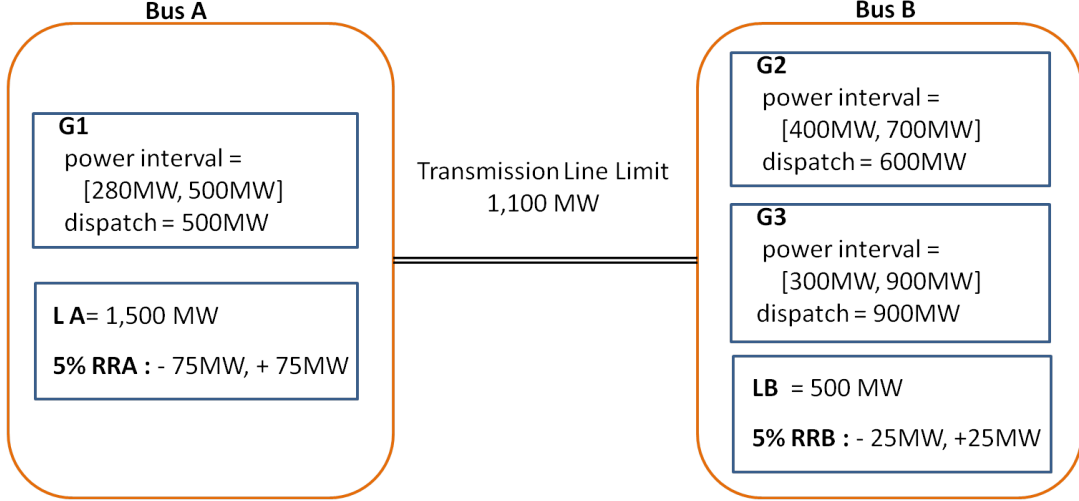
Figure 2.12: Depiction of an RTM ISOPort selection that satisfies local ZBG and RR$_{\alpha^*}$ constraints at each bus A and B at the end of minute M=15 for hour H of day D,where $\alpha^{D*} = \alpha^{U*} = 0.05$.

Consequently, the selection of ISOPort$_3$ permits the ISO to achieve a local ZBG at the end of minute M=15 with power flowing from bus B to bus A. Specifically, as depicted in Fig. 2.12, G1 at bus A can be dispatched at 500MW, which is its maximum possible power level. Also, G2 at bus B can be dispatched at 600MW, which is below its maximum possible power level of 700MW, and G3 at bus B can be dispatched at its maximum possible power level of 900MW. The load LA=1,500MW at bus A exceeds by 1,000MW the 500MW of power generated by G1. However, the 1,500MW of power generated at bus B by G2 and G3 exceeds the load LB=500MW at bus B by 1,000MW;

---

[7]Given ISOPort$_3$, the down/up ramp-rate limits for G1, G2, and G3 during M=15 are $r^D_{1,15} = r^U_{1,15}$ = 120MW/min, $r^D_{2,15} = r^U_{2,15}$ = 200MW/min, and $r^D_{3,15} = r^U_{3,15}$ = 300MW/min. Also, the min/max power limits for G1, G2, and G3 at the end of M=15 are $p^{min}_{1,15} = 0$MW, $p^{max}_{1,15} = 500$MW, $p^{min}_{2,15} = 0$MW, $p^{max}_{2,15} = 700$MW, $p^{min}_{3,15} = 0$MW, and $p^{max}_{3,15} = 900$MW. These conditions, together with the assumed generation levels for G1, G2, and G3 at the start of minute M=15, determine the feasible power intervals for G1, G2, and G3 at the end of M=15. For example, for G1 this feasible power interval is given by [FPI$^{min}_1$, FPI$^{max}_1$] where FPI$^{min}_1$ = max$\{400MW - 120MW, 0MW\}$ = 280MW and FPI$^{max}_1$ = min$\{400MW + 120MW, 500MW\}$ = 500MW.

and this 1,000MW can be transferred from bus B to bus A to satisfy the remaining load at bus A without violating the 1,100MW transmission line limit.

Now consider the additional RTM goal of ensuring a local $\text{RR}_{\alpha*}$ constraint at each bus A and B at the end of minute M=15, with $\boldsymbol{\alpha}^* = (0.05, 0.05)$. To satisfy the 5% up-power requirements of these local $\text{RR}_{\alpha*}$ constraints, the ISO needs +75MW of up-power reserve at bus A (5% of LA=1,500MW) and +25MW of up-power reserve at bus B (5% of LB=500MW). As seen in Fig. 2.12, the +75MW requirement at bus A is satisfied under ISOPort$_3$ because G2 at bus B has +75MW of unencumbered up-power that can flow to bus A without violation of the transmission line limit. Moreover, the +25MW requirement at bus B is satisfied under ISOPort$_3$ because G2 at bus B has +25MW of additional unencumbered up-power.

Conversely, to satisfy the 5% down-power requirements of these local $\text{RR}_{\alpha*}$ constraints, the ISO needs -75MW of down-power reserve at bus A and -25MW of down-power reserve at bus B. As seen in Fig. 2.12, the -75MW requirement at bus A is satisfied because G1 can feasibly reduce its 500MW dispatch level to 425MW. Moreover, the -25MW requirement at bus B is satisfied because G2 and G3 can feasibly reduce their total dispatch level by 25MW, either separately or in combination.

2.4   Linkages between the RTM and the DAM

2.4.1   Overview

This section extends the RTM illustrative example presented in Section 2.3 to include the prior operations of a DAM, as depicted in Fig. 2.13.

This DAM is assumed to operate in accordance with the general DAM description provided in Section 2.2.3. However, we maintain the simplifying assumptions introduced in Section 2.3 that all load is fixed and all line losses are negligible; and we also assume the absence of transmission congestion to further ease graphical depictions.
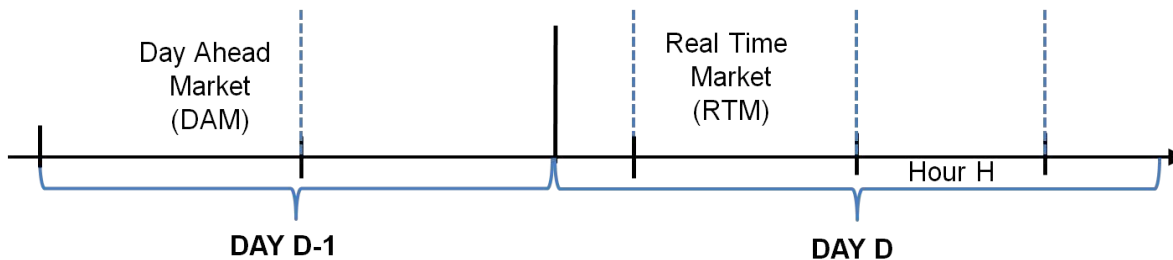
Figure 2.13: Illustrative time-line for DAM/RTM linkages

A key distinction between the DAM on day D-1 and the RTM on day D is that power-balance constraints in the DAM are based on LSE demand bids, not on the ISO's own load forecasts. In particular, for the illustrative example at hand, the loads appearing in the DAM power-balance constraints are the LSEs' DAM-submitted fixed (non-price-responsive) block-energy demand bids.

Nevertheless, the ISO has a fiduciary responsibility to balance *actual* real-time loads to ensure grid reliability. Consequently, the ISO is permitted to bid for SCs in the DAM on day D-1 to ensure reserve requirements are met, where these reserve requirements are informed by the ISO's own next-day load forecasts.[8] The ISO then matches and clears DAM-submitted SC bids and offers to achieve a least-cost ZBG subject to system constraints and reserve requirements. The ISO subsequently enters into the RTM on day D with a record of all DAM-cleared SCs and conducts RTM operations conditional on this SC inventory.

The operations of the RTM for a particular operating hour H in the absence of SC inventory conditioning were illustrated in Section 2.3. This illustration will now be extended to show how RTM operations for hour H could be affected by SC inventory conditioning. Section 2.4.2 considers the case in which reserve requirements are entirely for regulation (load-balancing) purposes. Contingency reserve requirements are considered in Section 2.4.3.

---

[8]As in Section 2.2.3, we require all costs arising from the ISO's DAM SC procurement to be charged to market participants in order to preserve the ISO's non-profit status.

2.4.2 DAM Linkages with Regulation Reserve Requirements

Let L_H denote the actual load profile for hour H of day D, and let $L_H^{F,DAM}$ denote the ISO's forecast for L_H at the start of the DAM. Figure 2.14 illustrates how the DAM-cleared LSE demand bids (all in block-energy form) imply a constant power level for hour H that can deviate from $L_H^{F,DAM}$. The difference between the two represents the down/up regulation reserve that the ISO would need to procure in the DAM in order to expect to be able to achieve *actual* load balancing for hour H, conditional on its own load forecasts. Hereafter this difference will be denoted by $L_H^{NF,DAM}$.
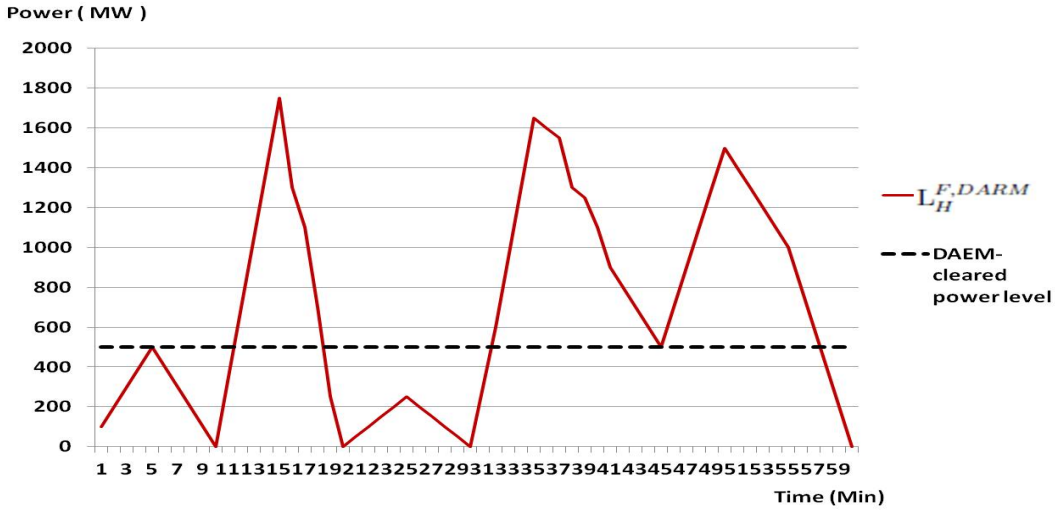
Figure 2.14: DAM-cleared LSE demand bids for hour H vs. the ISO's forecasted load profile $L_H^{F,DAM}$ for hour H at the time of the DAM

In addition to load-balancing, however, the ISO needs to ensure that it satisfies DAM down/up regulation reserve requirements. Suppose these requirements take the form of a system-wide RR constraint (2.18) with $\boldsymbol{\alpha}_{DAM}^* = (0.10, 0.10)$. This means that the ISO must procure SCs in the DAM with sufficient swing (flexibility) in their contractual terms that they are capable of covering a corridor of potential load profiles around the ISO's forecasted real-time net load profile $L_H^{NF,DAM}$ with a 10% width determined by $\boldsymbol{\alpha}_{DAM}^*$. This corridor, hereafter referred to as the *DAM 10% power corridor*, is depicted in Fig. 2.15.
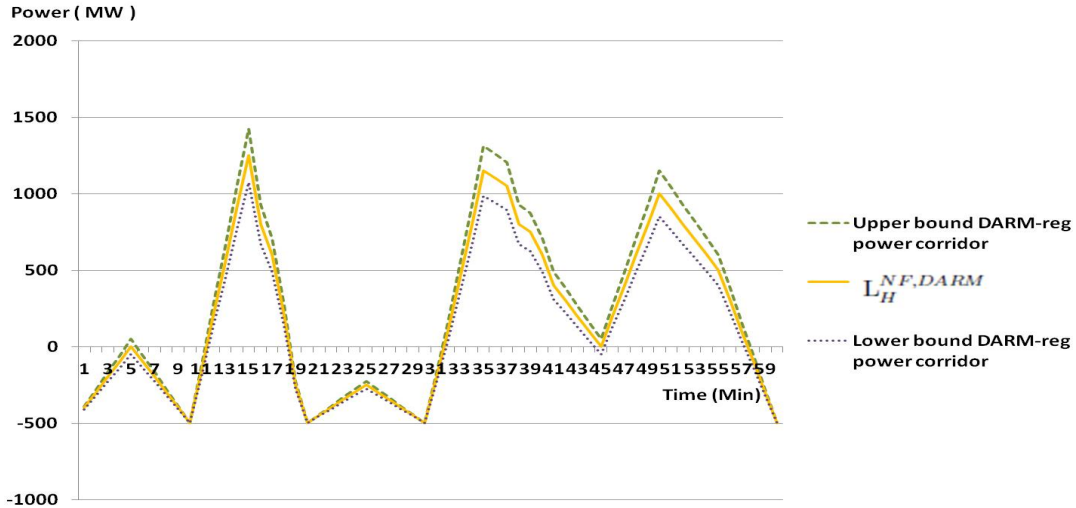
Figure 2.15: The DAM 10% power corridor for hour H of day D, conditional on the ISO's DAM-forecasted net load profile $L_H^{NF,DAM}$ for hour H of day D

As depicted in Fig. 2.16, the forecast $L_H^{F,DAM}$ that the ISO forms for L_H at the time of the DAM will typically differ from the forecast $L_H^{F,RTM}$ that the ISO forms for L_H at the time of the RTM.[9] For example, load could be affected by uncertain weather conditions, and the ISO could have improved information about these weather conditions at the time of the RTM relative to the information available to the ISO at the time of the DAM.
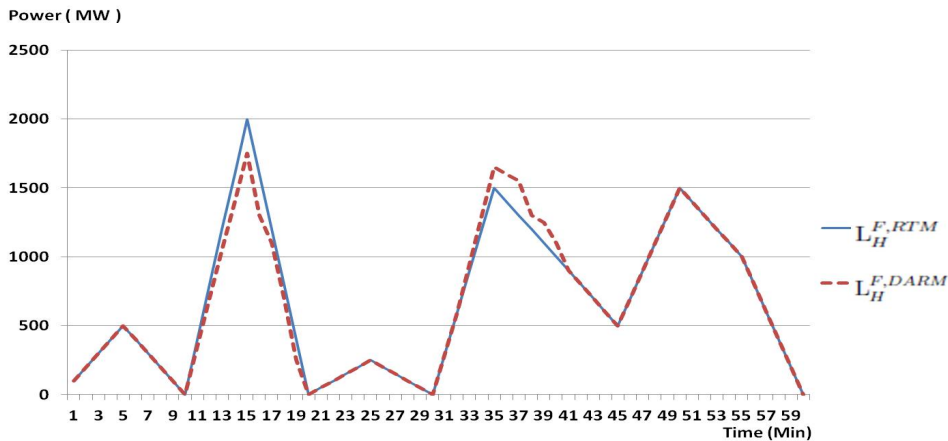
Figure 2.16: RTM vs. DAM ISO-forecasted load profiles $L_H^{F,RTM}$ and $L_H^{F,DAM}$ for hour H of day D

[9]Note $L_H^{F,RTM}$ in Fig. 2.16 coincides with the ISO-forecasted load profile in Fig. 2.4.

The ISO's RTM objective is to ensure a least-cost ZBG for hour H of day D subject to regulation reserve requirements, conditional on its updated load forecast $L_H^{F,RTM}$, GenCo/DRR/ESD RTM supply offers, and existing DAM-cleared SCs. Suppose the reserve requirements take the form of a system-wide RR constraint (2.18) with $\boldsymbol{\alpha}_{RTM}^* = (0.05, 0.05)$.[10] This means that the ISO must ensure, by the end of the RTM, that SCs have been procured with sufficient swing (flexibility) in their contractual terms that they are capable of covering a corridor of potential load profiles around the ISO's forecasted real-time load profile $L_H^{F,RTM}$ with a 5% width determined by $\boldsymbol{\alpha}_{RTM}^*$. Call this corridor the *RTM 5% power corridor*.

The gap $G_M^L = [PC_M^{L,RTM} - PC_M^{L,DA}]$ between the lower bound $PC_M^{L,RTM}$ of the RTM 5% power corridor and the lower bound $PC_M^{L,DA}$ of the DAM 10% power corridor for minute M of hour H determines the down-power amount P_M^{down} the ISO needs to procure in the RTM for injection during minute M of hour H. Specifically,

$$P_M^{down} = \min\{G_M^L, 0\} \tag{2.19}$$

Similarly, the gap $G_M^U = [PC_M^{U,RTM} - PC_M^{U,DA}]$ between the upper bound $PC_M^{U,RTM}$ of the RTM 5% power corridor and the upper-bound $PC_M^{U,DA}$ of the DAM 10% power corridor for minute M of hour H determines the up-power amount P_M^{up} that the ISO needs to procure in the RTM for injection during minute M of hour H. Specifically,

$$P_M^{up} = \max\{G_M^U, 0\} \tag{2.20}$$

Figure 2.17 illustrates the RTM down/up power requirements P_M^{down} and P_M^{up} that are implied by the lower and upper bounds $PC_M^{L,RTM}$, $PC_M^{L,DA}$, $PC_M^{U,RTM}$, and $PC_M^{U,DA}$ for each minute M of hour H. Note, for example, that no down-power procurement is needed in the RTM during minutes 10 to 20 of hour H because $PC_M^{L,DA} < PC_M^{L,RTM} \leq 0$ over this

---

[10]The ISO's load forecast errors in the RTM can be expected to be smaller than the ISO's load forecast errors in the DAM, and this is reflected in the specification of smaller component values for $\boldsymbol{\alpha}_{RTM}^*$ in comparison with $\boldsymbol{\alpha}_{DAM}^*$.

time interval. On the other hand, up-power procurement is needed in the RTM during minutes 10 to 20 of hour H because $\mathrm{PC}_M^{U,RTM} > \mathrm{PC}_M^{U,DA} \geq 0$ during this time interval.
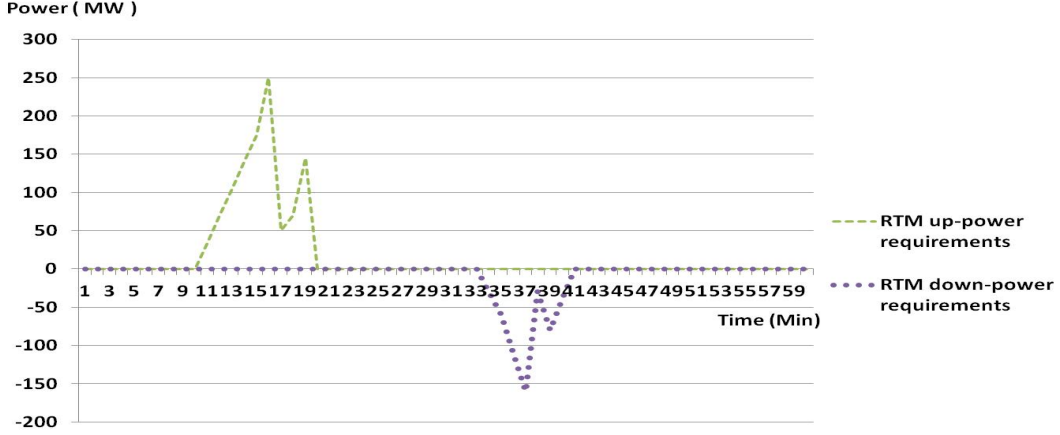
Figure 2.17: RTM down/up power procurement needed to satisfy load balancing with a 5% RR constraint for hour H of day D, conditional on $\mathrm{L}_H^{F,RTM}$ and the DAM 10% power corridor

In summary, permitting linkages between the DAM and the RTM changes the form of the ISOPorts available for ISO selection in the RTM. For the illustrative example developed in Section 2.3, each ISOPort in the collection $\mathcal{I}_{\alpha*}^{\mathcal{Z}}$ of ISOPorts achieving an RTM ZBG subject to the RTM RR constraint (2.18) for some given $\boldsymbol{\alpha}_{RTM}^*$ now takes the form

$$\mathrm{ISOPort} = \{\mathrm{GenPort}_1, \mathrm{GenPort}_2, \mathrm{GenPort}_3 \mid \mathrm{Contract\ Inventory}\} \qquad (2.21)$$

The *contract inventory* appearing in (2.21) consists of all SCs procured in the DAM whose exercise and/or use in combination with $\mathrm{GenPort}_1$, $\mathrm{GenPort}_2$, and $\mathrm{GenPort}_3$ permits the achievement of an RTM ZBG subject to the RTM RR constraint. For comparative selection purposes, the relevant (i.e., avoidable) expected total cost of ISOPort (2.21) thus consists of two parts:

(i) the performance payments arising from the exercise and/or use of the SCs in the contract inventory to achieve an RTM ZBG subject to the RTM RR constraint;[11]

---

[11]Note that the SCs in the contract inventory have already been procured, hence their procurement

(ii) the portfolio offer prices and performance payments arising from the RTM-procurement and implementation of the SCs comprising GenPort_1, GenPort_2, and GenPort_3.

The RTM is a balancing mechanism permitting the contract inventory to be supplemented as needed with new SC procurement to achieve real-time load balancing. As demonstrated in Fig. 2.17, the size of the RTM trade volume can be very small; it will tend to vary inversely with the amount of swing in the contract inventory.

Finally, under our proposed SC system, compensation obligations are separately incurred in the DAM (for service availability), in the RTM (for service availability), and in real time (for service performance). However, as illustrated in Fig. 2.18, the compensation obligations incurred for any particular operating hour H can in fact be settled at a single time point subsequent to H.
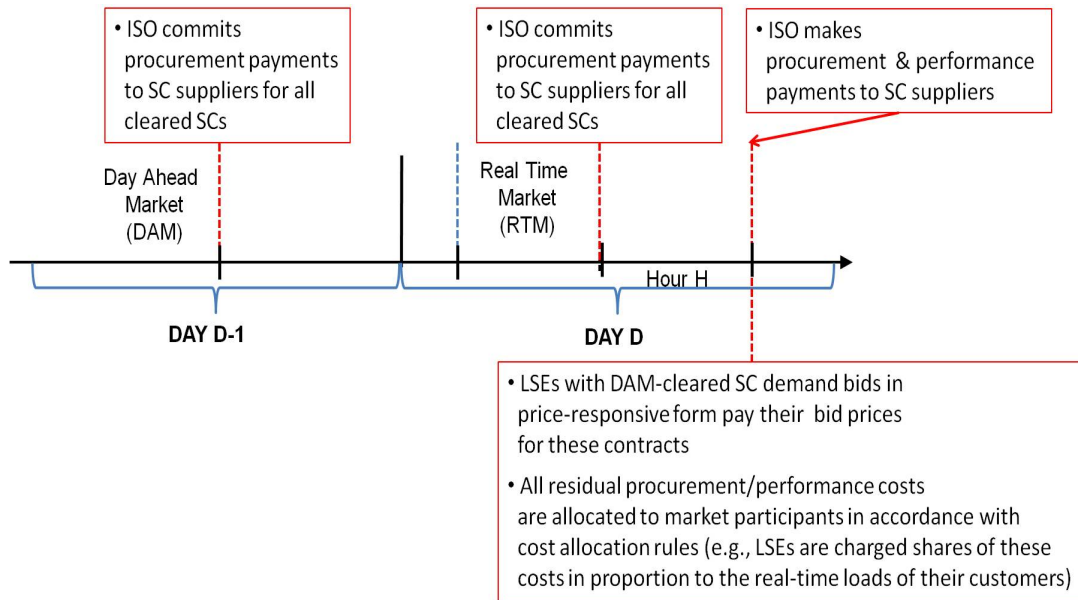
Figure 2.18: A possible time-line for hour-H settlements

---

costs are sunk (i.e., unavoidable) costs that should not affect the ISO's RTM selection of an ISOPort.

2.4.3 Contingency Reserve Considerations

Contingency reserve is spinning (synchronized) or non-spinning generation capacity that is able to reach a declared output level within a stated time interval in order to handle unusual power needs, such as the forced outage of a line or unit [30]. For resources with relatively slow ramp rates, the provision of contingency reserve through the RTM could be difficult if not impossible. In addition, regulation reserve can be efficiently substituted for contingency reserve under some market and system conditions.

Consequently, we propose that the ISO be permitted to clear an appropriate combination of SCs in the DAM to satisfy reserve requirements for both normal and contingency operating conditions, in addition to meeting load-balancing needs. As for regulation reserve, we require all of the ISO's DAM procurement costs for contingency reserve to be charged to market participants in order to preserve the ISO's non-profit status.

For resources with must-run constraints ($p^{min} > 0$) as well as UC costs (e.g., no-load and start-up/shut-down costs), we anticipate that the ISO's contingency reserve procurement would largely occur through the procurement of SCs in option form. These types of contracts provide a "no exercise" option that could be used to save UC costs in cases in which updated ISO forecasts of system conditions render some contingency reserve unnecessary as an operating point approaches.

For resources with no must-run constraints ($p^{min} = 0$), there is no operational difference for the ISO in securing contingency reserve either through an SC in firm form or through an SC in option form as long as these SCs have identical contractual terms apart from exercise option(s). This follows because the ISO can choose to implement the SC in firm form at a power level $p = 0$, thus effectively achieving the "no exercise" option of the SC in option form. However, the non-profit ISO has a fiduciary responsibility to ensure efficient operation of the power grid. Early signaling of "no exercise" decisions to the issuers of SCs in option form might permit these issuers to direct their resources to alternative uses, thus avoiding lost opportunity costs.

2.5 Discussion

2.5.1 Comparison with Real-World TSO/ISO Operations

Our ISO-managed DAM/RTM design for the support of SC trading is structurally similar to existing European and U.S. wholesale power market designs. European whole-sale power markets include "spot" (day-ahead) and intraday markets for energy and reserve managed by TSOs operating on a non-profit-making basis [32, 35]. U.S. whole-sale power markets include day-ahead and real-time imbalance markets for energy and reserve managed by non-profit ISOs [28].

Moreover, the idea of permitting resources to offer options into TSO/ISO-managed wholesale power markets is not new. For example, Moriarty and Palczewski [71] demonstrate how a small electricity storage unit could advantageously be permitted to offer American call options into a centrally-managed real-time imbalance market to facilitate load balancing.

On the other hand, our SC system differs sharply from current TSO/ISO operations in other regards. SCs with swing function as intrinsically combined energy and reserve products permitting the provision of a wide range of flexibly-provided services. Also, rewards and penalties can be included in SC performance payment methods to encourage good service performance, eg, accurate load forecasting and/or accurate following of dispatch instructions, where the rewards and penalties are assessed ex post based on actual performance. This inclusion could be required at the SC system level. Alternatively, SC suppliers could voluntarily undertake this inclusion as a way to signal the quality of their offered services to potential SC buyers.

Moreover, our SC system functions as a two-part pricing system under which all payments are compensations for value rendered, with no additional market or out-of-market adjustments required. Service availability compensation (in the form of SC offer-price payments) becomes obligatory at the commencement of service availability, ie, as

soon as SC supply offers are cleared. In contrast, service performance compensation (through SC performance payment methods) does not become obligatory until services have been performed in real time.

This two-part pricing system contrasts sharply with the Locational Marginal Pricing (LMP) systems currently implemented in U.S. ISO-managed wholesale power markets. Schweppe et al. [79] conceptualized LMPs for *true* spot markets in which there is no separation in time between payment and delivery, not for forward markets such as DAMs and RTMs. Currently, DAM LMP payment commitments are made in advance for the anticipated real-time dispatch of DAM-cleared generation, that is, in advance of value received. They must then subsequently be adjusted through RTM LMP payments to account for any deviations between DAM and RTM scheduled dispatch levels.

Moreover, DAM/RTM LMP payments do not necessarily provide adequate compensation for the costs incurred by resources to provide service availability. The perceived need to cover such costs more fully has led to the institution of capacity markets and various out-of-market uplift payments. More details about comparison between our proposed SC system and real-world ISOs are reported in Appendix A.

2.5.2 Comparison with Existing Standardized Power Contracts

The restructuring of European and U.S. electricity sectors, together with their increased reliance on VER generation, has resulted in increased price and volume risks for utilities and independent power producers as prices and net loads have become more volatile and difficult to forecast [53]. Financial and physical instruments are now heavily traded in Europe and the U.S. on exchanges and in over-the-counter markets as a means for hedging exposure to these risks [3, 25, 27, 75].

In Europe, standardized power contracts have been developed by the Agency for the Cooperation of Energy Regulators [1]. In the U.S., standardized power contracts have been developed by the Edison Electric Institute and the Western Systems Power Pool

[26, 95]. These widely used contracts are negotiated bilateral contracts between two counterparties.

Our proposed standardized contracts (SCs) differ in three important ways from ACER, EEI, and WSPP contracts. First, SCs are bids/offers for submission to an ISO-managed wholesale power market for possible clearing against other submitted offers/bids. In contrast, an ACER, EEI, or WSPP contract is a private agreement between two counterparties; it is subsequently self-scheduled in a TSO/ISO-managed wholesale power market only if fulfillment of the terms of the contract requires the use of power transmission lines.

Second, although the services provided through the contractual terms of SCs can cover the full range of product attributes included in ACER, EEI, and WSPP contracts, SC services are not rigidly separated into product types (capacity, reserve, and energy). Rather, SC services can be used to fulfill capacity requirements (general availability), reserve requirements (designated availability), and/or energy requirements (scheduled real-time dispatch) as appropriate.

Third, SCs permit swing (flexibility) in all of the services included in their contractual terms. In contrast, swing in ACER, EEI, and WSPP contracts is limited to option exercise dates in contracts taking an option form [1, 26, 95].

2.5.3 Discriminatory vs. Uniform Pricing of Contracts

A market is said to exhibit *market efficiency* if the total net surplus extracted from the market by the market participants is at a maximum. Total net surplus is measured in practice as the sum of the differences between the buyers' maximum willingness to pay and the sellers' minimum acceptable payment for each successively traded commodity unit; see Stoft [84] and Tesfatsion [85].

In order for market efficiency to hold, all valued attributes of the market-traded commodity must be properly priced and compensated at the margin. In a day-ahead energy

market organized as a bid/offer (double) auction, market efficiency can be achieved by means of a locally uniform pricing mechanism that assigns the same price to all energy units (MWh) being traded at a particular location for delivery at this location at a particular later time; see Tesfatsion [85] and Li and Tesfatsion [57]. This is because the units of the traded product, characterized by physical type (energy), delivery location, and delivery time, are homogeneous.

However, a uniform pricing mechanism applied to a traded product does not necessarily result in market efficiency if the units of this product are not homogeneous. In particular, in a market for which buyers and sellers are submitting bids and offers for differentiated products – referred to as a *monopolistically competitive market* within economics – the buyers and sellers must be permitted to bid and offer differentiated prices for units of these differentiated products in order for these prices to reflect the true value of these units to buyers and sellers at the margin, a necessary prerequisite for market efficiency.

As discussed in previous sections, the SCs traded in our proposed DAM and RTM can be highly differentiated products. First, SCs can differ in terms of the types of services they offer. Second, even if two SCs offer the same types of services, the two SCs can differ in terms of the amount of swing included in the specification of these services. Consequently, our DAM and RTM are monopolistically competitive markets. The most appropriate pricing mechanism for SCs in our DAM and RTM is thus a discriminatory pricing mechanism in which SC sellers are permitted to offer differentiated prices for the sale of their differentiated products and SC buyers are permitted to bid differentiated prices for the purchase of these differentiated products.

2.5.4 Comparison with Existing VER Initiatives

A major development in European and U.S. TSO/ISO-managed wholesale power markets is that increased VER penetration is increasing the volatility of net load (ie,

load minus as-available generation). Some TSOs/ISOs are revising their market rules and product definitions to accommodate this development.

For example, as discussed by Navid and Rosenwald [72] and Xu and Tretheway [96], MISO and CAISO have each proposed the introduction of "flexible ramping" products. Also, as discussed by Seliga et al. [80], ISO-NE has introduced a major rule change called "Energy Market Offer Flexibility." In addition, some ISOs are exploring innovative ways to incorporate VERs more fully into DAM/RTM operations. For example, MISO has introduced a new resource category called Dispatchable Intermittent Resource (DIR), designed primarily for its wind resources [64].

Our proposed SC system is not in conflict with the above market developments. To the contrary, as detailed in previous sections, SC trading would provide additional types of flexibility to both market participants and system operators that complement and extend these developments.

2.5.5 Robust-Control Management of Uncertain Net Load

A key requirement of standard two-stage stochastic SCUC formulations is the need to specify probability-weighted load scenarios with sufficient accuracy that a switch from currently-used deterministic SCUC formulations can be justified in terms of improved performance. For example, as shown in Krishnamurthy et al. [51], given a simulated "true" load distribution and an approximate set $\mathcal{S}$ of load scenarios, a deterministic SCUC formulation can result in lower energy costs than a stochastic SCUC formulation based on $\mathcal{S}$ if reserve requirements for the former are set within a "sweet spot" range of values.

The rapidly growing reliance on VERs, resulting in increased net load uncertainty and volatility, has encouraged efforts to develop improved stochastic SCUC formulations based on *net* load scenarios. See, for example, Morales et al. [69], Papavasiliou et al. [77], and Vrakopoulou et al. [90]. However, these approaches rely on having an accurate

modeling of the stochastic behavior of *net* load, a goal that has not yet been attained for as-available generation such as wind and solar power. In addition, to ensure tractability, they require the application of scenario reduction techniques capable of retaining the essential features of the net load scenarios derived from the original stochastic net load modeling.

Our proposed SC system offers an alternative robust-control approach to the management of uncertain net load. As detailed in Section 2.3, under this system the ISO considers in advance of an operating period how much swing (flexibility) will be needed in cleared SCs to cover a suitably wide corridor around an expected net load profile for this operating period. Consequently, a detailed specification of net load scenarios is not required.

2.5.6   Amelioration of Merit-Order and Missing-Money Issues

As noted in Section 2.5.4, centrally-managed wholesale power markets such as MISO are attempting to integrate VERs into the operations of their DAMs by permitting these resources to submit DAM supply offers based on generation forecasts. VERs tend to have relatively low marginal dispatch costs. Hence, increased VER participation tends to decrease the profits of thermal generators by reducing day-ahead energy prices, an outcome referred to in the power systems literature as the *merit-order effect* [82]. On the other hand, increased VER penetration requires an increase in flexibly-controllable generation to handle the resulting increased volatility of net load. Given the current state of electric energy storage development, this increase in flexibly-controllable generation must largely come from thermal generation.

The problem is then as follows. How can an adequate amount of flexibly-controllable thermal generation be ensured for matching the increased volatility of net load resulting from an increased penetration of VERs when the latter penetration reduces thermal generation profits and hence the incentive to invest in and maintain thermal generation?

This problem can be ameliorated by guaranteeing that thermal generators receive full compensation for all of the valuable services they provide, including flexibly-controllable generation. Our SC system permits this full compensation.

Specifically, under our SC system a thermal generator can offer a GenPort (ie, a portfolio of SCs) that accurately expresses the types of services it can provide as well as the degree of flexibility (swing) with which each of these types of services can be provided. The generator should offer this GenPort at a price that fully covers the costs it would incur to ensure the availability of these services, including capital and lost opportunity costs. If the GenPort is cleared, the generator receives an immediate compensation commitment for service availability equal to the GenPort's offer price. The generator also receives ex-post compensation for any real-time services performed under the terms of the GenPort, where this ex-post compensation is determined by the performance payment methods appearing in the SCs that comprise the GenPort.

Another problem arising in centrally-managed wholesale power markets is *missing money*. Cramton and Ockenfels [22] characterize this problem as follows: "In 'normal' periods, when there is no shortage of capacity, prices are below the level needed to cover operating and capital costs of new capacity, and in scarcity events, prices are unlikely to accurately reflect the scarcity."

For concreteness, our current paper focuses on the support of SC trading through relatively short-horizon DAM and RTM operations. More generally, however, SC trading could be supported by a sequence of linked forward markets that includes longer-term forward markets with planning horizons spanning a year or more. In these longer-term forward markets, the two-part pricing of SCs would permit investors to receive availability and performance payments that fully cover their capital, lost opportunity, and operating costs, thus helping to resolve the missing-money problem.

2.6   Conclusion: Energy Policy Implications

Key policy implications of our proposed market-supported trading of standardized contracts (SCs) permitting swing (flexibility) in their contractual terms are noted throughout Sections 2.1 through 2.5. These policy implications are concisely summarized below:

(i) The SC system permits separate full market-based compensation for service availability and service performance

SCs can function both as standardized instruments for the procurement of service *availability* in forward markets and as standardized blueprints for the procurement of service *performance* in real-time system operations. Thus, SC trading supports the goals of FERC Order 755 [38]; but this support is for a much broader array of services than envisioned in this order.

ii) The SC system facilitates a level playing field for market participation

The SC system focuses on service provision capability rather than on the physical characteristics of resources. This should permit and encourage the participation of a wider array of resources in wholesale power markets.

(iii) The SC system facilitates co-optimization of energy and reserve markets

SCs with swing intrinsically function as both energy and reserve products, eliminating the need to provide separate eligibility requirements and settlement processes for energy versus reserve services.

(vi) The SC system supports forward-market trading of energy and reserve

The *offer price* of an SC, determined through market processes, compensates the SC issuer for a guarantee of *service availability*. In contrast, the *performance payment method* of an SC, appearing among its contractual terms, determines how the SC issuer is to be compensated ex post for *actual services rendered* in real-time operations.

(iv) The SC system permits resources to offer flexible service availability

SCs with swing permit the *providers* of these contracts to be compensated for flexibility in offered services, such as offered exercise times, begin-times, end-times, down/up ramp rates, and down/up power levels. Moreover, the ability of one or more resources to offer services in the combined form of an SC portfolio (GenPort) can enhance the ability of resources to obtain appropriate compensation for the full value of their services.

(v) The SC system gives system operators flexibility in their real-time use of offered services

SCs with swing permit system operators who *procure* these SCs to implement the services offered in these SCs in a flexible manner during real-time operations.

(vii) The SC system encourages accurate load forecasting and the accurate following of real-time dispatch instructions

Rewards and/or penalties can be incorporated into the performance payment methods ϕ appearing among the contractual terms of SC demand bids to encourage LSEs and other wholesale intermediaries who bid for services on behalf of retail customers to submit bids that accurately reflect the service needs of these customers. Similarly, rewards and/or penalties can be incorporated into the performance payment methods ϕ appearing among the contractual terms of SC supply offers to encourage service suppliers to follow real-time service performance instructions with high accuracy.

(viii) The SC system permits resources to internally manage unit commitment and generation-capacity constraints

By offering an SC for a particular operating period, a resource is guaranteeing that it can feasibly perform the services represented in this SC during this period. For generators, this feasibility includes the assurance that power generation units with suitable capacities will be synchronized to the grid as necessary to perform these services.

(ix) The SC system permits robust-control management of uncertain net load

Under the SC system, the ISO considers in advance of an operating period how much swing (flexibility) will be needed in cleared SCs to cover a suitably wide corridor around an expected net load profile for this operating period. The SC system thus provides a robust-control alternative to standard stochastic formulations for SCUC/SCED requiring detailed specifications of net load scenarios and scenario probabilities.

(x) The SC system eliminates need for out-of-market payment adjustments

SC offer prices for service availability and SC performance payments for service performance provide full compensation for all rendered value, without need for additional market or out-of-market (OOM) adjustments.

(xi) The SC system reduces the complexity of market rules

Properties (i)-(x) reduce the complexity of power market rules, hence the opportunity for market participants to game these rules for own advantage.

51

CHAPTER 3.   AN IMPROVED METHOD FOR THE SHORT TERM FORECASTING OF ELECTRIC POWER MARKET PERFORMANCE WITH INCREASED PENETRATION OF RENEWABLE ENERGY

3.1   Introduction

Recently, several environmental and electricity market policies have been introduced in an attempt to increase the share of renewable energy in power markets. For example, the California Renewables Portfolio Standard Program requires investor-owned utilities, electric service providers, and community choice aggregators to increase procurement from eligible renewable energy resources to 33% of total procurement by 2020. The penetration of renewable energy mainly affects electric power markets in two ways. First, it increases volatility and uncertainty in a Real-Time Market (RTM) because renewable resources are non-dispatchable. When the penetration of renewable energy reaches relatively high levels, characteristics and operations of the current power system will be significantly changed and additional costs will be incurred in order to ensure sufficient resources for system reliability. Second, it decreases the market price and the dispatch level of conventional generation in a day-ahead and a real-time market. This can decrease profit of conventional generation. Thus it can change investment and operation plans of conventional generation [36]. When it comes to dealing with new coming challenges, the precise forecasting of system variables, such as *Locational Marginal Prices* (LMPs),

generation dispatch levels and power flows in transmission lines, becomes more difficult and more important for both market participants and system managers.

Several studies have focused on the forecasting of the system variables. Specifically, electricity price forecasting methods have been developed in several ways. Aggarwal et al. [2] provides an extensive review of electricity price forecasting methods. Two of the most widely used methods are stochastic time series and causal models. Examples of stochastic time series are autoregressive (AR), moving average (MA), autoregressive moving average (ARMA), autoregressive integrated moving average (ARIMA), and generalized autoregressive conditional heteroskedastic (GARCH). Examples of causal models are transfer function and ARMA with exogenous variables (ARMAX) models. Aggarwal et al. also provide extensive reviews of artificial intelligence models in electricity price forecasting, such as multilayer feed forward neural networks (FFNN), radial basis function networks (RBF), support vector machines (SVM), self-organizing maps (SOM), recurrent neural networks (RNN), and so on.

The transmission congestion forecasting methods have been developed based on time series to predict shadow prices of transmission lines [56] and also based on sequential Monte Carlo simulation [63]. Løland et al. [58] suggests semi-naive predictor comparing the statistics with several time series models for the congestion forecasting. Bo and Li [10] and Li and Bo [55] consider LMPs and congestion under load uncertainty and under load variation respectively. Most of time series and artificial intelligence forecasting models for the power system variables deal with only one type of system variable at a time. Also, these models do not consider the physical attributes of the power system that govern system variable characteristics.

On the other hand, structural simulation methods can forecast the system variables at a time and fully reflect the physical attributes of the power system, such as system operating requirements and constraints. Two structural simulation methods are mainly used: i) a market assessment and portfolio strategies (MAPS) algorithm developed by GE

Power System Consulting [5], and ii) the UPLAN software developed by LLC Consulting [23]. These simulation models require more specified input variables than statistical models, such as bidding behavior, generating unit data, transmission network data, fuel prices, demand forecasts. Also, computational costs of these method are very high.

Zhou et al. [98] proposes a new short-term forecasting algorithm for congestion, LMPs, and other power system variables based on the concept of "system patterns (SPs)" in the conventional power system. Specifically, this forecasting algorithm generates short-term forecasts for the system variables by separating the load space into convex sub-load spaces, where each sub-load space is a collection of loads that leads to the same physical status for each generation and transmission line. This method derives a linear-affine mapping between interiors of the sub-load spaces and the system variables. This method has mainly two advantages: i) it enables large-scale power system forecasts with less computational costs, and ii) it permits more accurate forecasting to be obtained through DC-OPF solutions than time series models by considering the physical constraints of the power system. The validity of the system pattern forecasting method is supported by means of an NYISO case study.

Uncertainty and volatility caused by renewable energy integration can change not only system variables but also system patterns, given conventional fixed load in the power system. Non-dispatchable renewable energy is treated as negative load in power system operations and it determines system patterns together with conventional fixed load. Thus considering penetration of non-dispatchable renewable energy in the system pattern method is necessary.

This study incorporates non-dispatchable renewable energy into the conventional system pattern method for the short-term forecasting of power markets. In addition, this study clarifies topological aspects of system pattern regions in net load space. This study also provides a linear-affine mapping between net load and CO_2 emissions that permits CO_2 emission forecasts to be derived from forecasted or actual load.

Moreover, this study introduces the concept of an empirically-based system pattern transition matrix. This matrix can be applied to broaden the scope of system pattern method applications to permit status forecasting of system variables. Also, as will be clarified below, this paper investigates how the extended system pattern method can be used to classify potential future load scenarios into a smaller number of scenarios than required by other forecasting techniques.

This paper is organized as follows. Section 5.2 provides a review of the basic system pattern method and explains how I have extended this method by incorporating non-dispatchable renewable energy and CO_2 emissions. Also, this section introduces the concept of an empirically-based system pattern transition matrix and its applicability to the status forecasting of the system variables and outlines the applicability of the extended system pattern method to classify realized loads into the corresponding system pattern. The verification and performance test and the applicability of the proposed extended method are demonstrated in Section 3.3 by means of illustrative simulations conducted for a 5-bus test system based on Midcontinent Independent System Operator (MISO) data. Concluding remarks are given in Section 4.7.

3.2   Method

3.2.1   Basic Vs. Extended System Pattern Method

As will be clarified below, distinct from the basic system pattern method, the extended system pattern method i) incorporates non-dispatchable renewable energy resources, ii) broadens the scope of the basic system pattern method to permit the short-term forecasting of CO_2 emissions as well as other system variables, iii) introduces the concept of an empirically-based system pattern transition matrix and its applicability to the short-term status forecasting of system variables, and iv) enlarges the applicability of the extended system pattern method to a load scenario reduction technique. Figure 3.1

specifically compares the extended system pattern method with the basic system pattern method.
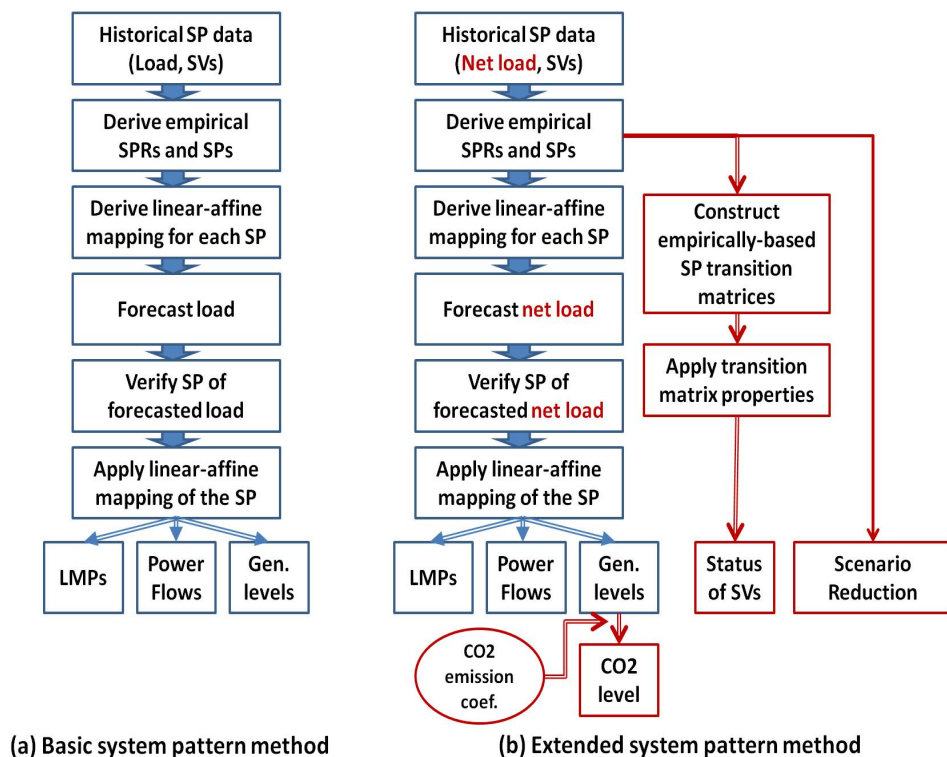
Figure 3.1: Basic vs. extended system pattern method

3.2.2 Review of Basic System Pattern Method

3.2.2.1 Standard DC-Optimal Power Flow (DC-OPF) Problem

Consider a wholesale power market system with K buses ($k \in K$), T transmission lines ($\tau \in T$) and I conventional dispatchable thermal generators ($i \in I$). Without loss of generality, assume that each bus k has load, L_k, and generation from dispatchable conventional thermal generators, P_k, for $k = 1, ..., K$. Assume that thermal generation at bus k has a quadratic total cost function with a linear coefficient, a_k, a quadratic coefficient, b_k, and no fixed costs.[1]

---

[1]Fixed costs do not affect finding optimal solutions because fixed costs drop out in the process of getting first order conditions.

Let the objective of the system operator in every time period be to minimize total cost subject to load balance, transmission line flow limits and generation capacity limits. Then the standard the standard DC Optimal Power Flow (OPF) formulation with a lossless transmission system can be constructed as follows:

$$\min_{P_k} \sum_{k=1}^{K} [a_k P_k + b_k P_k^2] \tag{3.1}$$

s.t.

$$\sum_{k=1}^{K} P_k - \sum_{k=1}^{K} L_k = 0 : \lambda \tag{3.2}$$

$$\sum_{k=1}^{K} \beta_{k\tau} [P_k - L_k] \leq F_\tau^+ : \mu_\tau^+ \qquad for \quad \tau = 1, ..., T \tag{3.3}$$

$$-\sum_{k=1}^{K} \beta_{k\tau} [P_k - L_k] \leq F_\tau^- : \mu_\tau^- \qquad for \quad \tau = 1, ..., T \tag{3.4}$$

$$P_k \leq C_k^{max} : \psi_k^{max} \qquad for \quad k = 1, ..., K \tag{3.5}$$

$$-P_k \leq C_k^{min} : \psi_k^{min} \qquad for \quad k = 1, ..., K \tag{3.6}$$

In these equations, $\beta_{k\tau}$ means the generation shift factor which measures how 1 MW injection of generation at bus k affects the transmission line τ. Equation (3.2) expresses the system balance constraint which guarantees that total generation is equal to total load. Equations (3.3) and (3.4) represent transmission line flow limit constraints in a positive and a negative direction respectively. Equations (3.5) and (3.6) denote upper and lower generation capacity limits.

3.2.2.2 Basic System Patterns and System Pattern Regions

Zhou et al. [98] introduces the idea of a system pattern which denotes structural generation capacities and transmission line conditions as "consisting of a vector of flags

indicating the marginal status of committed generation and the congestion status of available transmission lines at any given system operating point". Each transmission line is categorized as positively congested, negatively congested or not congested adopting the convention that, for each transmission line, one direction of power flow is positive and the opposite direction of power flow is negative.

Table 3.1: Flags used for system pattern

Status	Generating units			Transmission lines		
	Min capacity	Marginal unit	Max capacity	Neg Congestion	No Congestion	Pos Congestion
Flag	-1	0	1	-1	0	1

Specifically, given I conventional thermal generators and T transmission lines, the system pattern (SP) can be represented as the vector form:

$$SP = (g_1, ..., g_i, ...g_I, l_1, ..., l_\tau, ..., l_T) \tag{3.7}$$

where g_i denotes the power generation flag for generating unit i and l_τ denotes the congestion flag for transmission line τ.

Each flag has three statuses. Mathematically, the total number of system patterns is 3^{I+T}. Therefore, we expect that we may observe large numbers of system patterns in a huge power system. However, the total number of system patterns includes systematically infeasible patterns. For example, suppose that there is no generation in the power system, then transmission lines can not be congested. Moreover, only a limited number of system patterns are realized in real world power systems. For example, although the *Midcontinent Independent System Operator* (MISO) has 42,521 network buses and 60,009 generating units, at most 35 constraints were binding for each particular hour in the DAM during 2012 [65, 66].

System patterns contain the information of the system status at any given time. In addition, changes of system patterns imply changes of binding generation capacities and transmission line limit constraints in the optimization problem. Thus, some system pattern changes can drastically change values of system variables, such as LMPs, power generation levels and power flows in transmission lines.

Zhou et al. [98] applies convex polytopes to constitute load space coverings called *System Pattern Regions* (SPRs). SPRs are determined by capacity and transmission line limit constraints of the DC-OPF problem. A collection of load in the same SPR corresponds to a unique system pattern.

For example suppose a specific power system which has two buses (Bus 1, Bus 2) and one and one transmission line (TL). Each bus has one conventional thermal generator ($G1$ or $G2$) and one load ($L1$ or $L2$). $G1$ has lower marginal cost than $G2$ in generating the same amount of power. The minimum and the maximum capacities of each conventional generator are 0MW and 50MW respectively. The transmission line constraints are given by $-50MW \leq TL \leq 50MW$ and define the positive power flow when power flows from Bus 1 to Bus 2. Figure 3.2 describes this specific two-bus example.
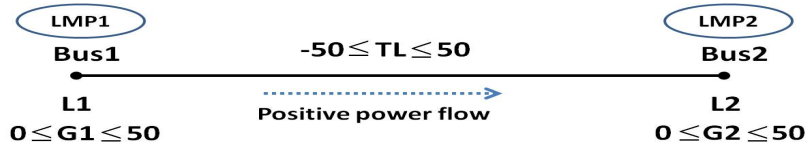
Figure 3.2: Description of two-bus example

Figure 3.3 illustrates all feasible SPRs of the specific two-bus example. Mathematically, the total number of system patterns (or equivalently SPRs) is 27 ($= 3^{2+1}$). However, only 9 system patterns are feasible among these 27 system patterns. DC-OPF solutions do not exist when collections of load are located in the "Infeasible Area" because collections of load in this area violate at least one of generating capacity or transmission line limit constraints in the DC-OPF problem. Thus, this study does not consider the

infeasible area. The probability of each system pattern realization depends on the area of its corresponding SPR in the feasible load space. SPRs can be open, closed, or neither open nor closed sets.
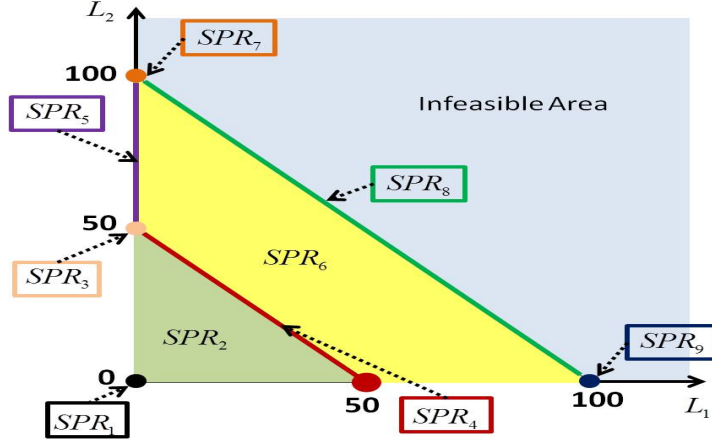
Figure 3.3: System pattern regions for the two-bus example

Also, each feasible SPR corresponds to a unique system pattern and each unique system pattern can be denoted in the vector form described in equation (3.7).

$$
\begin{aligned}
SPR_1 &\Rightarrow SP_1 = (-1, -1, 0), & SPR_2 &\Rightarrow SP_2 = (0, -1, 0) \\
SPR_3 &\Rightarrow SP_3 = (1, -1, 1), & SPR_4 &\Rightarrow SP_4 = (1, -1, 0) \\
SPR_5 &\Rightarrow SP_5 = (1, 0, 1), & SPR_6 &\Rightarrow SP_6 = (1, 0, 0) \\
SPR_7 &\Rightarrow SP_7 = (1, 1, 1), & SPR_8 &\Rightarrow SP_8 = (1, 1, 0) \\
SPR_9 &\Rightarrow SP_9 = (1, 1, -1)
\end{aligned}
\tag{3.8}
$$

3.2.2.3   Basic Linear-Affine Mapping

The system pattern method is structurally constrained by the physical conditions of power systems. The system pattern method needs to be classified and defined under the same operation plan. Thus system pattern data need to be classified for each system operation plan in practice.

For empirical applications, abundant historical data are necessary to collect sufficient samples of system patterns. Thus, to apply the system pattern method to a power system, this system needs to be mature. Therefore, hereafter, this study assumes that the power system under consideration is a mature system functioning under a normal system operation plan.

Zhou et al. [98] shows that a mapping between load and system variables can be expressed as a linear-affine function.

Proposition 1. *Suppose that a standard DC-OPF formulation with fixed load and quadratic generation cost function is used by a system operator to determine system variable solutions. Then, conditional on any given system patterns, the load space can be covered by convex polytopes such that: i) the interior of each convex polytope corresponds to a unique system pattern and ii) the system variable solutions can be expressed as a linear-affine function of the distributed load vector within the interior of each convex polytope.*

A linear-affine function between load and system variables for system pattern $j \in J$ where J is the set of system patterns can be expressed as follows:

$$SV^j = J^{SV,j} L^j + O^{SV,j} \tag{3.9}$$

where SV^j denotes a $K \times 1$ system variable vector, L^j denotes a $K \times 1$ load vector, $J^{SV,j}$ denotes a $K \times K$ sensitivity matrix and $O^{SV,j}$ denotes a $K \times 1$ ordinate vector when SV denotes the generation dispatch or LMP, or SV^j denotes a $T \times 1$ system variable vector, $J^{SV,j}$ denotes a $T \times K$ sensitivity matrix and $O^{SV,j}$ denotes a $T \times 1$ ordinate vector when SV denotes power flows in the transmission line. For ease of exposition, hereafter, this paper focuses on the case when SV denotes the generation dispatch or LMP without loss of generality.

The sensitivity matrix and ordinate vector in a linear-affine function can be estimated from historical data for each system pattern j. Suppose that the system pattern j is historically observed n_j times. Also assume that $SV^{h,j}$ denotes a $K \times n_j$ historically observed system variable matrix and $L^{h,j}$ denotes a $K \times n_j$ historically observed load matrix corresponding to the system pattern j. Then the multivariate least squares method [46] can be applied to estimate $J^{SV,j}$ and $O^{SV,j}$ as follows:

$$\left[\ \widehat{J}^{SV,j} | \widehat{O}^{SV,j} \ \right] = SV^{h,j} X'(XX')^{-1} \qquad (3.10)$$

where $\widehat{J}^{SV,j}$ is the estimate for $J^{SV,j}$, $\widehat{O}^{SV,j}$ is the estimate for $O^{SV,j}$, $X = \begin{bmatrix} L^{h,j} \\ \mathbf{1} \end{bmatrix}$, and $\mathbf{1}$ is an $1 \times n_j$ vector consisting of entirely 1s.

3.2.2.4 Forecasting Procedure for Basic System Pattern Method

By combining these estimates in equation (3.10) with the linear-affine function in equation (3.9), system variables can be forecasted for any given forecasted load as follows. First, estimate SPRs from total historically observed load data. Given any system pattern, consider a collection of sufficiently large historically observed load data. Second, partition this collection of historical load into subsets, one subset for each distinct system pattern. For each subset of load, the convex hull in the load space that covers this subset of load can be established by the QuickHull algorithm [5]. Each convex hull corresponds to a unique system pattern. Third, find the estimated SPR corresponding to the forecasted load. Any forecasted load can be associated with one of these estimated SPRs through the probabilistic point inclusion test described in Zhou et al. [98]. Third, forecast the system variables given the forecasted load by combining estimates of the sensitivity matrix and the ordinate vector corresponding to the estimated SPR for the forecasted load.

For example, the estimation of the SPR corresponding to the system pattern j, $SPR_{E,j}$, can be estimated from $L^{h,j}$ by the Quick Hull algorithm. Suppose that the forecasted load, L^f, corresponds to the $SPR_{E,j}$ as determined from a point inclusion test. Denote the forecasted load corresponding to the system pattern j as $L^{f,j}$. Finally, forecast the system variables, $SV^{f,j}$, given $L^{f,j}$, by using the estimates $\widehat{J}^{SV,j}$ and $\widehat{O}^{SV,j}$, and the following linear-affine function.

$$SV^{f,j} = \widehat{J}^{SV,j} L^{f,j} + \widehat{O}^{SV,j} \tag{3.11}$$

3.2.3 Extended System Pattern Method

3.2.3.1 Extended DC-OPF Problem

The basic DC-OPF problem can be extended by incorporating renewable energy. Similar with the basic DC-OPF case, consider a wholesale power market system with K buses ($k \in K$), T transmission lines ($\tau \in T$), I conventional thermal generators ($i \in I$) and $\mathcal{I}$ renewable power generators ($\tilde{i} \in \mathcal{I}$). Without loss of generality, assume that each bus k has load, L_k, generation from conventional thermal generators, P_k, and generation from renewable energy resources, P_k^W, for $k = 1, ..., K$. Assume that the conventional generation and the renewable energy resources have quadratic total cost functions with linear and quadratic coefficients a_k, b_k and a_k^W, b_k^W respectively.

Renewable energy has very low variable cost. Thus, this study assumes that the variable cost of renewable energy is zero, i.e., a_k^W and b_k^W are set to zero. This implies that renewable energy is cleared in most cases if total load is greater than total renewable generation and if power systems have enough available transmission capacity. In practice, most of electric power markets have total renewable energy capacity less than 20% of their total nameplate capacity. This amount is usually quite a bit lower than total load. For this reason, this study assumes that renewable energy is always cleared. In addition, renewable energy is variable and non-dispatchable. Thus non-dispatchable renewable

energy can be treated as an exogenous variable in the power system. By incorporating non-dispatchable renewable energy, the basic DC-OPF problem can be replaced by the extended DC-OPF problem as follows:

$$\min_{P_k} \sum_{k=1}^{K} [a_k P_k + b_k P_k^2] \tag{3.12}$$

s.t.

$$\sum_{k=1}^{K} P_k + \sum_{k=1}^{K} P_k^W - \sum_{k=1}^{K} L_k = 0 : \lambda \tag{3.13}$$

$$\sum_{k=1}^{K} \beta_{k\tau} [P_k + P_k^W - L_k] \leq F_{\tau}^+ : \mu_{\tau}^+ \qquad for \quad \tau = 1, ..., T \tag{3.14}$$

$$-\sum_{k=1}^{K} \beta_{k\tau} [P_k + P_k^W - L_k] \leq F_{\tau}^- : \mu_{\tau}^- \qquad for \quad \tau = 1, ..., T \tag{3.15}$$

$$P_k \leq C_k^{max} : \psi_k^{max} \qquad for \quad k = 1, ..., K \tag{3.16}$$

$$-P_k \leq -C_k^{min} : \psi_k^{min} \qquad for \quad k = 1, ..., K \tag{3.17}$$

The meaning of parameters and constraints in the extended DC-OPF problem is identical with the basic DC-OPF case. It is well known that the LMP at each bus k is equivalent to the sum of energy and congestion shadow price components.

$$LMP_k = \lambda + \sum_{\tau=1}^{T} \beta_{k\tau} \mu_{\tau}^+ + \sum_{\tau=1}^{T} \beta_{k\tau} \mu_{\tau}^- \tag{3.18}$$

In the extended DC-OPF problem, load and non-dispatchable renewable power are exogenous variables and they share same parameters at each bus. Therefore, we can define net load at bus k, L_k^{NET}, as load minus non-dispatchable renewable power at bus k and substitute it in place of $L_k - P_k^W$ in the extended DC-OPF problem. For more compactness, generation capacity and transmission constraints can be expressed as vector

forms; let $\mathbf{C}$ denote a vector of capacity limits; let $\mathbf{F}$ denote a vector of transmission limits; and let $\bar{\alpha}'$ denote a $2K \times K$ matrix consisting of -1, 1 or 0. The element of $\bar{\alpha}'$, $\alpha_{kk'}$, would be -1 or 1 when it corresponds to $-C_k^{min}$ or C_k^{max} respectively; otherwise, it would be 0. Then the previous extended DC-OPF problem can be rewritten as follows:

$$\min_{P_k} \sum_{k=1}^{K} [a_k P_k + b_k P_k^2] \tag{3.19}$$

s.t.

$$\sum_{k=1}^{K} P_k - \sum_{k=1}^{K} L_k^{NET} = 0 : \lambda \tag{3.20}$$

$$\bar{\beta}' \mathbf{P} - \bar{\beta}' \mathbf{L}^{NET} \leq \mathbf{F} : \mu \tag{3.21}$$

$$\bar{\alpha}' \mathbf{P} \leq \mathbf{C} : \psi \tag{3.22}$$

where

$$\bar{\alpha}' = \begin{bmatrix} \alpha_{11} & \alpha_{21} & \cdots & \alpha_{K1} \\ \alpha_{12} & \alpha_{22} & \cdots & \alpha_{K2} \\ \vdots & \vdots & \alpha_{kk'} & \vdots \\ \alpha_{1(2K)} & \alpha_{2(2K)} & \cdots & \alpha_{K(2K)} \end{bmatrix}$$

$$\bar{\beta}' = \begin{bmatrix} \beta_{11} & \beta_{21} & \cdots & \beta_{K1} \\ \beta_{12} & \beta_{22} & \cdots & \beta_{K2} \\ \vdots & \vdots & \beta_{k\tau} & \vdots \\ \beta_{1(2T)} & \beta_{2(2T)} & \cdots & \beta_{K(2T)} \end{bmatrix}$$

$$\mathbf{P} = [P_1, P_2, ..., P_K]'$$

$$\mathbf{L}^{NET} = [L_1^{NET}, L_2^{NET}, ..., L_K^{NET}]'$$

$$\mathbf{C} = [C_1, C_2, ..., C_{2K}]'$$

$$\mathbf{F} = [F_1, F_2, ..., F_{2T}]'$$

3.2.3.2 Extended System Patterns and System Pattern Regions

The system patterns in the basic method can be directly applied to the extended method by replacing the load space with the net load space, because SPRs are invariant under the same physical constraints of the power system. The forecasting method for short-term load has been developed in several ways by previous researchers, and is now quite accurate. However, non-dispatchable renewable energy, such as wind and solar power, is more difficult to forecast accurately because it totally depends on weather conditions which are affected by many random variables. In practice, the day-ahead load forecasting error is usually less than 3% [2], whereas the wind power forecasting error is approximately 20% [54]. Therefore, this study assumes that short-term DAM conventional load is deterministic (forecasted without error) but that short-term DAM non-dispatchable renewable energy is stochastic and hence forecasted with error. Consequently, as will be clarified below, the transition probabilities governing the system pattern corresponding to any given net load depend on the non-dispatchable renewable power generation probability density function.

Consider an extended two-bus example that is identical to the previous two-bus model depicted in Fig. 3.2 except it includes non-dispatchable wind power generators $G1_W$ and $G2_W$ at Bus 1 and Bus 2 respectively. Let each wind power generator have minimum and maximum capacities 0MW and 20MW respectively. This extended two-bus example is depicted in Fig. 3.4.

Figure 3.5 illustrates the SPRs and system pattern changes when wind power generation is incorporated into the conventional power system. For simplicity, it is assumed
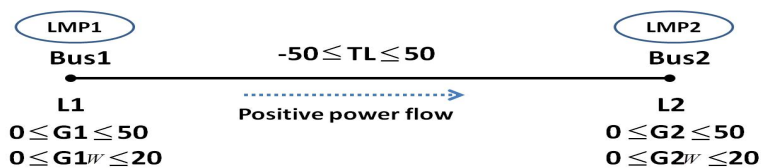
Figure 3.4: Description of extended two-bus example

that Bus 1 is geographically far away from Bus 2, so that the wind power generation at Bus 1 and Bus 2 are uncorrelated. Also, it is assumed that, with probability one, no wind blows at Bus 2 during the specific time period under consideration, and that the wind power generation at Bus 1 is governed by the wind power probability density function depicted at the bottom of Fig. 3.5. This wind power probability density function is depicted in the opposite direction to net load because non-dispatchable renewable energy is treated as negative load. Then net load decreases as wind power increases. Point A in this depicted probability density function denotes the net load when wind power is not generated at either Bus 1 or Bus 2. The point A moves toward the left as wind power generation at Bus 1 increases and the transition probabilities governing the system pattern change at point A depend on the wind power generation probability density function at Bus 1.[2]

3.2.3.3 Extended Linear-Affine Mapping

The basic linear-affine relation can be extended to incorporate non-dispatchable renewable energy by substituting net loads in place of conventional loads. Moreover, this extended linear-affine function relation can be used to map net loads into CO_2 emissions.

All generation capacities and transmission constraints for the extended DC-OPF problem depend linearly on net loads. Thus, each feasible combination of binding constraints corresponds to a unique convex polytope in the net load space. Consequently,

---

[2]The assumption that only Bus 1 has wind power generation can be easily relaxed to have wind power generation at each bus. In this case, the transition probabilities governing system pattern changes at point A depend on the joint probability density function for all wind power generation.
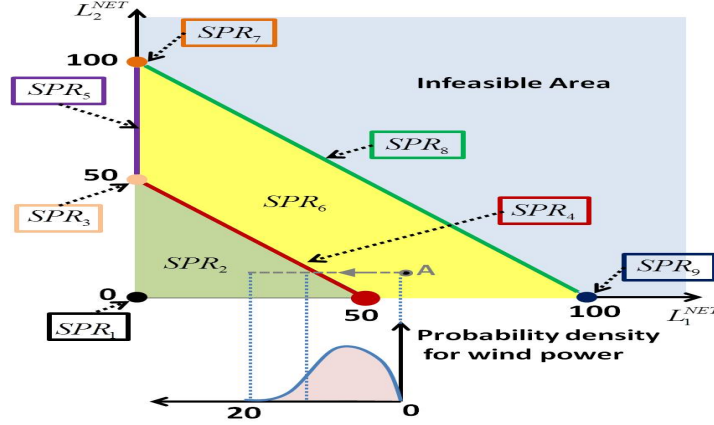
Figure 3.5: System pattern regions for the extended two-bus example

the system pattern method can be defined for the interior of the sub-load spaces. By including net load and the relationship between CO_2 emissions and net loads, **Proposition 1** in Zhou et al. [97] can be extended to the following **Proposition 2**:

Proposition 2 *Suppose that an extended DC-OPF formulation with net load and quadratic generator cost functions is used by a system operator to determine system variable solutions. Then, conditional on any given system patterns, the net load space can be covered by convex polytopes such that: i) the interior of each convex polytope corresponds to a unique system pattern and ii) the system variable solutions and CO_2 emissions can be expressed as linear-affine functions of the net load vector.*[3]

The extended linear-affine function between net load and the system variables, including CO_2 emissions, can be expressed in a form similar to the basic linear-affine function by replacing load with net load in equation (3.9), as follows:

$$SV^j = J^{SV,j} L^{NET,j} + O^{SV,j} \qquad (3.23)$$

where J is the collection of system patterns, and $L^{NET,j}$ denotes a net load vector corresponding to system pattern j, $j \in J$. Also, SV^j, $J^{SV,j}$ and $O^{SV,j}$ denote the

---

[3]***Proposition 2** is proved in Appendix B.*

system variables (including CO_2 emissions), the sensitivity matrix, and the ordinate vector corresponding to system pattern j; they have the same meanings and dimensions as in the case of the basic linear-affine function.

As for the basic system pattern case, the multivariate least squares method can be applied to equation (3.23) to obtain the estimates for $J^{SV,j}$ $(\widehat{J}^{SV,j})$ and the estimate for $O^{SV,j}$ $(\widehat{O}^{SV,j})$, as follows:

$$\left[\ \widehat{J}^{SV,j} | \widehat{O}^{SV,j'}\ \right] = SV^{h,j} X^{NET'} (X^{NET} X^{NET'})^{-1} \tag{3.24}$$

where $X^{NET} = \begin{bmatrix} L^{NET,h,j} \\ \\ \mathbf{1} \end{bmatrix}$, $L^{NET,h,j}$ denotes a $K \times n_j$ historically observed net load vector, and $\mathbf{1}$ is an $1 \times n_j$ vector consisting entirely of 1s, as for the basic system pattern method.

3.2.3.4   Forecasting Procedure for Extended System Pattern Method

The forecasting procedure for the extended system pattern method is similar to the procedure for the basic system pattern method developed in Section 3.2.2.4. By combining the estimates in equation (3.24) with the linear-affine function in equation (3.23), system variables can be forecasted for any given forecasted net load as follows. First, estimate SPRs from total historically observed net load data. Given any system pattern, consider a collection of sufficiently large historically observed net load points. Second, partition this collection of historical net load into the subsets, one subset for each distinct system pattern. For each subset of net load, the convex hull in the net load space that covers this subset of net load can be established by the QuickHull algorithm [5]. Each convex hull corresponds to a unique SPR. Third, find the estimated SPR corresponding to the forecasted net load. Any forecasted net load can be associated with one of these estimated SPRs through the probabilistic point inclusion test described in Zhou et al. [98]. Fourth, forecast the system variables given the forecasted net load by

combining estimates of the sensitivity matrix and the ordinate vector corresponding to the estimated SPR for the forecasted net load.

For example, estimation of the SPR corresponding to the system pattern j, $SPR_{E,j}$, can be estimated from $L^{NET,h,j}$ by the Quick Hull algorithm. Suppose that the forecasted net load, $L^{NET,f}$, corresponds to the $SPR_{E,j}$ as determined from a point inclusion test. Denote the forecasted net load corresponding to the system pattern j as $L^{NET,f,j}$. Finally, forecast the system variables, $SV^{f,j}$, given $L^{f,j}$, by using the estimates $\widehat{J}^{SV,j}$ and $\widehat{O}^{SV,j}$ and the following linear-affine relationship.

$$SV^{f,j} = \widehat{J}^{SV,j} L^{NET,f,j} + \widehat{O}^{SV,j} \tag{3.25}$$

3.2.4 Constructing Empirically-Based System Pattern Transition Matrix and Its Applicability

3.2.4.1 Empirically-Based System Pattern Transition Matrix Construction

From historically observed system pattern data, an empirically-based system pattern transition matrix can be constructed for each particular hour. Suppose the current time is Day D at Hour H and historically observed system pattern data since the beginning of Day $D - \mathcal{K}$ are available for constructing the empirically-based system pattern transition matrix. In addition, assume that $\mathcal{J}$ is the total number of observed system patterns from the historically observed data. Then the system pattern transition matrix from Hour H to the next Hour $H + 1$, denoted by $\Gamma_{H+1|H}$, is a $\mathcal{J} \times \mathcal{J}$ square matrix as follows:

$$\Gamma_{H+1|H} = \begin{bmatrix} \gamma_{11}^{H+1|H} & \gamma_{12}^{H+1|H} & \cdots & \gamma_{1\mathcal{J}}^{H+1|H} \\ \gamma_{21}^{H+1|H} & \gamma_{22}^{H+1|H} & \cdots & \gamma_{2\mathcal{J}}^{H+1|H} \\ \vdots & \vdots & \gamma_{jj'}^{H+1|H} & \vdots \\ \gamma_{\mathcal{J}1}^{H+1|H} & \gamma_{\mathcal{J}2}^{H+1|H} & \cdots & \gamma_{\mathcal{J}\mathcal{J}}^{H+1|H} \end{bmatrix} \tag{3.26}$$

where $\gamma_{jj'}^{H+1|H}$ denotes the sample probability of the system pattern transition from pattern j at Hour H to pattern j' at Hour $H+1$. The component $\gamma_{jj'}^{H+1|H}$ is calculated by dividing the total frequency of the historically observed system pattern transition from pattern j at Hour H to pattern j' at Hour $H+1$ by the total frequency of the historically observed system pattern j at Hour H.[4] The transition matrix has the following well-known property:

$$\Gamma_{H+2|H} = \Gamma_{H+1|H} \times \Gamma_{H+2|H+1} \,, ..., \, \Gamma_{H+\mathfrak{h}|H} = \Gamma_{H+1|H} \times \cdots \times \Gamma_{H+\mathfrak{h}|H+\mathfrak{h}-1} \tag{3.27}$$

Thus, the system pattern transition matrix from Hour H to $H+\mathfrak{h}$ can be easily calculated by means of matrix multiplications.

Net load patterns can be different by weekday and weekend, seasons, and months (or combinations of these factors). For better goodness of fit, the historically observed system pattern data can be segmented based on these factors and their combinations. The segmented empirically-based system pattern transition matrix can be constructed from the corresponding segmented data. For example, the system pattern transition matrix from Hour 12 to Hour 13 during a weekday can be constructed from the corresponding historical data. As the number of segmentations increases, however, the sample size of each specific system pattern transition matrix decreases. Thus, a sufficiently large amount of historically observed system pattern data is necessary for more segmentation.

---

[4] These numbers can be directly obtained from the historical system pattern data.

3.2.4.2 Applicability to Status Forecasting of System Variables

System patterns are derived from solutions of DC-OPF problems subject to the physical power system constraints. Therefore, historically observed system pattern data contain reduced forms of information for the power generation levels and the line congestion.

For each generating unit i, we can define sets corresponding to i) a minimum power level system pattern set, $SP^{i,-1}$, ii) a marginal power level system pattern set, $SP^{i,0}$, and iii) a maximum power level system pattern set, $SP^{i,+1}$, as follows:

$$SP^{i,-1} = \{\cup SP_j, \ j \in J : \ g_i = -1\} \tag{3.28}$$

$$SP^{i,0} = \{\cup SP_j, \ j \in J : \ g_i = 0\} \tag{3.29}$$

$$SP^{i,+1} = \{\cup SP_j, \ j \in J : \ g_i = 1\} \tag{3.30}$$

Assume that the system pattern at Hour H is j. Then, for each generator i, the sample probability of minimum capacity generation at Hour $H + \mathfrak{h}$ conditional on the given SP_j at Hour H, $Pr^{i,-1}_{H+\mathfrak{h}|H}$, the sample probability of marginal generation at Hour $H + \mathfrak{h}$ conditional on the given SP_j at Hour H, $Pr^{i,0}_{H+\mathfrak{h}|H}$, and the sample probability of maximum capacity generation at Hour $H + \mathfrak{h}$ conditional on the given SP_j at Hour H, $Pr^{i,+1}_{H+\mathfrak{h}|H}$, can be expressed as follows:

$$Pr^{i,-1}_{H+\mathfrak{h}|H} = \sum_{j' \in SP^{i,-1}} \gamma^{H+\mathfrak{h}|H}_{jj'} \tag{3.31}$$

$$Pr^{i,0}_{H+\mathfrak{h}|H} = \sum_{j' \in SP^{i,0}} \gamma^{H+\mathfrak{h}|H}_{jj'} \tag{3.32}$$

$$Pr^{i,+1}_{H+\mathfrak{h}|H} = \sum_{j' \in SP^{i,+1}} \gamma^{H+\mathfrak{h}|H}_{jj'} \tag{3.33}$$

The status of each transmission line can also be forecasted from this matrix. For each transmission line $\tau \in T$, we can define sets by congestion status: i) a negative congestion system pattern set, $SP^{\tau,-1}$, ii) a non-congestion system pattern set, $SP^{\tau,0}$, and iii) a positive congestion system pattern set, $SP^{\tau,+1}$. These sets are defined as follows:

$$SP^{\tau,-1} = \{\cup SP_j, \ j \in J: \ l_\tau = -1\} \tag{3.34}$$

$$SP^{\tau,0} = \{\cup SP_j, \ j \in J: \ l_\tau = 0\} \tag{3.35}$$

$$SP^{\tau,+1} = \{\cup SP_j, \ j \in J: \ l_\tau = +1\} \tag{3.36}$$

Then the sample probability of negative congestion at Hour $H + \mathfrak{h}$ conditional on the given SP_j at Hour H, $Pr^{\tau,-1}_{H+\mathfrak{h}|H}$, the sample probability of no congestion at Hour $H + \mathfrak{h}$ conditional on the given SP_j at Hour H, $Pr^{\tau,0}_{H+\mathfrak{h}|H}$, and the sample probability of positive congestion at Hour $H + \mathfrak{h}$ conditional on the given SP_j at Hour H, $Pr^{\tau,+1}_{H+\mathfrak{h}|H}$, can be denoted as follows:

$$Pr^{\tau,-1}_{H+\mathfrak{h}|H} = \sum_{j' \in SP^{\tau,-1}} \gamma^{H+\mathfrak{h}|H}_{jj'} \tag{3.37}$$

$$Pr^{\tau,0}_{H+\mathfrak{h}|H} = \sum_{j' \in SP^{\tau,0}} \gamma^{H+\mathfrak{h}|H}_{jj'} \tag{3.38}$$

$$Pr^{\tau,+1}_{H+\mathfrak{h}|H} = \sum_{j' \in SP^{\tau,+1}} \gamma^{H+\mathfrak{h}|H}_{jj'} \tag{3.39}$$

Thus this approach can forecast the status of the system variables by means of the corresponding calculated probabilities although it cannot provide the specific forecasting values of the system variables.

3.2.5 Applicability of Extended System Pattern Method to Load Scenario Reduction

Centrally-managed wholesale power markets in the U.S. are structured as forward markets in advance of real-time operations. To make informed decisions in the forward markets for electric energy and reserve, market managers would ideally like to be able to forecast system variables under the set of all possible load scenarios [70]. However, the set of all possible load scenarios is too large to consider in practice. To reduce computational

complexities and time requirements, forecasting models with large number of scenarios are often approximated by models with relatively small number of scenarios [44].

The system pattern method can be applied to load scenario reduction processes in two ways. First, it can reduce all net load variations into a limited number of scenarios. As pointed out in Section 3.2.2, although the total number of system patterns in a huge power system is expected to be a large number, the total number of feasible system patterns would be less than the total number of system patterns and the total number of historically observed system patterns would be even less than the total number of feasible system patterns. Thus, the historically observed system patterns can be small enough to handle in practice, even in a huge power system.

Second, the system pattern method can provide reasonable criteria for the classification of load scenarios. Each SPR corresponds to a unique combination of binding constraints in the power system. Any severe net load volatility cannot affect power system constraints, such as the status of the generating units and the transmission line congestion, if the load fluctuations are bounded within the same SPR. Thus any net load volatility within the same SPR is manageable under the same operating condition (or binding constraints). Under this circumstance, we can conjecture that the LMP volatility is relatively lower when the net load fluctuates within the same system pattern, while the LMP volatility is relatively higher when the net load fluctuates across the system patterns, because LMPs are piecewise linear functions of net load, hence bigger net load fluctuations will typically result in bigger LMP deviations.

3.3   Illustrative Simulations

To test the verification and the performance of the extended system pattern method and its applicability described in Section 3.2.3 - Section 3.2.5, historical data for operating plans, system variables, loads, and wind power generation are required. In practice,

74

however, the full empirical data set for electric power market data is not publicly available.[5] Thus, instead of empirical market data for the system variables, this study use simulation data (or simulation outcomes) obtained via a specific electric power market test system given load to demonstrate the validity and the performance of extended system pattern method and its applicability for the status forecasting of the system variables and a scenario reduction method.

Specifically, this study constructs a 5-bus test system based on the AMES wholesale power market test bed [4] reflecting the physical attributes of MISO. Also, historical net load data from MISO during July 2013 are used as input data. Given these input data, simulation outcomes for the system variables during this period are obtained by running simulation via the 5-bus test system. These net load and simulation outcomes for the system variables during July 2013 are used as data sets for estimating SPRs, estimating the sensitivity matrices and the ordinate vectors corresponding to the estimated system patterns, and constructing the empirically-based system pattern transition matrices.

These estimates are used to forecast the system variables given forecasted net load data following the procedures described in Section 3.2.3.4. To test the verification of the extended system pattern method, this study compares forecasted system variables obtained via the extended system pattern method with simulated system variables obtained via the simulation outcomes given forecasted net load profile.

Also, the 5-bus test system is used to analyze the effects of wind power penetration on the system pattern frequencies in the DAM and the effects of wind power uncertainty on the system patterns and the system variables given fixed load in the DAM. These effects are demonstrated by comparing the simulation outcomes obtained via the 5-bus test system with wind power penetration with the simulation outcomes obtained via the 5-bus test system without wind power penetration.

---

[5]Specific data for operating plan, generating units' capacities and power generation levels, power flows in transmission lines, and demand are not publicly available.

In addition, this study constructs the empirically-based system pattern matrices from simulation outcomes during July 2013. To demonstrate the applicability of these matrices in the status forecasting of the system variables, this study compares the forecasted system pattern obtained via these matrices with the simulated system pattern obtained via the 5-bus test system for a specific time period.

Finally, this study demonstrates the applicability of the extended system pattern method to the scenario reduction method based on the total number of realized system patterns during July 2013. Following subsections provide more details for the illustrative simulations. Figure 3.6 describes these simulation and demonstration procedures.
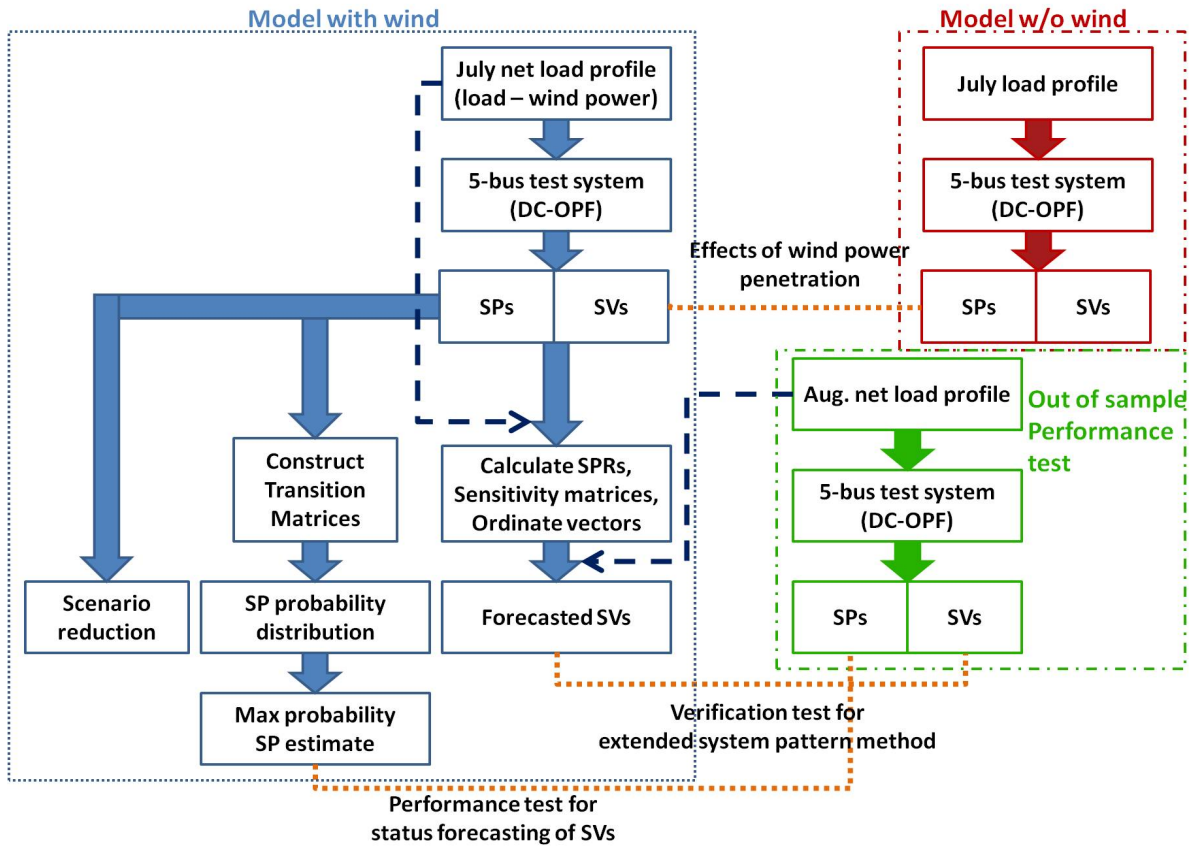
Figure 3.6: Verification and performance test procedure

3.3.1   5-Bus Test System

The 5-bus test system consists of five generation units (G1-G5), six transmission lines (TL1-TL6), three Load Serving Entities (LSE1-LSE3) and wind power generation embedded as negative load at Bus 2, Bus 3 and Bus 4 respectively. Power flows in a transmission line are represented by positive values if power flows from a smaller numbered bus to a larger numbered bus, otherwise negative. For example, the power flow in TL1 is represented by a positive value if the power flows from Bus 1 to Bus 2 and as a negative value otherwise. This test system assumes that the day-ahead market (DAM) is a market for energy only, ignoring reserve considerations, and that all generating units are committed for every hour. This 5-bus test system is depicted in Fig. 3.7
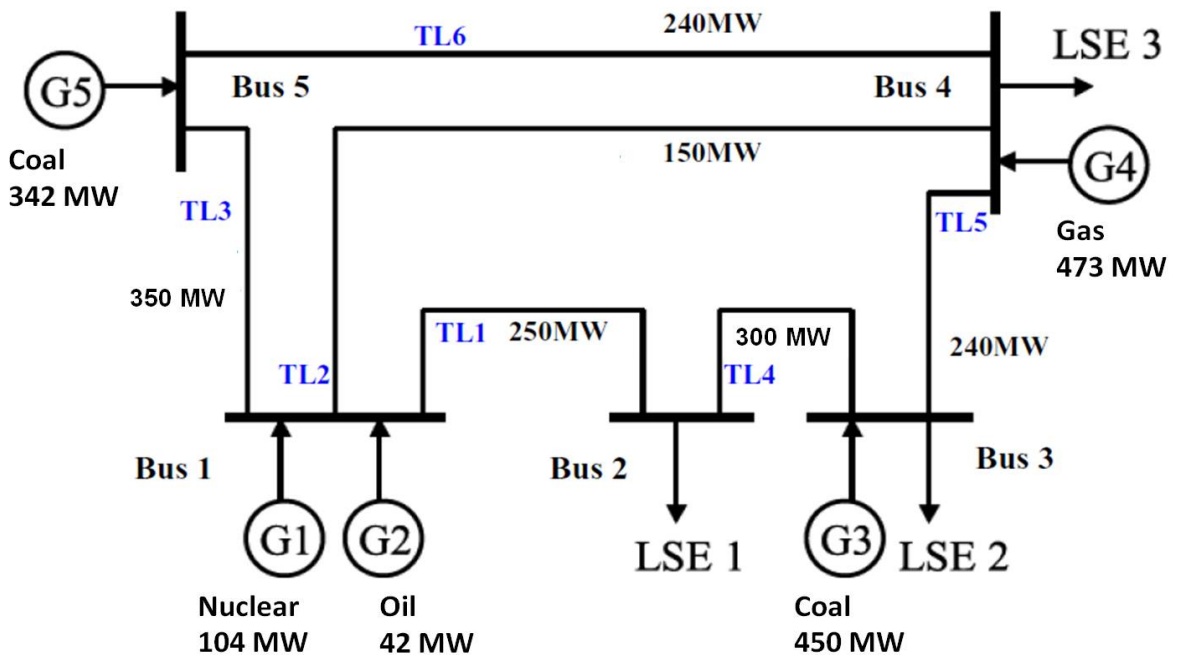
Figure 3.7: 5-bus test system

3.3.1.1   Generating Unit Attributes

To determine the characteristics of the generating units, capacity by fuel type is assigned based on the 2013 Midwest Independent System Operator (MISO) data [68] in this test system. The MISO region can be divided into two sub-regions: the MISO Midwest region and the MISO South region. The MISO South region was integrated into the pre-existing MISO Midwest region on December 9th, 2013. Thus this study only focuses on the MISO Midwest region.

The fuel type of generation in the MISO Midwest region includes nuclear, coal, natural gas, oil, hydro, pumped storage, biomass, and wind. The 2013 MISO Midwest capacity by fuel type is reported in Table 3.2. For simplicity, this study focuses only on the thermal generating units (nuclear, coal, natural gas, oil) and on wind power, the largest renewable energy resource in the MISO Midest region.

Table 3.2: 2013 MISO generation capacity by fuel type

Fuel type	Capacity (MW)
Nuclear	8,309
Coal	63,369
Gas	37,876
Oil	3,372
Hydro	1,103
Pumped Storage	2,490
Biomass	752
Wind	12,069

As depicted in the extended DC-OPF problem in Section 3.2.3.1, each generating unit has a quadratic cost function. The dispatch cost coefficients of a generation unit depend

on its fuel type. Cost coefficients by fuel type can be estimated from data provided by the U.S. Environmental Protection Agency (EPA) [34]. Specifically, Table 4.5 reports these estimated coefficients from Krishnamurthy et al. [51].

Table 3.3: Dispatch cost coefficients by fuel type

Fuel	a ($/MW)	b ($/MW^2)
Nuclear	15	0.003
Coal	15	0.008
Gas	75	0.020
Oil	35	0.016

To calculate CO_2 emissions from thermal generation, this study uses CO_2 emission coefficients by fuel type processed from EIA data.[6] CO_2 emissions from nuclear and wind power generation are negligible. Thus this study assumes that no CO_2 is emitted from nuclear and wind power generation. CO_2 emission coefficients by fuel type are reported as CO_2 tonnage per megawatt hour (tCO_2/MWh) in Table 5.1

Table 3.4: Average CO_2 emissions by fuel type (tCO_2/MWh)

Fuel Type	tCO_2/MWh
Nuclear	0.0000
Coal	0.9716
Gas	0.5539
Oil	0.7922

---

[6] http://www.eia.gov/tools/faqs/faq.cfm?id=74&t=11

For simplicity, the 5-bus test system uses scaled-down MISO Midwest generating capacity and wind power data that are determined by dividing the data by 80 without loss of generality. Thermal generating units are assumed to be assigned as depicted in Table 3.5. By considering practical capacity limits of gas generating units, this study assumes that G4 consists of four identical gas power plants.

Table 3.5: Capacity by fuel type in the 5-bus test system

	Fuel Type	Capacity (MW)
G1	Nuclear	104
G2	Oil	42
G3	Coal	450
G4	Gas	473
G5	Coal	342

The MISO Midwest region has three sub-regions: namely, the West, Central, and East sub-regions. These three sub-regions correspond to Bus 2, Bus 3, and Bus 4 in the 5-bus test system as depicted in Fig. 4.4.
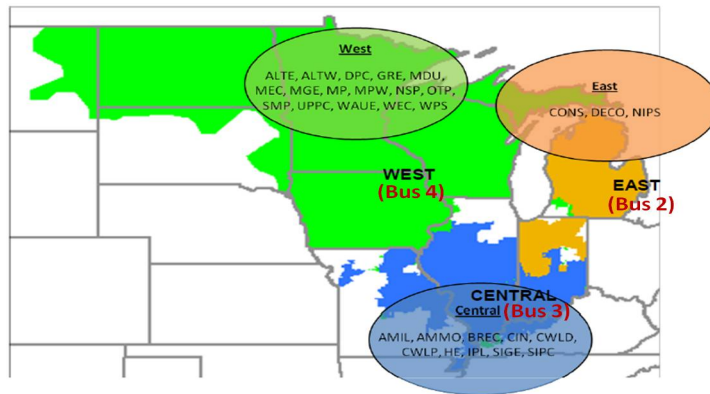
Figure 3.8: 2013 MISO sub-region

Wind power generation is distributed on Bus 2, Bus 3, and Bus 4 based on the proportion of wind power generation capacities across the MISO Midwest sub-regions. Figure 3.9 reports these proportions by sub-region.
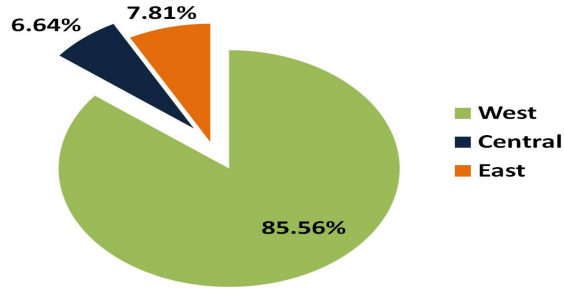
Figure 3.9: Wind power capacity proportion by Miwdwest sub-region

3.3.1.2 LSE Attributes

Bus 2, Bus 3 and Bus 5 each have a single representative aggregated LSE in this 5-bus test system. An LSE has an intermediary responsibility between generating units and retail customers in electric wholesale power markets. An LSE procures necessary energy for retail customers by submitting demand bids into the DAM on each day D-1. Based on the LSE's regional next-day load forecasting for operating day D, the LSE submits a demand bid into the DAM in the form of a 24-hour regional load profile for day D. For simplicity, it is assumed that this load profile is not responsive to price. Historical exogenous loads for the three MISO Midwest sub-regions are obtained from MISO [68].

3.3.1.3 Data

Load and wind generation, i.e. net load, data are necessary to conduct simulations based on the 5-bus test system. Operating plan analysis during the daily peak demand hour is critical for system operations. Thus this study focuses on the hourly load and wind power generation data in the DAM during the 2013 MISO Midwest peak month (July), which consists of 744 hours. These data can be obtained from the MISO homepage [68].

Data for system variables such as LMPs, power generation levels, and congestion in transmission lines can be obtained via the 5-bus test system by conducting simulations using the MISO net load data as input data. Through these procedures, we can obtain data for the system variables during July 2013.

Net loads and simulation outcomes for the system variables corresponding to net loads during July 2013 are used to test the verification and the performance of the extended system pattern method and its applicability described in Section 3.2.3 - Section 3.2.5.

3.3.2 Illustration 1: Testing Verification of Extended System Pattern Method

The sensitivity matrix and the ordinate vector for the system variables can be estimated using the simulation outcomes during July 2013 by following the processes described in Section 3.2.3.3 for all system patterns. For example, the estimated sensitivity matrix and the estimated ordinate vector of the system variables including CO_2 emissions for system pattern 7 (SP_7) are reported in (3.40) - (3.43).

$$
\left[\; \widehat{J}^{P,7} | \widehat{O}^{P,7'} \; \right] =
\begin{bmatrix}
0.00 & 0.00 & 0.00 & 104.00 \\
-2.45 & -1.80 & 0.00 & 1713.71 \\
0.00 & 0.00 & 0.00 & 450.00 \\
3.45 & 2.80 & 1.00 & -2610.56 \\
0.00 & 0.00 & 0.00 & 342.00
\end{bmatrix}
\tag{3.40}
$$

$$
\left[\; \widehat{J}^{TL,7} | \widehat{O}^{TL,7'} \; \right] =
\begin{bmatrix}
0.00 & 0.00 & 0.00 & 250.00 \\
-1.33 & -0.98 & 0.00 & 1003.59 \\
-1.12 & -0.82 & 0.00 & 563.98 \\
-1.00 & 0.00 & 0.00 & 250.04 \\
-1.00 & -1.00 & 0.00 & 700.10 \\
1.12 & 0.82 & 0.00 & -905.98
\end{bmatrix}
\tag{3.41}
$$

$$
\left[\ \widehat{J}^{LMP,7} \middle| \widehat{O}^{LMP,7'}\ \right] =
\begin{bmatrix}
-0.01 & -0.01 & 0.00 & 40.48 \\
0.14 & 0.11 & 0.03 & 69.54 \\
0.11 & 0.09 & 0.03 & 64.03 \\
0.03 & 0.03 & 0.01 & 48.89 \\
0.00 & 0.00 & 0.00 & 41.97
\end{bmatrix}
\tag{3.42}
$$

$$
\left[\ \widehat{J}^{CO_2,7} \middle| \widehat{O}^{CO_2,7'}\ \right] =
\begin{bmatrix}
0.00 & 0.00 & 0.00 & 0.00 \\
-1.94 & -1.43 & 0.00 & 1357.60 \\
0.00 & 0.00 & 0.00 & 437.22 \\
1.91 & 1.55 & 0.55 & -1445.99 \\
0.00 & 0.00 & 0.00 & 332.29
\end{bmatrix}
\tag{3.43}
$$

where $\widehat{J}^{P,7}, \widehat{O}^{P,7'}$, $\widehat{J}^{TL,7}, \widehat{O}^{TL,7'}$, $\widehat{J}^{LMP,7}, \widehat{O}^{LMP,7'}$, and $\widehat{J}^{CO_2,7}, \widehat{O}^{CO_2,7'}$ are the estimated sensitivity matrices and the transpose of estimated ordinate vectors for power generation, power flows, LMPs, and CO_2 emissions respectively. The estimated sensitivity matrices and the estimated ordinate vectors are used to forecast the system variables given forecasted load profile. The forecasting procedures of the system variables using these matrices and ordinate vectors are described in Section 3.2.3.4.

To test the verification for the extended system pattern method, this study compares the forecasted system variables to the simulated system variables given forecasted load profile. For example, Figure 3.10 provides the forecasted system variables obtained via the extended system pattern method and the simulated system variables obtained via the 5-bus test system given the MISO Midwest region net load profile on August 30th, 2013. The forecasted SVs are very similar to the simulated SVs. Thus the extended system pattern method contains full information of the extended DC-OPF on the relations between SVs and net load.
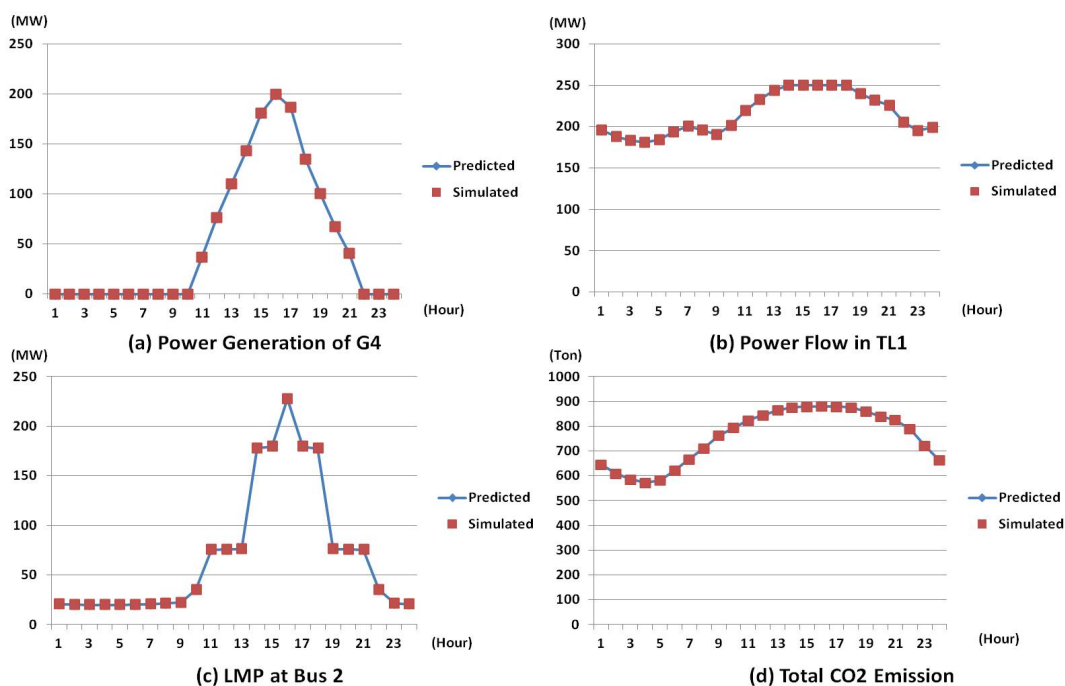
Figure 3.10: Forecasted vs. simulated values of system variables

3.3.3   Illustration 2: Wind Power Penetration Effects on System Patterns

3.3.3.1   Effects of Wind Power Penetration on System Pattern Frequencies in the Day-Ahead Market

The simulation outcomes during July 2013 show that there are seven system patterns (SP_1-SP_7) with/without wind power penetration. Thus the total number of system patterns in the DAM is not changed with/without wind power penetration in these illustrative simulations. Flags for these seven system patterns are depicted in Table 3.6.

Table 3.6: System patterns from simulation outcomes

	G1	G2	G3	G4	G5	TL1	TL2	TL3	TL4	TL5	TL6
SP_1	1	-1	0	-1	0	0	0	0	0	0	0
SP_2	1	-1	0	-1	1	0	0	0	0	0	0
SP_3	1	0	1	-1	1	0	0	0	0	0	0
SP_4	1	1	1	0	1	0	0	0	0	0	0
SP_5	-1	-1	1	0	0	1	0	0	0	0	0
SP_6	0	-1	1	0	1	1	0	0	0	0	0
SP_7	1	0	1	0	1	1	0	0	0	0	0

Wind power penetration can affect the frequencies of system pattern occurrences in the DAM. To analyze these effects, this study compares the DAM system pattern frequencies without wind power penetration (f^{WO}) to the DAM system pattern frequencies with wind power penetration (f^W).

Although the simulation outcomes show that there is no change for the type of realized system patterns in each case during July 2013, the simulation outcomes show that the system pattern frequencies with wind power penetration differ from the system pattern frequencies without wind power penetration during July 2013. When wind penetration is introduced, the frequencies of SP_1 and SP_7 are increased, the frequencies of SP_2, SP_3, SP_4, and SP_5 are decreased, and the frequency of SP_6 is not changed. Thus the penetration of wind power can induce system pattern changes in electricity markets. The specific system pattern frequencies obtained both with and without wind power penetration during July 2013 are reported in Table 3.7.

Table 3.7: Frequency of system patterns with/without wind power penetration

	SP_1	SP_2	SP_3	SP_4	SP_5	SP_6	SP_7	Total
f^{WO}	369	208	41	81	11	25	9	744
f^{W}	438	168	26	69	8	25	10	744

3.3.3.2   Effects of Wind Power Uncertainty on System Patterns

Renewable energy is basically non-dispatchable. Thus, day-ahead wind power fore-casts typically differ from actual real-time wind power generation. This uncertainty can be estimated via a kernel probability density estimation for wind power generation [50]. For example, Figure 3.11 depicts the kernel probability density function (PDF) for wind power generation at Bus 4 estimated from hourly MISO West sub-region wind power generation data during July 2013.
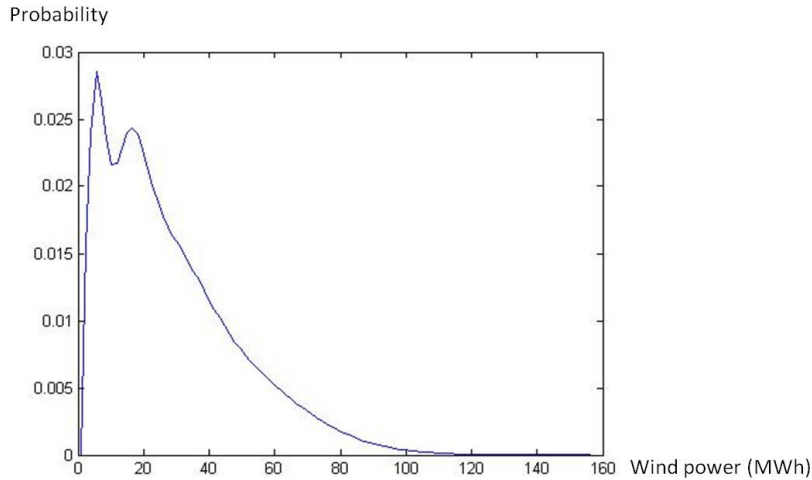
Figure 3.11: Kernel PDF for wind power generation at Bus 4 during July 2013

To test the possibility of system pattern changes caused by wind power uncertainty for a specific Hour H, given fixed load, this section focuses on the load at Hour 13 on

July 23rd, 2013, which is the peak load hour that occurred during 2013. In addition, this section focuses on the wind power at Bus 4, which is the bus with the largest capacity proportion of wind power generation in the 5-bus test system.[7] The system pattern at Hour 13 on July 23rd, 2013, is given as SP_4.

For sensitivity studies, 1,000 wind power generation samples are drawn from this kernel PDF. Each sample, together with the given fixed load data for hour H, is then used to solve the resulting extended DC OPF problem.

The resulting simulation outcomes show that the system pattern at Hour 13 does not change with probability 0.339, while it changes from SP_4 to SP_2 with probability 0.087 and changes from SP_4 to SP_3 with probability 0.574. Thus, wind power uncertainty can change system patterns given fixed load.
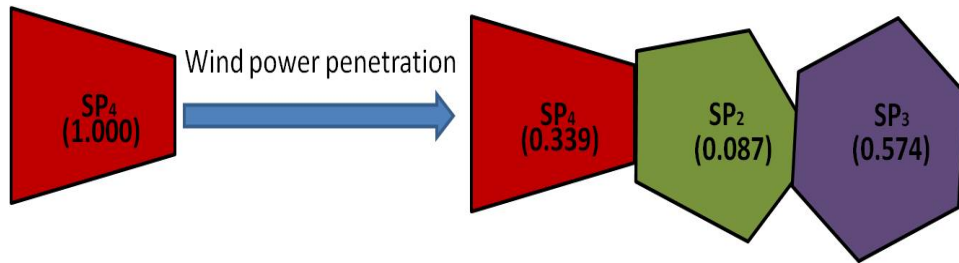
Figure 3.12: Example of system pattern changes under wind power unceratinty

These system pattern changes can cause significant changes for the system variables. For example, Figure 3.13 depicts LMPs at Bus 1 in results of 1,000 simulation runs. In this figure, the upper dots labeled as SP_4, the middle dots labeled as SP_3, and the lower dots labeled as SP_2 describe LMPs when each sample of net load belongs to SP_4, SP_3, and SP_2 respectively. As we can see, LMPs are slightly changed within the same system pattern while LMPs are significantly changed across the system patterns.

---

[7] For simplicity, the wind power generation at Bus 2 and Bus 3 are assumed to be zero during Hour 13 for this illustrative case.
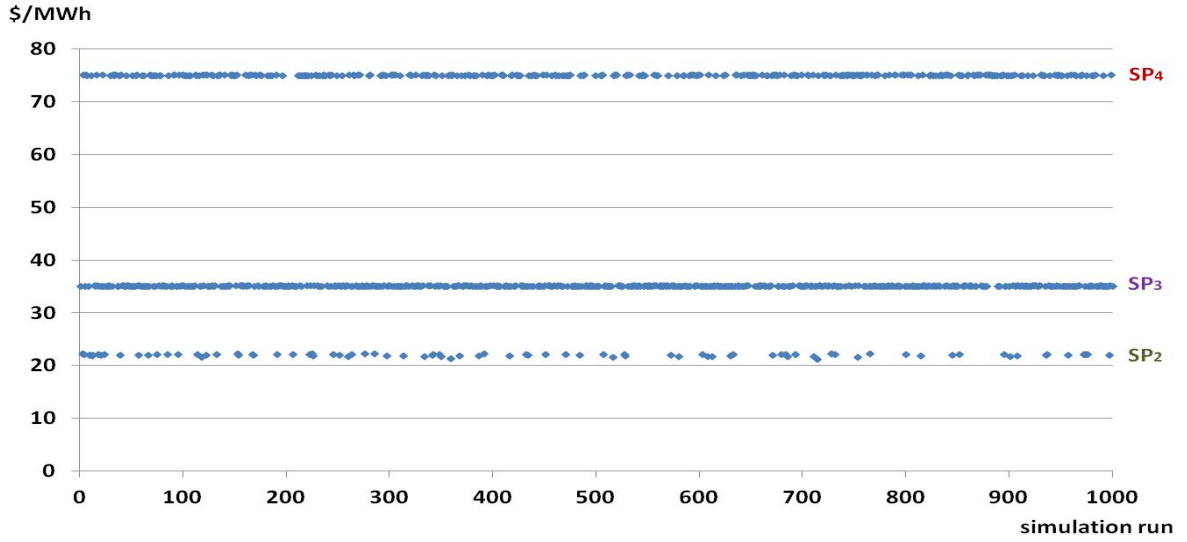
Figure 3.13: Simulation outcome for LMP at Bus 1 under wind power uncertainty

3.3.4 Illustration 3: Applicability of Empirically-Based System Pattern Transition Matrix to Status forecasting of System Variables

The derivation of empirically-based system pattern transition matrices is explained in Section 3.2.4.1. Equations (3.44) and (3.45) depict the empirically-based system pattern transition matrices from Hour 18 to Hour 19 and from Hour 19 to Hour 20 calculated from the simulation outcomes during July 2013 via the 5-bus test system.

$$\Gamma^{19|18} = \begin{bmatrix} 1 & 0 & 0 & 0 & 0 & 0 & 0 \\ 0.15 & 0.85 & 0 & 0 & 0 & 0 & 0 \\ 0 & 0 & 1 & 0 & 0 & 0 & 0 \\ 0 & 0 & 0.2 & 0.8 & 0 & 0 & 0 \\ 0 & 0 & 0 & 0 & 0 & 0 & 0 \\ 0 & 0 & 0 & 0 & 0 & 0.6 & 0.4 \\ 0 & 0 & 0 & 0 & 0 & 0 & 0 \end{bmatrix} \tag{3.44}$$

$$\Gamma^{20|19} = \begin{bmatrix} 1 & 0 & 0 & 0 & 0 & 0 & 0 \\ 0.27 & 0.73 & 0 & 0 & 0 & 0 & 0 \\ 0 & 1 & 0 & 0 & 0 & 0 & 0 \\ 0 & 0 & 0.5 & 0.5 & 0 & 0 & 0 \\ 0 & 0 & 0 & 0 & 0 & 0 & 0 \\ 0 & 0 & 0 & 0 & 0 & 0 & 1 \\ 0 & 0 & 0 & 0 & 0 & 0 & 0 \end{bmatrix} \tag{3.45}$$

These transition matrices can be used to forecast the system patterns (or status of system variables) by following equations (3.26) and (3.27) in Section 3.2.4.1 and by taking maximum probability system pattern estimate. To demonstrate the applicability of these transition matrices in system pattern forecasts, this section compares forecasted system pattern obtained via these matrices with simulated system pattern obtained via the 5-bus test system for Hour 19 and Hour 20 on August 1st conditional on given system pattern at Hour 18.

The simulation outcomes report that the system pattern given the net load at Hour 18 on August 1st is SP_2. Conditional on SP_2 at Hour 18, the probability for the occurrence of SP_1 at Hour 19 on August 1st is 0.15 ($= \gamma_{2,1}^{19|18}$) and the probability for the occurrence of SP_2 at Hour 19 on August 1st is 0.85 ($= \gamma_{2,2}^{19|18}$) obtained from equation (3.44). Thus, by taking maximum probability system pattern estimate, we can predict that the system pattern at Hour 19 would be SP_2 conditional on SP_2 at Hour 18.

Also, by multiplying these two matrices (3.44) and (3.45), we can calculate the empirically-based system pattern transition matrix from Hour 18 to Hour 20 (3.46).

$$\Gamma^{20|18} = \begin{bmatrix} 1 & 0 & 0 & 0 & 0 & 0 & 0 \\ 0.38 & 0.62 & 0 & 0 & 0 & 0 & 0 \\ 0 & 0 & 1 & 0 & 0 & 0 & 0 \\ 0 & 0 & 0.2 & 0.4 & 0.4 & 0 & 0 \\ 0 & 0 & 0 & 0 & 0 & 0 & 0 \\ 0 & 0 & 0 & 0 & 0 & 0 & 1 \\ 0 & 0 & 0 & 0 & 0 & 0 & 0 \end{bmatrix} \tag{3.46}$$

Equation (3.46) reports that, conditional on SP_2 at Hour 18 on August 1st, the probability for the occurrence of SP_1 at Hour 20 on August 1st is 0.38 $(= \gamma_{2,1}^{20|18})$ and the probability for the occurrence of SP_2 at Hour 20 on August 1st is 0.62 $(= \gamma_{2,2}^{20|18})$. Thus, by taking maximum probability system pattern estimate, we can forecast that the system pattern at Hour 20 would be SP_2 conditional on SP_2 at Hour 18.

The simulation outcomes report that system patterns at Hour 19 and Hour 20 on August 1st are both SP_2. Thus the predictions for the system patterns using these transition matrices show the same system patterns with simulation outcomes at Hour 19 and Hour 20 on August 1st as depicted in Table 3.8.

Table 3.8: Illustration of system pattern prediction via transition matrices

	Probability of SP_1	Probability of SP_2	Forecasted SP	Simulated SP
Hour 19	0.15	0.85	SP_2	SP_2
Hour 20	0.38	0.62	SP_2	SP_2

Under SP_2, we can predict that G1 generates its full capacity level, G2 and G5 do not generate, G3 and G5 generate less than their capacity levels, and there is no transmission congestion in the power system.

3.3.5 Illustration 4: Applicability of Extended System Pattern Method to Load Scenario Reduction

The total number of possible system patterns for the 5-bus test system is 177,147 ($= 3^{5+6}$). However, as we can see from Table 3.7 in Section 3.3.3.1, only seven system patterns are actually observed in the simulation outcomes during July 2013.

The variation in system variable predictions within any one SPR can be bounded as a function of the size of the SPR, and the average system variable outcomes for any one SPR might exhibit a small enough standard deviation that the deviations can be ignored. In this case, without much loss of predictive power for system variables, each SPR can be associated with a single net load, taken to be the average net load within the SPR; and the system variable predictions associated with this average net load can be taken to be the system variable prediction for this single net load. Consequently, the number of net load scenarios can be reduced to only seven scenarios (namely, the average net loads for the seven SPRs). Thus, the system operator can mainly focus on the seven system patterns for operation plans. Moreover, as we can see from Fig. 3.13 in Section 3.3.3.2, the price volatility is relatively low within the same system pattern, while it is relatively high across system patterns.

Form these illustrations, we can consider the system pattern method as a scenario reduction techniques because the method can provide the limited number of scenarios that can be small enough to handle in practice. Also, the system pattern method can provide reasonable criteria for the classification of load scenarios; i) each system pattern corresponds to a unique combination of binding constraints in the power system; and ii) the LMP volatility is relatively lower when the net load fluctuates within the same system pattern, while the LMP volatility is relatively higher when the net load fluctuates across the system patterns.

3.4   Conclusion

Several electric power markets all around the world have increased and will increase the penetration of renewable energy. Electricity markets become more volatile and uncertain as the penetration of renewable energy resources increases. This can incur additional operating costs and more frequent contingent events. Under this circumstance, the accurate forecasting of system variables becomes more difficult and more important for both market participants and system operators.

This study extends the basic system pattern method developed by Zhou et al. [97, 98] for short-term forecasting in electricity markets with conventional generation to include generation by renewable resources. Although the current system pattern method does not consider the penetration of non-dispatchable renewable energy resources, it can be applied directly to the power system with non-disaptchable renewable energy resources by substituting net load in place of conventional load. Moreover, this study derives a linear-affine mapping between net load and CO_2 emissions that permits CO_2 emission forecasting. Thus, this extended system pattern method can be used to jointly derive forecasts of CO_2 emissions as well as a wide range of system variables, including LMPs, generation dispatch levels, and transmission line power flows.

This paper demonstrates that the penetration of renewable energy resources can change the realization of system patterns. Also, uncertainties embedded in the non-dispatchable renewable energy can change the system pattern given fixed load. The transition probabilities governing the system pattern changes depend on the probability density function of the non-dispatchable renewable power generation.

This study introduces the concept of empirically-based system pattern transition matrix which can be constructed from historical system pattern data. This transition matrix can be applicable to the prediction of system patterns (or status of system variables). In addition, the system pattern method can be applicable to a load scenario reduction

method, because i) each system pattern corresponds to a unique combination of binding constraints in the power system; and ii) the LMP volatility is relatively lower when the net load fluctuates within the same system pattern, while the LMP volatility is relatively higher when the net load fluctuates across the system patterns.

A 5-bus test system is provided to test the verification and the performance of the extended system pattern method and to illustrate all applicability of the extended system pattern method presented in this paper. The simulation outcomes from this 5-bus test system well illustrate the verification of the extended system pattern method and the performance of its applicability to the status forecasting of system variables and to a load scenario reduction method.

CHAPTER 4.   A NINE ZONE ELECTRIC POWER MARKET TEST SYSTEM BASED ON DATA FROM MISO

4.1   Introduction

In a series of reports culminating in a 2003 White Paper [37], the U.S. Federal Energy Regulatory Commission (FERC) recommended that U.S. energy regions be organized as day-ahead and real-time wholesale electric power markets centrally operated by non-profit entities capable of providing fair and impartial management with regard to the business interests of market participants such as Generation Companies (GenCos) and Load Serving Entities (LSEs). This design recommends wholesale electric power markets should be centrally operated by Independent System Operator (ISO). ISO uses Locational Marginal Prices (LMPs) to reflect local transmission congestion on pricing in transmission grid. To date, this market design has been adopted by seven U.S. energy regions managing over 60% of U.S. electric power generation capacity: namely, CAISO, ERCOT, ISO-NE, MISO, NYISO, PJM, and SPP.

Several test beds for analyzing electric wholesale power markets have been developed [4, 9, 94, 78]. Among these test beds, this study focuses on one of the open source test bed, AMES V3.0 [4]. This AMES V3.0 is developed in Java/Python platform. Its first implementation is 8-zone test system based on data received from the Independent System Operator of New England (ISO-NE) [51]. AMES wholesale power market test bed allows the dynamic study of product and design issues for centrally managed electric wholesale power markets through intensive computational experiments. This study de-

velops the Midcontinent Independent System Operator (MISO) 9-zone test system based on AMES.

MISO has integrated the South region into the pre-existing Midwest region since December 9, 2013. This South region adds over 18,000 miles of transmission, 50,000 MW of generation capacity, and up to 30,000 MW of load into MISO.[1] This additional capacity is around 40% of the established MISO Midwest capacity in 2013. Thus this integration is expected to cause significant changes in the pre-existing Midwest region.

A MISO 9-zone test system also permits a wide range of implementable sensitivity studies. To illustrate the applicability, this study reports change of simulated DA LMPs through a comparative study of a Midwest 7-zone test system prior to the integration of the South region versus a 9-zone test system after the integration of the South region. The Midwest 7-zone test system is a special case of the MISO 9-zone test system.[2] Thus, this study focuses on the development of the MISO 9-zone test system without loss of generality. Simulated DA LMPs are determined through Security Constrained Unit Commitment (SCUC) and Security Constrained Economic Dispatch (SCED) processes for both test systems.

This study is organized as follows. Section 4.2 demonstrates the computational plat form, AMES. Section 4.3 describes the components of the MISO 9-zone test system construction. Section 4.5 provides an illustration for the sensitivity study to analyze the LMP changes prior to and after the integration of the South region. Key findings from the illustrative application are provided in Section 4.6. Finally, concluding remarks are presented in Section 4.7.

---

[1] https://www.misoenergy.org/WhatWeDo/StrategicInitiatives/SouthernRegionIntegration/Pages/SouthernRegionIntegration.aspx

[2] If generation capacities, transmission line limits and loads in the South region are set to zero, then the MISO 9-zone test system is automatically reduced into the 7-zone Midwest test system.

4.2 The AMES Test Bed

In a 2003 White Paper [37] FERC proposed the adoption of market design to improve electric wholesale power market operations. The key feature of this market design is a centrally managed two-settlement system operated by independent system operator.

Figure 4.1 depicts two-settlement system consisting of a day-ahead market (DAM) and a real-time market (RTM). Generating units are committed and scheduled their generations for next-day operation in the DAM. The RTM is functioned as a balancing mechanism to manage any residual load-balancing in case of discrepancies between DAM-scheduled generation and ISO forecasted real-time loads. Transmission congestion is handled through LMPs in both markets.

Figure 4.1: Two-Settlement System: ISO activities on a typical day D-1

AMES (Agent-based Modeling of Electricity Systems) [4] is an agent-based computational platform (Java/Python) allowing the systematic study of a dynamic electric wholesale power market operating under FERC's two-settlement system.

Figure 4.2 describes an ISO-managed wholesale power market operating during $h = 1, 2, ...$, over an AC transmission grid in AMES V3.0. Market participants in this test system include Generation Companies (GenCos) and Load Serving Entities (LSEs). The GenCos can include not only conventional dispatchable generating units such as thermal

power plants but also non-dispatchable renewable energy generating units such as wind and solar power plants. Non-dispatchable renewable energy can be treated as negative load. The DAM is cleared through Security Constrained Unit Commitment (SCUC) and Security Constrained Economic Dispatch (SCED), and the RTM is cleared through SCED in this test bed.
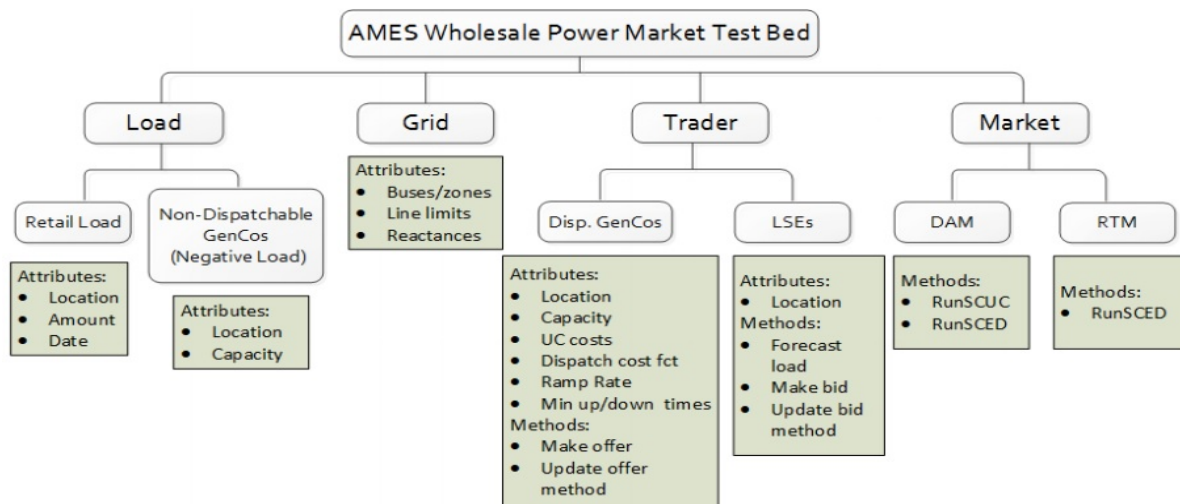
Figure 4.2: Key components of AMES V3.0

If GenCos are committed in the DAM, then unit commitment (UC) costs such as start-up, no-load and shut-down cost are incurred by the GenCos to synchronize them to the grid. Also, dispatch costs are incurred by the GenCos to deliver the cleared amounts of power to the grid. Dispatchable thermal GenCos in AMES can incur both UC and dispatch costs. For more details, see the Krishnamurthy et al. [51, Section II].

4.3   MISO 9-Zone Test System Construction

This section discusses how to construct and configure the 9-zone test system with MISO data. The MISO load and generation capacity by fuel type can be obtained directly from the MISO website. However, this data set is incomplete to construct the

9-zone test system. Especially, cost structures and technology information of generating units are necessary for each fuel type. The needed missing data were obtained from Krishnamurthy et al. [51] and other reliable sources.

4.3.1 MISO Market Topology

MISO is the largest centrally-managed energy market in the U.S. MISO covers all or most of North Dakota, South Dakota, Nebraska, Minnesota, Iowa, Wisconsin, Illinois, Indiana, Michigan and parts of Montana, Missouri, Kentucky, Arkansas, Texas, Louisiana, and Mississippi. MISO can roughly be divided into two regions: the pre-existing Midwest region and the newly added South region. The Midwest region is originally-covered area by MISO. The South region has been integrated since December 9, 2013. The South region adds over 18,000 miles of transmission, 50,000 MW of generation capacity, and up to 30,000 MW of load into the pre-existing MISO Midwest region. The map of the MISO region is depicted in Fig. 4.3.
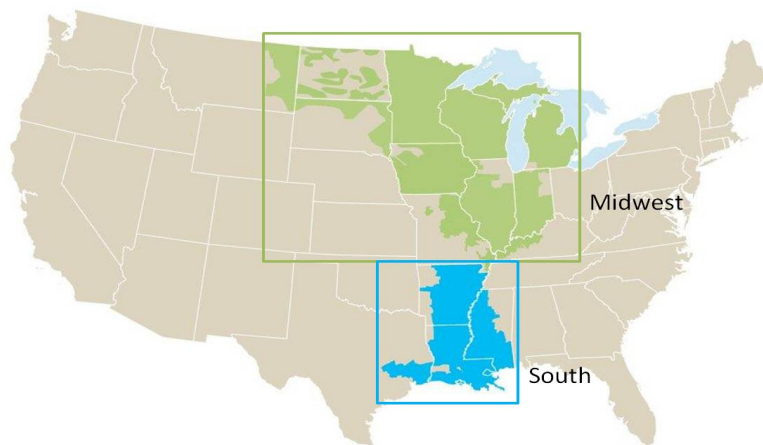
Figure 4.3: MISO regions: Midwest and South

As depicted in Fig. 4.4, the MISO Midwest region is divided into seven Local Resource Zones (LRZs) : namely, Zone 1 ,..., Zone 7. Also, the South region is divided into two

LRZs : namely, Zone 8 and Zone 9. The Midwest region is connected with the South region. This study assumes that all neighboring zones are connected with one another as depicted in Fig. 4.4. Also, the capacity import and export limits of each zone are described in Table 4.1.
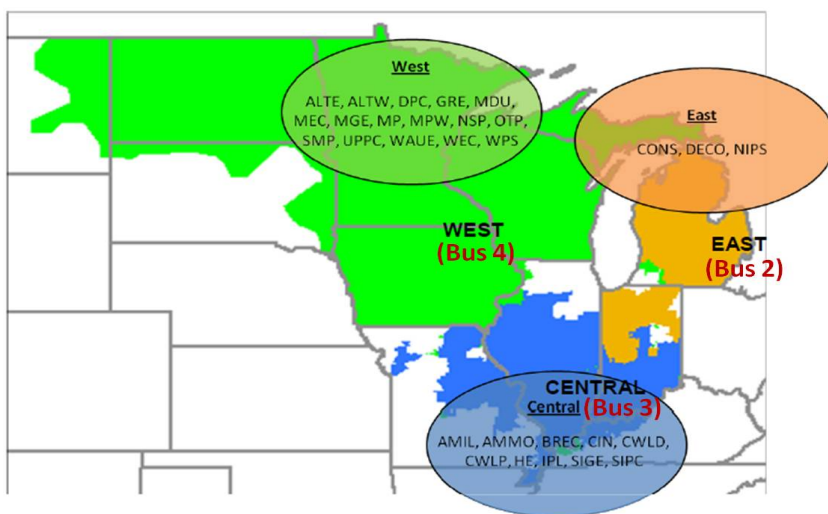
Figure 4.4: MISO local resource zone (LRZ)

Table 4.1: Year 2013 - 2014 capacity import and export limits by LRZ

Zone	Import Limit(MW)	Export Limit (MW)
1	4,085	1,416
2	4,144	1,766
3	3,717	1,612
4	6,614	2,230
5	5,035	1,616
6	6,838	3,432
7	4,576	4,306
8	5,933	3,464
9	3,554	2,716

As depicted in Fig. 4.5, the MISO Midwest region is also divided into the three transmission provider planning sub-regions: namely, the West, the Central and the East sub-region.

LRZ	Local Balancing Authorizes
1	DPC, GRE, MDU, MP, NSP, OTP SMP
2	ALTE, MGE, UPPC, WEC, WPS
3	ALTW, MEC, MPW
4	AMIL, CWLP, SIPC
5	AMMO, CWLD
6	BREC, DUK(IN, KY), HE, IPL, NIPSCO, SIGE
7	CONS, DECO
8	EAI
9	CLEC, EES, LAFA, LAGN, LEPA, SME

MISO - using Ventyx, Velocity Suite © 2013
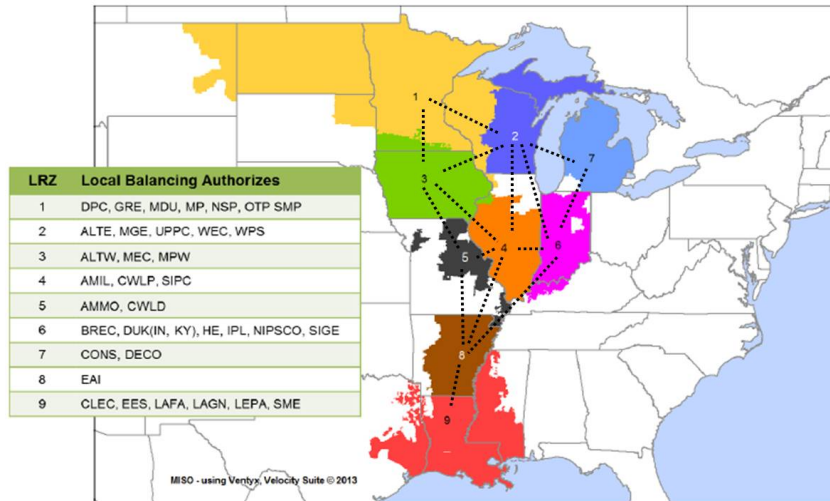
Figure 4.5: Transmission provider planning sub-regions

MISO historical load data can be obtained as the sub-region levels. To adjust sub-region level data with LRZ level data, this study divides the West sub-region into Zone 1, Zone 2 and Zone 3, and the Central sub-region into Zone 4, Zone 5 and Zone 6. The East sub-region is Zone 7 by itself. Finally, the South region is divided into Zone 8 and Zone 9. Table 4.2 depicts these classifications. Also, each sub-regional load is assumed to be distributed to the corresponding zones weighted by transmission import limits described in Table 4.1.

Table 4.2: Planning sub-regions and LRZ classifications

Planning Sub-Region	LRZs
West	Zone 1, Zone 2, Zone 3
Central	Zone 4, Zone 5, Zone 6
East	Zone 7
South	Zone 8, Zone 9

4.3.2 MISO Market Operations

MISO market participants include GenCos and LSEs. The GenCos can include both conventional dispatchable generating units such as thermal power plant and non-dispatchable renewable energy generating units such as wind and solar power plant. Non-dispatchable renewable energy is treated as negative load.

Market operations are based on a double auction mechanism for the DAM. The dispatchable GenCos submit supply offers into the DAM. Also, the LSEs submit demand bids into the DAM in the form of a 24-hour regional load profile for day D. In the DAM, MISO conducts Security-Constrained Unit Commitment (SCUC) and Security-Constrained Economic Dispatch (SCED) optimizations based on given bids and offers subject to system constraints. SCUC and SCED processes determine cost-minimized unit commitments and scheduling of generation to meet forecasted next-day load implied by LSE demand bids. In the RTM, the ISO conducts an offer-based SCED optimization to balance discrepancies between the DAM-scheduled generation and the ISO forecasted real-time load subject to system constraints. Locational Marginal Prices (LMPs) are determined through these optimization processes by considering transmission and other system constraints. Simplified MISO market operations are depicted in Fig. 4.6.
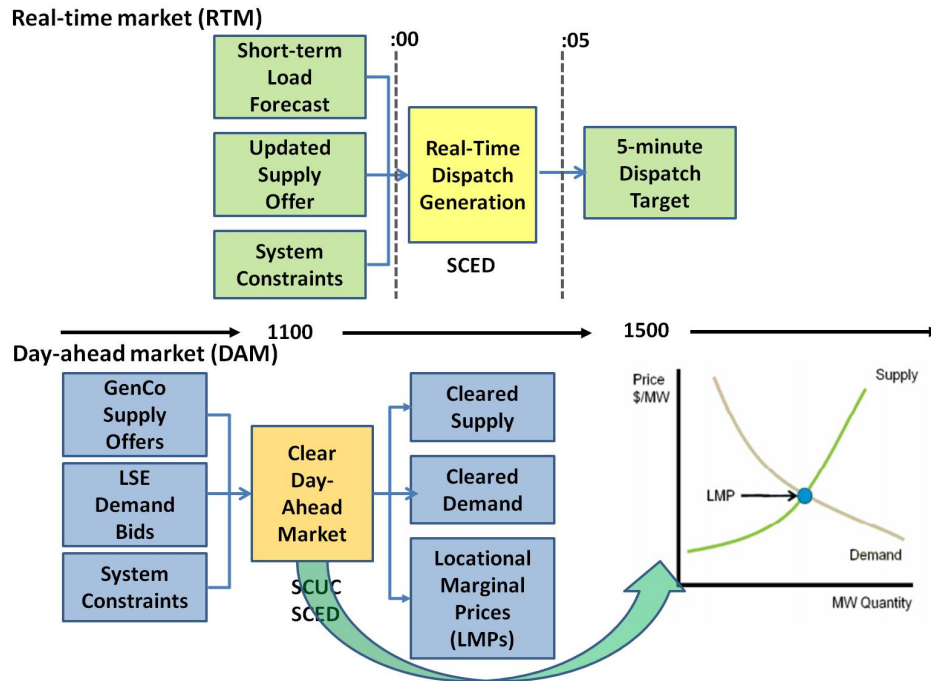
Figure 4.6: Simplified MISO day-ahead and real-time market operations

4.3.3 Generator Attributes

Data provided by MISO [68] include nameplate capacity by fuel type. Fuel types include nuclear, coal, natural gas, oil, hydro, pumped storage, biomass, and wind. This study focuses only on the thermal generating units (nuclear, coal, natural gas, oil) and the largest renewable energy, wind power. Figure 4.7 presents capacity proportion and capacity by fuel type for MISO and each LRZ.

For simplicity, the 9-zone test system applies a scale-down factor without loss of generality; all capacities and transmission line limits in this test system are re-scaled as "Capacities/10" and "line limits/10".[3] In this test system, the fuel mix of the thermal generation capacities is maintained in the same proportions as in the original MISO data for each zone. The number of GenCo by fuel type at each zone in the test system is determined by considering the scale-down total capacities and capacity proportions by

---

[3]While the generation capacity by fuel type and line limits are derived from MISO data, reactances are arbitrarily decided in this test system.

	MISO	Zone 1	Zone 2	Zone 3	Zone 4	Zone 5	Zone 6	Zone 7	Zone 8	Zone 9
Wind	6.90%	18.95%	4.24%	36.47%	3.58%	0.06%	1.33%	3.86%	0.00%	0.00%
Oil	3.64%	4.06%	2.89%	3.03%	2.52%	2.42%	2.23%	1.76%	2.64%	6.72%
Gas	39.64%	28.56%	36.91%	16.56%	19.28%	33.68%	25.86%	44.41%	31.38%	69.75%
Coal	39.35%	40.27%	46.53%	40.23%	67.03%	51.79%	70.57%	41.96%	45.00%	3.74%
Nuclear	10.46%	8.16%	9.43%	3.72%	7.59%	12.06%	0.00%	8.02%	20.98%	19.79%
Capacity (MW)	174,995	22,287	17,111	14,741	14,193	10,752	21,522	24,389	8,795	4 1,205

Figure 4.7: Capacity proportion and capacity by fuel type

fuel type at each zone. The number of GenCos by fuel type at each zone is provided in Table 4.3.

Table 4.3: Number of GenCos by fuel type at each zone

	Nuclear	Coal	Gas	Oil	Total
MISO	8	19	67	8	102
Zone 1	1	3	7	1	12
Zone 2	1	2	2	1	6
Zone 3	1	3	3	1	8
Zone 4	1	2	5	1	9
Zone 5	0	2	6	1	9
Zone 6	1	3	9	1	14
Zone 7	1	2	5	1	9
Zone 8	1	1	2	0	4
Zone 9	1	1	28	1	31

All GenCos in the MISO 9-zone test system incur both the Unit Commitment (UC) and dispatch costs. The UC costs include start-up, no-load, and shut-down costs. This test system uses same additional generator attributes such as ramp rates, minimum up/down times as described in Krishnamurthy et al. [51].[4]

No-load cost data for generators by fuel type in this test system are derived from the IEEE 24-Substation Test Case data [9]. Table 4.4 provides these no-load costs by fuel type and capacity.

---

[4] Although ISO-NE 8-zone test system data in Krishnamurthy et al. [51] are based on the ISO New England, it is natural to assume that each generator by fuel type has similar cost structures and technologies across the U.S. energy regions.

Table 4.4: No-load costs by fuel type and capacity

Fuel	Capacity (MW)	No-load cost ($/hr)
Coal	0 - 75	212.307
Coal	76 - 155	382.239
Coal	156 - 350	665.109
Coal	> 350	877.417
Oil	0 - 12	086.385
Oil	13 - 20	400.684
Oil	21 - 100	781.521
Oil	101 - 200	832.757
Gas	—	400.000
Nuclear	—	385.374
Wind	—	000.001
Photovoltaic	—	000.001

The MISO 9-zone test system assumes that each thermal generator i offers based on a quadratic dispatch cost function in each time period h as follows:

$$C_i^R = a_i^R p_i + b_i^R p_i^2 \tag{4.1}$$

where C_i^R ($/h) is a reported dispatch cost of generator i, p_i (MW) is the generator i's dispatch level measured in MW, a_i^R ($/MWh) and b_i^R ($/(MW)^{2}h) are the reported coefficients on a linear term and a quadratic term in the cost function respectively for each generator i. These cost coefficients in (4.1) depend on the fuel types of generators. The dispatch cost coefficients by fuel type are listed in Table 4.5.

Table 4.5: Dispatch cost coefficients by fuel type

Fuel	a ($/MWh)	b ($/(MW)^{2}h)
Coal	15	0.008
Fuel Oil	35	0.016
Jet Fuel	45	0.024
Kerosene	30	0.009
Landfill Gas	75	0.006
Municipal Solid Waste	15	0.004
Natural Gas	75	0.020
Nuclear	15	0.003
Tire Derived Fuel	75	0.020

All thermal generators incorporate ramp rate attributes in this test system. Ramp rate (MW/min) is basically the speed at which a generator can increase (ramp up) or decrease (ramp down) generation in one minute. Table 4.6 lists ramp rates by fuel type. These ramp rates are displayed as % of capacity MW per minute.

Table 4.6: Ramp rate by fuel type

Fuel	Ramp Rate (% of capacity MW)/min
Coal	3 - 5
Oil	10 - 15
Natural Gas	20 - 25
Nuclear	1

4.3.4 Load Serving Entity Attributes

In the MISO 9-zone test system, each zone has a single representative aggregated Load Serving Entity (LSE). An LSE has an intermediary responsibility between GenCos and retail customers in electric wholesale power markets. An LSE procures necessary energy for retail customers by submitting demand bids into the DAM on each day D-1. Based on the LSE regional next-day load forecasting for operating day D, the LSE submits demand bid in the form of a 24-hour regional load profile for day D.

4.4 Performance Test of Test System

This study compares the simulation outcomes for the thermal and the wind generation dispatch proportions from the MISO Midwest 7-zone test system and the actual thermal and wind generation dispatch proportions from the MISO Midwest region during July, 2013 [67], for the performance check of the test system.

To get the simulation outcomes, this study uses 30-day load and wind generation profile drawn from empirical probability density functions of load and wind generation. Specifically, for each LRZ, hourly empirical probability density functions of load and wind generation are estimated based on hourly weekday load and wind power generation data during 2011 - 2013. From these empirical probability density functions, hourly load and wind power generation profile data are constructed for 30 simulated days.[5]

Specific comparison between proportions of capacities and dispatches by fuel type from the simulation outcomes under the 7-zone test system with proportions of capacities and dispatches by fuel type from actual MISO data during July 2013 is depicted in Table 5.3.

---

[5] MATLAB 'default seed' is used to generate 30 simulated days' load and wind power generation profile from the estimated empirical probability density functions.

Table 4.7: Comparision bewteen simulated dispatch proportions and actual MISO dispatch proportions by fuel type (%)

	Capacity	Simulated Dispatch	Actual MISO Dispatch
Nuclear	6.65	10.08	11.28
Coal	50.70	75.65	74.97
Gas	30.30	8.65	9.03
Oil	2.70	2.23	0.00
Wind	9.66	3.39	4.72
Total	100.00	100.00	100.00

As we can see in this table, proportions of simulated dispatch by fuel type are similar to proportions of actual MISO dispatch data during July 2013 given the same capacity proportions. Thus the test system can well demonstrate actual MISO situation.

4.5   Illustrative Example

4.5.1   Purpose and General Scope

To illustrate the applicability of the MISO 9-zone test system, this study reports day-ahead LMP changes for each pre-existing Midwest 7-zone through a comparative study of the 7-zone Midwest test system prior to the integration of the South region versus the 9-zone test system after the integration of the South region. For simplicity, this illustrative example assumes: (i) generators consist of thermal generators and wind power generators; (ii) There is no measurement error on day-ahead zonal load forecasting and wind power generation; (iii) the MISO grid is not connected with other energy region, i.e., there are no energy imports or exports; (iv) MISO requires reserve requirements at 8% of total capacity and, (v) all line reactances are set to 0.001.

4.5.2 Day-Ahead Security Constrained Unit Committment

This test system used the same day-ahead SCUC described in Section IV-B of Krishnamurthy et al. [51]. The objective of this day-ahead SCUC is to minimize expected total costs including UC costs and dispatch costs subject to system constraints based on the next-day load forecasting. For more details, see the Krishnamurthy et al. [51] Section IV-B.

4.5.3 Sensitivity Design

For sensitivity analysis, this study compares the average day-ahead LMPs during specific time period T in Midwest zones between prior to and after the integration of the South region. Expected hourly day-ahead LMPs are calculated through DAM SCUC/SCED process in each zone both prior to and after the integration of the South region. Given day-ahead LMPs for pre- and post-integration of the South region, % change of average day-ahead LMPs during the time period T in Zone k are measured as follows:

$$\Delta_{B,A,k}^{T} = \frac{AvgLMP_{k}^{T,A} - AvgLMP_{k}^{T,B}}{AvgLMP_{k}^{T,B}} \times 100 \quad (\%) \tag{4.2}$$

where $\Delta_{B,A,k}^{T}$ is the average % change of day-ahead LMPs during the time period T between prior to and after the integration of the South region at Zone k, $AvgLMP_{k}^{T,A}$ is the average of day-ahead LMPs during the time period T after the integration of the South region at Zone k, and $AvgLMP_{k}^{T,B}$ is the average of day-ahead LMPs during the time period T prior to the integration of the South region at Zone k.

4.6 Key Findings from Illustrative Example

The integration of the South region is the key treatment factor in this illustrative example. The 24-hour zonal day-ahead load data for simulation focus on 18th of July

load profile: the day marked the peak hourly load during 2013 in the MISO Midwest region.

This section reports the outcomes for the illustrative example described in Section 4.5. The key finding is that the South region integration decreases simulated day-ahead LMPs of all pre-existing Midwest zones given load and wind generation profile during July 17. Specifically, as reported in Fig. 4.8, simulated day-ahead LMP is decreased 3.49% at Zone 1, 3.80% at Zone 2, 3.20% at Zone 3, 3.33% at Zone 4, 2.22% at Zone 5, 4.24% at Zone 6, 2.22% at Zone 7, and 3.20% at the Midwest region on average.

	Midwest Avg.	Zone 1	Zone 2	Zone 3	Zone 4	Zone 5	Zone 6	Zone 7
Price Change	-3.20%	-3.49%	-3.80%	-3.20%	-3.33%	-2.22%	-4.24%	-2.22%
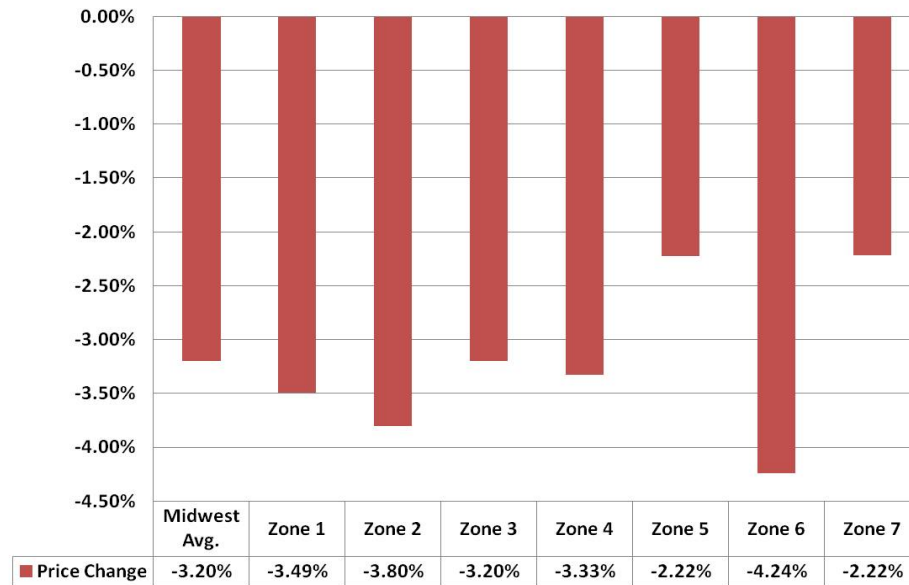
Figure 4.8: Simulated average % changes in the Midwest LMPs between pre- and post-integration of the South region using 2013 MISO peak load data

To check the performance of the MISO 9-zone test system, this study provides actual average day-ahead LMP changes for the MISO Midwest region at each pricing hub[6] prior to/after the South region integration by comparing average day-ahead LMP between the peak months, July 2013 and July 2014.[7] Specifically, as depicted in Fig. 4.9,

[6] MISO day-ahead LMP data are not published by local resource zone level but published by pricing hub level. Thus, this section provides average day-ahead LMP changes at each pricing hub level.

[7] Peak load profile in 2013 and 2014 is different, so it is hard to directly compare the peak day LMPs

day-ahead LMP is decreased 1.17% at Illinois hub, 4.42% at Michigan hub, 13.57% at Minnesota hub, 3.68% at Indiana hub and 5.68% at Midwest region on average. Thus, this study demonstrates that LMPs are decreased after the South region integration in both simulation outcomes and actual MISO data during the peak load time.
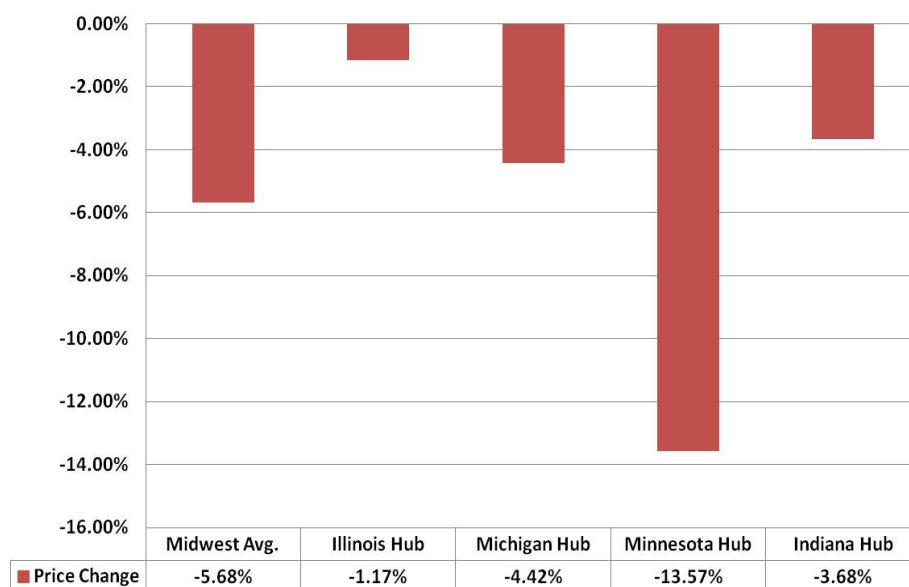
Figure 4.9: Actual % changes in the Midwest LMPs between July 2013 (pre-integration of the South region) and July 2014 (post-integration of the South region)

4.7 Conclusion

Constructing of electricity wholesale power market test systems is important to analyze the effect of power market policies and environment changes on power markets. The test systems can also help to forecast changes of system variables and market participant's performances. This study constructs a 9-zone test system using 2013 MISO data. This test system is implemented through AMES test bed. AMES permits systematic

---

between two different time periods. Thus this study compares the average LMP during July 2013 with the average LMP during July 2013 to analyze the effects of the South region integration on the MISO Midwest region LMPs during July.

study of dynamic electric wholesale power markets allowing FERC's centrally managed two-settlement market design.

The limitations of data acquisition hinder to construct a sufficiently large test system to fully reflect actual MISO situations. However, this small test system can be extended to a sufficiently large test system, if we have the corresponding data set. Although the small test system cannot embed all characteristics of MISO, it embeds important features of actual MISO attributes such as generating capacity and technology by fuel type, transmission constraints and operation processes. Thus, this small test system can be applicable to finding implications for actual power markets by conducting various sensitivity studies.

For the performance check of the test system, this study compares the simulation outcomes for thermal and wind generation dispatch proportions from the MISO Midwest 7-zone test system with actual thermal and wind generation dispatch proportions from the actual MISO Midwest region. Proportions of dispatches from the simulation outcomes are is similar to proportions of actual MISO dispatches. Thus, the test system can well demonstrate the actual MISO situations.

For sensitivity studies, this study compares the simulation outcomes for day-ahead LMP changes with the actual MISO day-ahead LMP changes prior to/after the integration of the South region that has been incorporated into the pre-existing MISO Midwest region since 9th of December in 2013.

The simulation outcomes report that the average day-ahead LMP decreases during after the integration of the South region at each zone. Actual MISO LMP data also report that overall LMPs at Midwest pricing hubs are decreased after the integration of the South region. Thus, the simulation outcomes demonstrates similar trend in day-ahead LMPs to the actual MISO day-ahead LMP after the integration of the South region.

CHAPTER 5.   EFFECTS OF A CARBON TAX AND WIND POWER PENETRATION ON WHOLESALE ELECTRIC POWER MARKETS

5.1   Introduction

There is evidence that human activities produce large quantities of greenhouse gases. Greenhouse gases can affect human activities through changes in the global climate. The magnitude of such changes remains uncertain. However, there is growing recognition that theses changes could be catastrophic [83]. Several governments all around world agreed that greenhouse gases, especially CO_2, cause climate change and accepted CO_2 reduction targets in order to counter climate change under the Kyoto Protocol [87]. Global climate change is also one of the most significant long-term policy challenges [17].

Although the U.S. is the second largest CO_2 emitter and historically the largest cumulative contributor to global CO_2 emissions, accounting for approximately 16 percent of the world's emissions, the U.S. did not ratify the acceptance of the Kyoto Protocol [88]. However, the U.S. President Obama committed to reduce emissions in the range of 17 percent below 2005 levels by 2020, 42 percent below 2005 levels by 2030, and 83 percent below 2005 levels by 2050 during 2009 Copenhagen Climate Change Summit. These targets are aligned with the energy and climate legislation passed by the House of Representatives [89]. Thus the U.S. Federal Government is considering several policy options to reduce CO_2 emissions.

Under these circumstances, it is important to analyze the effects of possible CO_2 emission reduction options in the U.S. Experimenting the effects of carbon tax policy is usually analyzed at the economy-wide level. Two promising methods are input-output (I-O) models and computable general equilibrium (CGE) models. I-O models derive the inter-industry price effects of carbon taxes or emission charges. Several I-O models show that the energy sector including the electricity sector is highly affected by carbon tax policies [16, 12, 61, 45]. A CGE model is a general equilibrium model including the industry, factor market and consumption sector. Several CGE models also show consistent results with I-O models about the effects of carbon tax imposition on the electricity sector [49, 41, 11].

Agent-Based Model (ABM) is one of the most promising methods to construct the field of energy system modeling [59]. The application of ABM in the energy market reform and energy policy simulation is mainly focused on electricity markets. In previous studies, analysis of carbon policy impacts in electricity markets through ABM mainly focuses on a cap-and-trade system rather than a carbon tax. Weidlich et al. [92] provides a conceptual simulation platform which can be used to test the impacts of different CO_2 emission market designs, policy measures on market outcomes and the development of the electricity sector through the multi-agent-based approach. Chappin and Dijkema [19] develops ABM to elucidate the effect of a cap-and-trade on the decisions of power generators under an oligopolistic market setting in the Netherlands electricity market. This study shows that a cap-and-trade has an impact but the effect of it is relatively small and materialized late. Even after the introduction of a cap-and-trade, the coal generation is preferred in the capacity expansion plan and the economic effect of a cap-and-trade is not sufficient to outweigh the economic incentives to choose for coal generation. Wang et al. [91] shows that the initial allowance will influence the operation of power producers and that some generation companies may need to raise the bid prices to recover their expenses for buying additional allowances. Cong and Wei [20] establishes ABM with cap-

and-trade in China power sector. This study finds that cap-and-trade internalizes the environmental cost and increases the average electricity price by 12% and its volatility by 4%.

Recently, ABM models analyzing the effects of the renewable energy and carbon tax policy on electric power markets have been developed. Sensfuß et al. [81] analyzes the impact of the renewable electric generation on CO_2 emissions and power plant utilization portfolio in Germany based on ABM. This study shows that most of the renewable resources replace coal power plants. Wild et al. [93] investigates the impact of the introduction of a carbon price signal on wholesale electricity prices, carbon-pass-through rates and retail electricity rates in the states making up the Australian National Electricity Market based on AMES test bed [4]. This study shows that a carbon tax increases both wholesale spot market prices and retail tariffs but the increasing amounts are different across states.

Distinct from previous studies, this study focuses on the joint effects of carbon tax and renewable energy options on the U.S. electric wholesale power market based on the data of the largest centrally-managed energy region in the U.S., the Midcontinent Independent System Operator (MISO). For analysis, a test bed has been developed based on empirical data from MISO such as rules of operation, physical attributes of market generation technology and capacity, and transmission constraints. Also, effects on CO_2 emissions of alternative carbon tax levels based on a proposal in the U.S. Congressional Budget Office Report [17] and wind power penetration levels based on 2025 MISO projection [43] have been studied.

This study is implemented through ABM platform. ABM is one of the most promising methods to construct the field of energy system modeling and to analyze the effects of exogenous shocks on energy markets [59]. The application of ABM in the energy market reform and energy policy simulation is mainly focused on electricity markets. Specifically, ABM can investigate the effects of extensive scenarios of CO_2 reduction

options on CO_2 emissions and other electric wholesale power market key outcomes at the market participant-level.

This study is organized as follows. Section 5.2 explains the method of this study such as MISO 7-zone model construction, implementation of ABM, experimental design, scenarios and types of reported simulation outcomes. Scenario-based simulated effects of CO_2 reduction options on CO_2 emissions and other electricity market key outcomes are provided in Section 5.3. Finally, concluding remarks are presented in Section 5.4.

5.2   Method

5.2.1   MISO Midwest 7-Zone Test System

This study constructs the MISO Midwest 7-zone test system based on Chapter 4 for sensitivity analysis. Physical attributes of MISO such as zonal capacity by fuel type and transmission line constraints are incorporated in the test system. Also, this test system embeds rules of MISO market operations, cost structures and technology information of generating units by each fuel type and attributes of LSEs. This test system is implemented through AMES test bed [4]. More detailed descriptions are presented in Chapter 4.

This study focus on the CO_2 emission reduction options such as carbon tax and wind power penetration. Thus characteristics of carbon intensity by fuel type and cost structures of wind power generation are added to the MISO Midwest 7-zone test system.

Unlike thermal power generation, wind power generation has some unique characteristics. First, wind power is volatile and uncontrollable. Thus this study considers wind power as non-dispatchable energy. Second, wind power has high fixed cost but very low dispatch cost. Thus this study assumes that wind power has zero dispatch cost. This implies that wind power is dispatched in most cases if the total load is greater than the total wind power generation and the power system has enough available transmission ca-

pacity. By combining these two characteristics of wind power, we can treat wind power as negative load.

This study uses levelized cost of wind power estimated by EIA, \$80.6/MWh to calculate the total cost of wind power generation.[1] Levelized cost represents the per-MWh cost (in real dollars) of building and operating a generating plant over an assumed financial life and duty cycle.

All generators in this test bed emit CO_2 when they generate electricity except nuclear and wind power generators.

Each fuel type of generator has different carbon intensity. Each carbon intensity per MWh of electricity generation by fuel type measured in CO_2 tonnage (tCO_2) per MWh is reported in Table 5.1. The amount of CO_2 emission from a specific fuel type generation is calculated by multiplying the amount of generation by carbon intensity per MWh of a specific fuel type.

Table 5.1: Average carbon intensity per MWh of electricity generation by fuel type

Fuel Type	tCO_2/MWh
Nuclear	0.0000
Coal	0.9716
Gas	0.5539
Oil	0.7922

Although the identical carbon tax (\$/tCO_2) is imposed on each fuel type, the carbon tax per MWh is different across fuel type because each fuel type has different carbon intensity.

[1] http://www.eia.gov/forecasts/aeo/electricity_generation.cfm

5.2.2 Experimental Design

5.2.2.1 Purpose and General Scope

To analyze the effects of CO_2 reduction options, an increased renewable energy and a carbon tax imposition, on CO_2 emissions and electricity market performance, this study uses the test bed to conduct a comparative study of base case, electricity market without a increased renewable energy and a carbon tax imposition, versus CO_2 reduction scenario based cases, electricity market with the renewable energy penetration or the carbon tax imposition with MISO load and wind power data.

5.2.2.2 Simulated CO_2 Reduction Scenarios

This study focuses on two CO_2 emission reduction options as treatment factors: a renewable energy penetration and a carbon tax imposition.

First, the renewable energy policy is represented by two different wind power penetration rates: MISO's 2013 wind power penetration rate, 9.66% (low level), and MISO's projected 2025 wind power penetration rate, 17.70% (high level), of 2013 MISO's total capacity [43]. Wind power is embedded as negative load for each zone in this study.

Second, two different level of upstream carbon taxes are imposed on each GenCo and are embedded in each GenCo's dispatch cost based on the carbon intensity by fuel type. The carbon tax levels are based on the 2013 EU ETS average carbon spot price and proposed bills for carbon tax imposition in the U.S.The historical EU ETS average carbon spot price is around €5/tCO_2 and the historical euro-to-dollar exchange rate is around 1.3 during 2013. [2] Based on this, \$6.5/tCO_2 (low level) carbon tax rate is set to be equivalent to the 2013 EU ETS average carbon spot price. Also, \$20/tCO_2 (high level) carbon tax rate is set based on proposed bills for carbon tax imposition in the U.S.

---

[2] https://www.eex.com/

This study sets up CO_2 emission reduction scenarios for sensitivity studies by combining two different levels of these two treatment factors. A hypothetical base case (BC), an electricity market without a wind power penetration and a carbon tax imposition, is established to analyze the effects of these two treatment factors on the electricity market performance.

Under scenario 1 (SC1), the test bed embeds MISO's 2013 wind power penetration rate, 9.66%. Thus SC1 is similar to the current MISO market situation. Under scenario 2 (SC2), the test bed embeds a wind power penetration rate based on MISO's projected 2025 wind power penetration rate, 17.70%.

Under scenario 3 (SC3), the test bed embeds $6.5/tCO_2 (upstream) carbon tax imposition. Under scenario 4 (SC4), the test bed embeds $20/tCO_2 carbon tax imposition.

Scenario 5-8 (SC5-SC8) mix these two treatment factors: SC5 embeds 9.66% wind power penetration rate and $6.5/tCO_2 carbon tax imposition, SC6 embeds 17.7% wind power penetration rate and $6.5/tCO_2 carbon tax imposition, SC7 embeds 9.66% wind power penetration rate and $20/tCO_2 carbon tax imposition, and SC8 embeds 17.7% wind power penetration rate and $6.5/tCO_2 carbon tax imposition. Details about base case and all other scenario characteristics are described in Fig. 5.1.

		Wind Penetration Rate (%)		
		0	9.66	17.7
CO2 Tax ($/tCO2)	0	BC	SC1	SC2
	6.5	SC3	SC5	SC6
	20.0	SC4	SC7	SC8

Figure 5.1: Simulated scenarios for sensitivity study

5.2.2.3   Data

We can only obtain exogenous hourly planning sub-region level load and hourly MISO total wind power generation from the MISO website [68]. The test bed is established by zone level. Thus we need to assign planning sub-region level load and MISO total wind power generation to each zone.

To obtain zonal load, each sub-regional load is assumed to be distributed to the corresponding zones weighted by transmission import limits described in Chapter 4.

To obtain zonal wind power generation, total wind power generation is assumed to be distributed to the corresponding zones weighted by wind power capacity proportion of each zone. Also, this study assumes that the increase in wind power penetration rate increases total wind power generation at a rate proportional to the increase of wind penetration rate. For example, suppose that wind power generation is 100MWh for a specific hour H under 9.66% of wind power penetration rate, then wind power generation for a specific hour H under 17.70% of wind power penetration rate would be 183MWh calculated by multiplying 100MWh by 1.83 (= 17.70/9.66).

Relatively high contingent situations on the power market can arise during the peak season because of the scarcity of resources. Price volatility is also high and all other key outcomes in the power market are more sensitive during the peak season. This implies that we may observe the significant impact of possible policies on electric power markets during the peak season. Thus this study focuses on the peak load month, July, and uses average hourly load and wind power generation data during this month.

For sensitivity studies, hourly empirical distributions of load and wind power generation are estimated based on hourly weekday load and wind power generation data during 2011 - 2013 in zonal level. From these empirical distributions, hourly load and wind power generation profile data under 9.66% of wind power penetration rate are constructed for 30 simulated days. MATLAB R2014b 'default seed' is used to generate 30 simulated days load and wind power generation profile from the estimated empirical

distributions. We can obtain 30-day wind power generation profile data under 17.7% of wind power penetration rate by multiplying 1.83 (= 17.70/9.66) by constructed 30-day wind power generation profile under 9.66% wind power penetration rate.

Load and wind power generation are also scaled down with the same scale-down factor applied to generating capacity and transmission line limits as described in Chapter 4.

Also, the increase of dispatch cost ($/MWh) data by fuel type incurred by carbon tax imposition can be calculated as follows: multiplying carbon intensity per MWh presented in Table 5.1 by imposed carbon tax level. The increase of dispatch cost under $6.5/tCO_2$ and $30/tCO_2$ carbon tax imposition by fuel type is provided in Table 5.2

Table 5.2: Additional dispatch cost from carbon tax imposition by fuel type ($/MWh)

	$6.5/tCO_2$	$20/tCO_2$
Nuclear	0.0000	0.0000
Coal	6.3154	19.4320
Gas	3.6004	11.0780
Oil	5.1493	15.8440

5.2.2.4 Sensitivity Design

The main purpose of this study is to investigate the effects of CO_2 reduction options on CO_2 emissions and other market performances. The effects are measured relative to base case, electricity market without CO_2 reduction options. The key treatment factors for CO_2 reductions in electricity market are embedded in each scenario as described in Section 5.2.2.2.

For each comparative study of CO_2 emissions and other market performances between base case and scenario sj, $sj = 1, 2, ...8$, expected difference (%) in outcomes are calculated as follows.

First, draw day D load profile, L(D), and day D wind power generation profile, W(D), during 30 simulated days, $D = 1, 2, ..., 30$, from empirical distributions and adjust wind power generation profile corresponding to scenario sj as described in Section 5.2.2.3

Second, adjust each GenCo's dispatch cost based on the carbon tax level and carbon intensity by fuel type corresponding to scenario sj as described in Section 5.2.2.3.

Third, calculate specific outcome V under base case and scenario sj determined by means of SCUC and SCED given load and wind power profile of day D, i.e., L(D) and W(D). SCUC and SCED solutions are provided by hourly basis, $H = 1, 2, ..24$, during day D. To get outcome V during day D, V_D, we need to add all hourly outcomes, V_H, during day D as follows.

$$V_D = \sum_{H=1}^{24} V_H \tag{5.1}$$

Fourth, letting $V_D(bc)$ and $V_D(sj)$ denotes a outcome V during day D under base case and scenario sj respectively, calculate difference (%) in daily outcome V between base case and scenario sj, $\Delta_{V,D}(sj)$, as follows for each day D.

$$\Delta_{V,D}(sj) = \frac{V_D(bc) - V_D(sj)}{V_D(bc)} \times 100\% \tag{5.2}$$

Fifth, calculate the average and the standard deviation of daily difference in outcome V between base case and scenario sj for 30 simulated days, $D = 1, 2, ..., 30$ as follows:

$$\Delta_V^{avg}(sj) = \frac{\sum_{D=1}^{30} \Delta_{V,D}(sj)}{30} \tag{5.3}$$

$$\Delta_V^{std}(sj) = \sqrt{\frac{\sum_{D=1}^{30} (\Delta_{V,D}(sj) - \Delta_V^{avg}(sj))^2}{29}} \tag{5.4}$$

Sixth, repeat this process for all or selected outcomes and scenarios based on the objective of research.

Throughout all scenarios, it is assumed that market participants have no learning capabilities and LSE demands are not price responsive.

5.2.2.5   Types of Reported Simulation Outcomes

This study reports the average and the standard deviation of difference of outcomes between base case and each scenario to measure the effects of CO_2 reduction policies on CO_2 emissions, net load[3] and its volatility, average LMP and its volatility, dispatch and profits of thermal generators as described in Section 5.2.2.[4]

Unlike the previous outcomes, wind power generation profit and government carbon tax revenue are reported as the average and the standard deviation of their simulated values instead of the difference of outcomes between base case and scenarios, because these outcomes are newly incorporated in the model due to two treatment factors, so these values on each scenario can not be measured relative to base case. The calculation process of average and standard deviation of wind power generation profit and government tax revenue are same with equation (5.3) and (5.4) respectively.

In addition to these outcomes, all simulated outcomes (total CO_2 emissions and CO_2 emissions by fuel type, net load and its volatility, average LMP and its volatility, total dispatch and dispatch by fuel type, total generation revenue and generation revenue by fuel type, total cost and cost by fuel type, total profit and profit by fuel type, total carbon tax revenue and carbon tax revenue by fuel type) are reported in Table C.1 of Appendix C.

Note that all figures and tables in following sections report average values together with standard deviations (in parenthesis).

5.2.2.6   Test Bed Vs. Real-World MISO Outcomes

As mentioned in Section 5.2.2.2, SC1 in our test bed is similar to the current MISO market situation. Thus this study compares simulated results of thermal and wind

---

[3]Net load = load - wind power generation

[4] Net load volatility and LMP volatility are measured as Coefficient of Variation (CV) which is defined as the ratio of the standard deviation to the mean, $\frac{StandardDeviation}{Average}$, to get normalized variable volatility.

generation dispatch to the actual thermal and wind generation dispatch levels of MISO during July 2013 for a validation check of the test bed.

Note that this test bed has the same capacity proportion by fuel type with actual 2013 MISO capacity proportion. The dispatch proportion in SC1 is calculated from simulated results for dispatch by fuel type provided at Table C.1 in Appendix C and actual MISO dispatch proportion by fuel type during July 2013 is obtained from July 2013 Monthly Market Assessment Report [67].

In simulation results for SC1, the proportion of dispatch level by fuel type show different pattern from the proportion of capacities by fuel type. Although the capacity of gas generation is over one third of total capacity, gas generation is only dispatched 8.65% in total dispatch even given the peak month load data because it has the highest dispatch cost as depicted in Chapter 4. This is equivalent to the actual MISO situation. Gas generation is usually peaker and most gas capacity is maintained for reserves. Oil generation is only dispatched 2.23% because it has the smallest capacity proportion and the second highest dispatch cost. Nuclear power dispatch is 10.08% in total generation which is more than its capacity proportion (7.36%) because nuclear generation has the lowest dispatch cost. Coal generation is dominantly dispatched. Coal generation dispatch proportion (75.65%) is more than its capacity proportion (56.12%) because it has the largest capacity proportion and the second lowest dispatch cost. Specific comparison between the capacity and the dispatch proportion by fuel type in SC1 with the capacity and the dispatch proportion by fuel type in MISO during July 2013 is depicted in Table 5.3. As we can see in this table, simulated dispatch results by fuel type are similar to actual MISO dispatch level by fuel type during July 2013 given the same capacity proportions. Thus the test bed can represent the real-world MISO situation well.

Table 5.3: Comparision bewteen simulated dispatch proportions under SC1 and actual MISO dispatch proportions by fuel type (%)

	Capacity	Simulated Dispatch for SC1	Actual MISO Dispatch
Nuclear	6.65	10.08	11.28
Coal	50.70	75.65	74.97
Gas	30.30	8.65	9.03
Oil	2.70	2.23	0.00
Wind	9.66	3.39	4.72
Total	100.00	100.00	100.00

5.3 Results

5.3.1 Effects on Total CO_2 Emissions

The wind power penetration and the carbon tax imposition can reduce total CO_2 emissions. The wind power generation can reduces CO_2 emissions by directly substituting for the dispatch of fossil-fuel generation, such as coal, gas and oil generation. The carbon tax imposition can also reduces CO_2 emissions by changing fuel mix from high carbon intensive fuel type generation to low carbon intensive fuel type generation implied by relative dispatch cost changes.

In the simulation results, total CO2 emissions are decreased by 3.03% under low level wind power penetration rate (SC1) and 5.61% under high level wind power penetration rate (SC2) relative to base case. Thus the increase in wind power penetration rate decreases total CO2 emissions.

Total CO_2 emissions are decreased by 0.23% under both low level carbon tax imposition (SC3) and high level carbon tax imposition (SC4) relative to base case. These

results imply that a much higher carbon tax rate than $20/tCO_2$ needs to be imposed to derive major fuel mix changes and to reduce additional CO_2 emissions in electricity markets during the peak season.

Total CO_2 emissions are also decreased in mixed options (SC5-SC8) relative to base case. The amount of total CO_2 emission reduction in mixed options is slightly higher than the sum of reduction from each separate option. Thus joint effects of these two options show weakly positive correlation in total CO_2 emission reduction. More detailed results about CO_2 emission reduction are described in Fig. 5.2.[5]

		Wind Penetration Rate (%)		
		0	9.66	17.7
CO2 Tax ($/tCO2)	0	0.00% (0.00)	-3.03% (1.36)	-5.61% (2.05)
	6.5	-0.23% (0.31)	-3.39% (1.22)	-6.16% (2.14)
	20	-0.23% (0.31)	-3.39% (1.22)	-6.17% (2.14)

Figure 5.2: Effects of CO_2 reduction options on total CO_2 emissions

5.3.2 Effects on CO_2 Emissions by Fuel Type

The effects of wind power penetration and carbon tax imposition on CO_2 emissions can differ by fuel type. The wind power generation can reduces CO_2 emissions by directly substituting for the dispatch of fossil-fuel generation, such as coal, gas and oil generation, but it can not affect CO_2 emissions from nuclear generation because nuclear generation dose not emit CO_2.

The carbon tax imposition can also reduces CO_2 emissions from high carbon intensive fuel type generation, such as coal and oil generation, but it can increase CO_2 emissions

---

[5] All figures and tables in this section report average outcomes together with standard deviations (in parenthesis).

from low carbon intensive fuel type generation, such as gas generation. High carbon intensive fuel type generation can be substituted by low carbon intensive fuel type generation under the carbon tax imposition by changing the relative dispatch cost between different fuel type generation; the increase in dispatch cost of high carbon intensive fuel type generation is relatively higher than the increase in dispatch cost of low carbon intensive fuel type generation. The carbon tax imposition can not affect CO_2 emissions from nuclear generation because nuclear generation dose not emit CO_2 at all.

In the simulation results, CO_2 emissions from nuclear generation do not change relative to base case through all scenarios because nuclear generation does not emit CO_2. Detailed results of CO_2 emissions from nuclear generation are displayed in Fig. 5.3 (a).

CO_2 emissions from coal generation are decreased by 1.33% under low level wind power penetration rate (SC1) and 2.93% under high level wind power penetration rate (SC2) relative to base case. Thus the increase in wind power penetration rate decreases CO2 emissions from coal generation. CO_2 emissions from coal generation are decreased by 0.26% under both low level carbon tax imposition (SC3) and high level carbon tax imposition (SC4) relative to base case. Thus there are no level effects on CO_2 reduction from coal generation between low and high level carbon tax imposition. CO_2 emissions from coal generation are also decreased in mixed options (SC5-SC8) relative to base case. The amount of total CO_2 emission reduction in mixed options is higher than the sum of reduction from each separate option. Thus joint effects of these two options show positive correlation in CO_2 emission reduction from coal generation. Detailed results of CO_2 emissions from coal generation are displayed in Fig. 5.3 (b).

CO_2 emissions from gas generation are decreased by 20.43% under low level wind power penetration rate (SC1) and 31.73% under high level wind power penetration rate (SC2) relative to base case. Thus the increase in wind power penetration rate decreases CO2 emissions from gas generation. CO_2 emissions from gas generation are increased by 0.02% under low level carbon tax imposition (SC3) and 0.07% under high level carbon

tax imposition (SC4) relative to base case. Thus the increase in carbon tax rate increases CO2 emissions from gas generation by substituting for other fossil-fuel generation. CO_2 emissions from gas generation are also decreased in mixed options (SC5-SC8) relative to base case. The amount of total CO_2 emission reduction in mixed options is lower than the sum of reduction from each separate option. Thus joint effects of these two options show negative correlation in CO_2 emission reduction from gas generation. Detailed results of CO_2 emissions from gas generation are displayed in Fig. 5.3 (c).

CO$_2$ emissions from oil generation are decreased by 13.69% under low level wind power penetration rate (SC1) and 26.51% under high level wind power penetration rate (SC2) relative to base case. Thus the increase in wind power penetration rate decreases CO2 emissions from oil generation. CO_2 emissions from oil generation are decreased by 0.02% under low level carbon tax imposition (SC3) and 0.14% under high level carbon tax imposition (SC4) relative to base case. Thus the increase in carbon tax rate decreases CO2 emissions from oil generation. CO_2 emissions from oil generation are also decreased in mixed options (SC5-SC8) relative to base case. The amount of total CO_2 emission reduction in mixed options is lower than the sum of reduction from each separate option. Thus joint effects of these two options show negative correlation in CO_2 emission reduction from oil generation. Detailed results of CO_2 emissions from oil generation are displayed in Fig. 5.3 (d).

5.3.3   Effects on Net Load

As earlier assumptions, this study does not consider price-responsive demand. Thus the carbon tax imposition can not affect net load and its volatility. Thus the wind power penetration level is the only treatment factor that can affect net load and its volatility. We can observe that wind power penetration decrease net load but increase net load volatility in actual electricity markets [36].

		Wind Penetration Rate (%)		
		0	9.66	17.7
CO2 Tax ($/tCO2)	0	0.00% (0.00)	0.00% (0.00)	0.00% (0.00)
	6.5	0.00% (0.00)	0.00% (0.00)	0.00% (0.00)
	20	0.00% (0.00)	0.00% (0.00)	0.00% (0.00)

(a) Nuclear generator

		Wind Penetration Rate (%)		
		0	9.66	17.7
CO2 Tax ($/tCO2)	0	0.00% (0.00)	-1.33% (0.43)	-2.93% (0.46)
	6.5	-0.26% (0.31)	-1.84% (0.22)	-3.54% (0.48)
	20	-0.26% (0.31)	-1.83% (0.22)	-3.55% (0.47)

(b) Coal generator

		Wind Penetration Rate (%)		
		0	9.66	17.7
CO2 Tax ($/tCO2)	0	0.00% (0.00)	-20.43% (9.96)	-31.73% (15.99)
	6.5	0.02% (0.06)	-19.57% (9.64)	-31.66% (15.97)
	20	0.07% (0.08)	-19.54% (9.67)	-31.57% (15.98)

(c) Gas generator

		Wind Penetration Rate (%)		
		0	9.66	17.7
CO2 Tax ($/tCO2)	0	0.00% (0.00)	-13.69% (7.21)	-26.51% (13.06)
	6.5	-0.02% (0.48)	-12.47% (6.44)	-26.40% (13.03)
	20	-0.14% (0.43)	-12.72% (6.47)	-26.65% (13.51)

(d) Oil generator

Figure 5.3: Effects of CO_2 reduction options on CO_2 emissions by fuel type

In the simulation results, net load is decreased by 3.39% under low level wind power penetration rate and 6.38% under high level wind power penetration rate relative to base case. Thus the increase in wind penetration rate decreases net load. Detailed results of net load are displayed in Fig. 5.4 (a).

Net load volatility is increased by 5.20% under low level wind penetration rate and 10.39% under high level wind penetration rate relative to base case in terms of CV. Thus the increase in wind penetration rate increases net load volatility. Detailed results of net load are displayed in Fig. 5.4 (b).

5.3.4   Effects on Locational Marginal Prices (LMPs)

Net load can be decreased under the wind power penetration. Thus the wind power penetration can decrease average LMP, because a decrease in net load implies a shift down of demand.

		Wind Penetration Rate (%)		
		0	9.66	17.7
CO2 Tax ($/tCO2)	0	0.00% (0.00)	-3.39% (1.26)	-6.38% (2.52)
	6.5	0.00% (0.00)	-3.39% (1.26)	-6.38% (2.52)
	20	0.00% (0.00)	-3.39% (1.26)	-6.38% (2.52)

(a) Net load

		Wind Penetration Rate (%)		
		0	9.66	17.7
CO2 Tax ($/tCO2)	0	0.00%	5.20%	10.39%
	6.5	0.00%	5.20%	10.39%
	20	0.00%	5.20%	10.39%

(b) Net load volatility

Figure 5.4: Effects of CO_2 reduction options on net load and its volatility

The wind power penetration can increase LMP volatility in terms of CV. CV is defined by "standard deviation/average". Thus CV can be increased (decreased) if standard deviation is increased (decreased) or average is decreased (increased).

As we can see from Fig. 5.4 (b), net load volatility can be increased under wind power penetration relative to base case. The increase in net load volatility can increase LMP volatility relative to base case because LMP is determined by load under given market construction. Thus the increase in LMP volatility and the decrease in average LMP can increase LMP volatility in terms of CV under wind power penetration.

LMP level is determined by the dispatch cost of marginal unit. The carbon tax imposition can increase average LMP by increasing the dispatch cost of fossil-fuel generators.

The carbon tax imposition can decrease LMP volatility; carbon tax imposition can bridge the dispatch cost gap between different fuel type generation. For example, the gas generation has the highest dispatch cost while the coal generation has the second lowest dispatch cost, but gas generation emits CO_2 around half less than coal generation in generating the same amount of electricity. Thus coal generation pays almost twice more carbon tax than gas generation and the dispatch cost gap between coal and gas generation can be decreased. This implies that the decrease in dispatch cost gap between different fuel type generation can decrease LMP volatility. The decrease in LMP volatility and the increase in average LMP can decrease LMP volatility in terms of CV.

When these two CO_2 reduction options are simultaneously used, the average LMP and its volatility would be determined by the relative magnitude of these two oppositely directed effects.

In the simulation results, average LMP is decreased by 9.29% under low level wind power penetration rate (SC1) and 16.87% under high level wind power penetration rate (SC2) relative to base case. Thus the increase in wind power penetration rate decreases average LMP. Average LMP is increased by 8.25% under low level carbon tax imposition (SC3) and 25.11% under high level carbon tax imposition (SC4) relative to base case. Thus the increase in carbon tax rate increases average LMP. The average LMP is decreased by 0.56% under low level wind power penetration rate and low level carbon tax imposition (SC5) and 8.34% under high level wind power penetration rate and low level carbon tax imposition (SC6) relative to base case. The average LMP is increased by 17.65% under low level wind power penetration rate and high level carbon tax imposition (SC7) and 10.44% under high level wind power penetration rate and high level carbon tax imposition (SC8) relative to base case. Detailed results of average LMP are displayed in Fig. 5.5 (a).

Volatility of LMP is increased by 14.61% under low level wind power penetration rate (SC1) and 24.65% under high level wind power penetration rate (SC2) relative to base case. Thus the increase in wind penetration rate increases volatility of LMP. Volatility of LMP is decreased by 12.68% under low level carbon tax imposition (SC3) and 33.62% under high level carbon tax imposition (SC4) relative to base case. Thus the increase in carbon tax rate decreases volatility of LMP. Volatility of LMP is decreased by 0.95% under low level wind power penetration rate and low level carbon tax imposition (SC5) while it is increased by 7.39% under high level wind power penetration rate and low level carbon tax imposition (SC6) relative to base case. Volatility of LMP is decreased by 25.55% under low level wind power penetration rate and high level carbon tax imposition (SC7) and 20.17% under high level wind power penetration rate and high level carbon

tax imposition (SC8) relative to base case. Detailed results of volatility of LMP are displayed in Fig. 5.5 (b).

		Wind Penetration Rate (%)		
		0	9.66	17.7
CO2 Tax ($/tCO2)	0	0.00% (0.00)	-9.29% (4.12)	-16.87% (8.45)
	6.5	8.25% (3.87)	-0.56% (6.42)	-8.34% (10.07)
	20	25.11% (7.24)	17.65% (9.29)	10.44% (11.57)

(a) Average LMP

		Wind Penetration Rate (%)		
		0	9.66	17.7
CO2 Tax ($/tCO2)	0	0.00%	14.61%	24.65%
	6.5	-12.68%	-0.95%	7.39%
	20	-33.62%	-25.55%	-20.17%

(b) Volatility of LMP

Figure 5.5: Effects of CO_2 reduction options on average LMP and its volatility

5.3.5 Effects on Thermal Generator Dispatch and Profit Levels

5.3.5.1 Effects on Dispatch Levels by Fuel Type

The effects of wind power penetration and carbon tax imposition on the dispatch can differ by fuel type. The wind power generation can decrease the dispatch by directly substituting for the dispatch of thermal generation such as nuclear, coal, gas and oil generation. But the degree of substitution can differ by fuel type; thermal generation with relatively high dispatch cost, such as gas and oil generation can be substituted by wind power generation more than thermal generation with relatively low dispatch cost, such as nuclear and coal generation. Even thermal generation with low dispatch cost can increase for balancing if the wind power generation substitutes generation with high dispatch cost much more than generation with low dispatch cost.

The carbon tax imposition can decrease relatively high carbon intensive fuel type generation dispatch such as coal and oil but increase relatively low carbon intensive fuel type generation dispatch such as nuclear and gas generation. This implies that high carbon intensive fuel type generation can be substituted by low carbon intensive fuel type

generation under the carbon tax imposition by changing relative dispatch cost between different fuel type generation; the increase in dispatch cost of high carbon intensive fuel type generation is relatively higher than the increase in dispatch cost of low carbon intensive fuel type generation.

In the simulation results, the nuclear generation dispatch are increased by 2.01% under low level wind power penetration rate (SC1) and 0.01% under high level wind power penetration rate (SC2) relative to base case. The nuclear generation dispatch is increased by 1.97% under both low level carbon tax imposition (SC3) and high level carbon tax imposition (SC4) relative to base case by substituting for high carbon intensive fossil-fuel generation, such as coal and oil generation. The nuclear generation dispatch are also increased in mixed options (SC5-SC8) relative to base case. The amount of the increase in nuclear generation dispatch in mixed options is higher than the sum of the increase in nuclear generation dispatch from each separate option. Thus joint effects of these two options show positive correlation in the increase in nuclear generation dispatch. Also, the amount of the increase in nuclear generation dispatch is identical across mixed options. Detailed results of the nuclear generation dispatch are displayed in Fig. 5.6 (a).

The coal generation dispatch is decreased by 1.33% under low level wind power penetration rate (SC1) and 2.93% under high level wind power penetration rate (SC2) relative to base case. Thus the increase in wind penetration rate decreases the coal generation dispatch. The coal generation dispatch is decreased by 0.26% under both low level carbon tax imposition (SC3) and high level carbon tax imposition (SC4) relative to base case. The coal generation dispatch are also decreased in mixed options (SC5-SC8) relative to base case. The amount of the decrease in coal generation dispatch in mixed options is higher than the sum of the decrease in dispatch from each separate option. Thus joint effects of these two options show positive correlation in the decrease in coal generation dispatch. Detailed results of coal generation dispatch are displayed in Fig. 5.6 (b).

The gas generation dispatch is decreased by 20.43% under low level wind power penetration rate (SC1) and 31.73% under high level wind power penetration rate (SC2) relative to base case. Thus the increase in wind penetration rate decreases the gas generation dispatch. The gas generation dispatch are increased by 0.02% under low level carbon tax imposition (SC3) and 0.07% under high level carbon tax imposition (SC4) relative to base case. Thus the increase in carbon tax rate increases the gas generation dispatch by substituting for high carbon intensive fossil-fuel generation, such as coal and oil generation. The gas generation dispatch is also decreased in mixed options (SC5-SC8) relative to base case. The amount of the decrease in gas generation dispatch in mixed options is smaller than the sum of gas generation dispatch from each separate option. Thus joint effects of these two options show negative correlation in the decrease in gas generation dispatch. Detailed results of the gas generation dispatch are displayed in Fig. 5.6 (c).

The oil generation dispatch is decreased by 13.69% under low level wind power penetration rate (SC1) and 26.51% under high level wind power penetration rate (SC2) relative to base case. Thus the increase in wind penetration rate decreases the oil generation dispatch. The oil generation dispatch is decreased by 0.02% under low level carbon tax imposition (SC3) and 0.14% under high level carbon tax imposition (SC4) relative to base case. Thus the increase in carbon tax rate decreases the oil generation dispatch. The oil generation dispatch is also decreased in mixed options (SC5-SC8) relative to base case. The amount of the decrease in oil generation dispatch in mixed options is smaller than the sum of the decrease in dispatch from each separate option. Thus joint effects of these two options show negative correlation in the decrease in oil generation dispatch. Detailed results of oil generation dispatch are displayed in Fig. 5.6 (d).

(a) Nuclear generator

		Wind Penetration Rate (%)		
		0	9.66	17.7
CO2 Tax ($/tCO2)	0	0.00% (0.0000)	2.01% (10.45)	0.01% (10.27)
	6.5	1.97% (1.95)	4.70% (10.23)	4.70% (10.23)
	20	1.97% (1.95)	4.70% (10.23)	4.70% (10.23)

(b) Coal generator

		Wind Penetration Rate (%)		
		0	9.66	17.7
CO2 Tax ($/tCO2)	0	0.00% (0.00)	-1.33% (0.43)	-2.93% (0.46)
	6.5	-0.26% (0.31)	-1.84% (0.22)	-3.54% (0.48)
	20	-0.26% (0.31)	-1.83% (0.22)	-3.55% (0.47)

(c) Gas generator

		Wind Penetration Rate (%)		
		0	9.66	17.7
CO2 Tax ($/tCO2)	0	0.00% (0.00)	-20.43% (9.96)	-31.73% (15.99)
	6.5	0.02% (0.06)	-19.57% (9.64)	-31.66% (15.97)
	20	0.07% (0.08)	-19.54% (9.67)	-31.57% (15.98)

(d) Oil generator

		Wind Penetration Rate (%)		
		0	9.66	17.7
CO2 Tax ($/tCO2)	0	0.00% (0.00)	-13.69% (7.21)	-26.51% (13.06)
	6.5	-0.02% (0.48)	-12.47% (6.44)	-26.40% (13.03)
	20	-0.14% (0.43)	-12.72% (6.47)	-26.65% (13.51)

Figure 5.6: Effects of CO_2 reduction options on dispatch by fuel type

5.3.5.2 Effects on Total Profit

Generally, the wind power penetration can decrease the total profit of thermal generator in two ways; it can decrease electricity price (average LMP) and the chance of thermal generation dispatch by directly substituting for it.

The carbon tax imposition can affects the profit of thermal generator in two ways; it can increase both electricity price and dispatch cost. The increase in electricity price and dispatch cost affects the profit of thermal generator in opposite way. Thus effects of the carbon tax imposition on the profit of thermal generator depend on the relative magnitude of these two opposite effects.

The effects of wind power penetration and carbon tax imposition on the profit of generator can differ by fuel type. More details about this issue are described in Section 5.3.5.3.

In the simulation results, the total profit of thermal generator is decreased by 12.10% under low level wind power penetration rate (SC1) and 22.05% under high level wind power penetration rate (SC2) relative to base case. Thus the increase in wind power penetration rate decreases the total profit of thermal generator.

The total profit of thermal generator is decreased by 2.43% under low level carbon tax imposition (SC3) and 7.79% under high level carbon tax imposition (SC4) relative to base case. Thus the increase in carbon tax imposition rate decreases total profit of thermal generator.

The total profit of thermal generator is also decreased in mixed options (SC5-SC8) relative to base case. The amount of the decrease in the total profit of thermal generator in mixed options is smaller than the sum of the decrease of profit from each separate option. Thus joint effects of these two options show negative correlation in the decrease in total profit of thermal generator. More detailed results about the total profit of thermal generator are described in Fig. 5.7.

		Wind Penetration Rate (%)		
		0	9.66	17.7
CO2 Tax ($/tCO2)	0	0.00% (0.00)	-12.10% (4.98)	-22.05% (9.37)
	6.5	-2.43% (3.81)	-14.01% (7.54)	-24.01% (11.99)
	20	-7.79% (10.16)	-17.45% (14.00)	-26.77% (18.23)

Figure 5.7: Effects of CO_2 reduction options on total thermal generator profit

5.3.5.3   Effects on Profits by Fuel Type

The effects of wind power penetration and carbon tax imposition on the profit of thermal generator can differ by fuel type. The wind power penetration can decrease electricity price and chance of thermal generator dispatch except nuclear power as men-

tioned in previous section. The decrease in electricity price and dispatch can decreases general profit of thermal generator. Also, the wind power penetration can increase net load volatility. This can give more chances for fast ramping unit, such as gas generator to be committed and dispatched for balance and reserve because frequency of the event for requiring fast raming unit increases as net load volatility increases. During the event for requiring fast raming unit, electricity price can be much higher than price in normal situation. Thus profit of fast ramping generator can be increased. Thus the profit of thermal generator by fuel type is determined relative to the magnitudes of these opposite effects under the wind power penetration.

The carbon tax imposition can increase both the electricity price and dispatch cost of thermal generator. Every thermal generator faces the same increase in electricity price but different increase in dispatch cost. High carbon intensive fuel type generator, such as coal and oil generator faces higher increase in dispatch cost than low carbon intensive fuel type generator, such as nuclear and gas generator. If the increase in electricity price is relatively higher than the increase in dispatch cost for low carbon intensive fuel type generator, then profit of low carbon intensive fuel type generator can be increased. Thus the profit of thermal generator by fuel type is determined relative to the magnitudes of these opposite effects under the carbon tax imposition.

In the simulation results, the profit of nuclear generator is decreased by 10.71% under low level wind power penetration rate (SC1) and 22.82% under high level wind power penetration rate (SC2) relative to base case. Thus the increase in wind power penetration rate decreases profit of nuclear generator. Profit of nuclear generator is increased by 12.29% under low level carbon tax imposition (SC3) and 36.90% under high level carbon tax imposition (SC4) relative to base case because nuclear power does not emit CO_2. The profit of nuclear generator is increased by 2.62% under low level wind power penetration rate and low level carbon tax imposition (SC5), 29.88% under low level wind power penetration rate and high level carbon tax imposition (SC7), and

18.25% under high level wind power penetration rate and high level relative to base case. However, profit of nuclear generator is decreased by 9.66% under high level wind power penetration rate and low level carbon tax imposition (SC6) relative to base case. Detailed results of nuclear generator profit are displayed in Fig. 5.8 (a).

Profit of coal generator is decreased by 12.08% under low level wind power penetration rate (SC1) and 21.90% under high level wind power penetration rate (SC2) relative to base case. Thus the increase in wind power penetration rate decreases profit of coal generator. Profit of coal generator is decreased by 4.31% under low level carbon tax imposition (SC3) and 13.46% under high level carbon tax imposition (SC4) relative to base case. Thus the increase in carbon tax rate decreases profit of nuclear generator. Profit of coal generator is also decreased in mixed options (SC5-SC8) relative to base case. The amount of the decrease in profit of coal generator in mixed options is smaller than the sum of the decrease in profit from each separate option. Thus joint effects of these two options show negative correlation in the decrease in profit of coal generator. Detailed results of the profit of coal generator are displayed in Fig. 5.8 (b).

Profit of gas generator is decreased by 21.94% under low level wind power penetration rate (SC1) but increased 31.93% under high level wind power penetration rate (SC2) relative to base case. This implies that the frequency of event for requiring high ramping unit increases as wind power penetration rate increases and the relative magnitude of this effect on the increase in profit of gas generator is greater than the effect on the decrease in profit by decreasing electricity price under high level wind power penetration rate. Profit of gas generator is increased by 0.08% under low level carbon tax imposition (SC3) and 0.60% under high level carbon tax imposition (SC4) relative to base case. Thus the increase in carbon tax rate increases profit of gas generator because gas generation is relatively low carbon intensive generation. Profit of gas generator is decreased by 20.12% under low level wind power penetration rate and low level carbon tax imposition (SC5) and 19.73% under low level wind power penetration rate and high level carbon tax

imposition (SC7) relative to base case. However, profit of gas generator is increased by 29.14% under high level wind power penetration rate and low level carbon tax imposition (SC6) and 24.24% under high level wind power penetration rate and high level carbon tax imposition relative to base case. Detailed results of gas generator profit are displayed in Fig. 5.8 (c).

Profit of oil generator is decreased by 16.76% under low level wind power penetration rate (SC1) and 33.24% under high level wind power penetration rate (SC2) relative to base case. Thus the increase in wind power penetration rate decreases profit of oil generator. Profit of oil generator is decreased by 3.09% under low level carbon tax imposition (SC3) and 11.05% under high level carbon tax imposition (SC4) relative to base case. Thus the increase in carbon tax rate decreases profit of nuclear generator. Profit of oil generator is also decreased in mixed options (SC5-SC8) relative to base case. The amount of the decrease in profit of oil generator in mixed options is smaller than the sum of the decrease in profit from each separate option. Thus joint effects of these two options show negative correlation in the decrease in profit of oil generator. Detailed results of oil generator profit are displayed in Fig. 5.8 (d).

5.3.6 Effects on Wind Power Generator Profit and Tax Revenue

Renewable power generator usually faces negative profit (loss) in real world because the life time cost of renewable generator is higher than the life time revenue of it. Thus governments provide subsidies for the loss of renewable power generator. For example, the U.S. Federal Government gives federal production tax credit (PTC), 2.3 cents per kilowatt-hour (3.4 to 3.7 cents per kilowatt-hour in pre-tax value), to subsidize for the loss of renewable electricity generation [48].

Governments can earn carbon tax revenue by imposing carbon tax. Carbon tax revenue can give several policy options to governments such as carbon tax swap with income tax, investing in renewable resources, and carbon capture-and-storage technology [62] or

		Wind Penetration Rate (%)		
		0	9.66	17.7
CO2 Tax ($/tCO2)	0	0.00% (0.00)	-10.71% (11.93)	-22.82% (16.96)
	6.5	12.29% (12.65)	2.62% (17.21)	-9.66% (22.05)
	20	36.90% (14.95)	29.88% (17.51)	18.52% (20.58)

(a) Nuclear generator

		Wind Penetration Rate (%)		
		0	9.66	17.7
CO2 Tax ($/tCO2)	0	0.00% (0.00)	-12.08% (5.31)	-21.90% (10.16)
	6.5	-4.31% (1.86)	-15.94% (5.13)	-25.77% (10.02)
	20	-13.46% (2.63)	-23.25% (7.29)	-32.42% (12.01)

(b) Coal generator

		Wind Penetration Rate (%)		
		0	9.66	17.7
CO2 Tax ($/tCO2)	0	0.00% (0.00)	-21.94% (23.62)	31.93% (26.58)
	6.5	0.08% (0.54)	-20.12% (23.98)	29.14% (26.28)
	20	0.60% (1.42)	-19.73% (24.11)	24.24% (25.56)

(c) Gas generator

		Wind Penetration Rate (%)		
		0	9.66	17.7
CO2 Tax ($/tCO2)	0	0.00% (0.00)	-16.76% (11.18)	-33.24% (23.19)
	6.5	-3.09% (1.84)	-19.38% (11.02)	-35.91% (23.10)
	20	-11.05% (2.67)	-25.35% (10.05)	-40.72% (24.44)

(d) Oil generator

Figure 5.8: Effects of CO_2 reduction options on profit by fuel type

can be used for further tax reforms [17].

The carbon tax imposition can increase profit of renewable generator because it increases electricity price but does not increase dispatch cost of renewable generator. Also, the wind power penetration can reduce carbon tax revenue by replacing thermal generation dispatch which is the source of carbon tax revenue.

In the simulation results, wind power generator faces loss in all scenarios, because its cost which is measured as exogenous levelized cost is usually greater than average LMP per MWh. The profit of wind power generator under low level wind power penetration rate is greater than the profit of wind power generator under high level wind power penetration rate given the same level of carbon tax imposition; profit of wind power generator in SC1, SC5 and SC7 is greater than the profit in SC2, SC6 and SC8 respectively. Thus profit of wind power generator decreases as wind power penetration rate increases.

On the other hand, profit of wind power generator under high level carbon tax imposition is greater than profit of wind power generator under low level carbon tax imposition given the same level of wind power penetration rate; profit of wind power generator in SC4, SC7 and SC8 is greater than the profit in SC3, SC5 and SC6 respectively. Thus profit of wind power generator increases as carbon tax rate increases.

The carbon tax revenue under low level wind power penetration rate is greater than carbon tax revenue under high level wind power penetration rate given the same level of carbon tax imposition; carbon tax revenue in SC3 and SC4 is greater than the profit in SC5 and SC6 respectively, and the profit in SC7 and SC8 is greater than the profit in SC5 and SC6 respectively. Thus the carbon tax revenue decreases as wind power penetration rate increases.

On the other hand, the carbon tax revenue under high level carbon tax rate is greater than the carbon tax revenue under low level wind power penetration rate given the same level of wind power penetration rate; carbon tax revenue in SC3 and SC4 is greater than the profit in SC5 and SC7 respectively, and the profit in SC5 and SC7 is greater than the profit in SC6 and SC8 respectively. Thus the carbon tax revenue increases as carbon tax rate increases.

Whenever the wind penetration and carbon tax imposition coexist in the simulated electricity market, carbon tax revenue is greater than the loss of wind power generator. Thus carbon tax revenues are sufficient to subsidize for all loss when these two options coexist in the simulated electricity market. More detailed results are presented in Table 5.4

Table 5.4: Simulated daily average profit of wind power generator and carbon tax revenues ($)

Scenarios	W. Profit	CT. Revenue	W. Profit + CT. Revenue
SC1	-190964	N/A	-190964
	(44621)		(44621)
SC2	-439281	N/A	-439281
	(165098)		(165098)
SC3	N/A	989400	989400
		(74703)	(74703)
SC4	N/A	3044257	3044257
		(229841)	(229841)
SC5	-159404	958025	798621
	(33663)	(62919)	(32198)
SC6	-380460	930562	550102
	(142272)	(53843)	(107421)
SC7	-94423	2947753	2853330
	(13788)	(193599)	(181856)
SC8	-251475	2863163	2611688
	(94894)	(165653)	(121768)

5.4 Conclusions and Policy Implications

This paper analyzes the impact of two treatment factors for CO_2 reduction options, a wind power penetration and a carbon tax imposition, on CO_2 emissions and other electricity market key outcomes using the Midcontinent Independent System Operator (MISO) data. The analysis is implemented based on the agent-based electricity market

platform called the AMES Wholesale Power Market Test Bed. Specifically, the MISO Midwest 7-zone test bed developed in Chapter 4 is used to study the effects of CO_2 reduction options on electricity market outcomes. This test bed captures the core features of MISO, such as MISO operations, physical attributes of MISO generation technology and capacity by fuel type, and MISO transmission constraints during 2013. Also, simulated scenarios are established based on practical grounds of carbon tax imposition and wind power policies: carbon tax scenarios are based on a proposal in the U.S. Congressional Budget Office Report [17] and wind power penetration rate scenarios are based on the current MISO wind power penetration rate and the 2025 MISO projection [43]. So, this model is not purely hypothetical but an empirically-based test bed. Thus this test bed can be useful to obtain meaningful results and implications for real-world electricity markets through sensitivity studies.

Based on these scenarios, various sensitivity studies are implemented to investigate the effects of CO_2 reduction options on CO_2 emissions, net load and its volatility, average LMP and its volatility, outcomes of thermal generators such as dispatch level and profit relative to base case, electricity markets without the wind power penetration and the carbon tax imposition. The effects of CO_2 reduction options on profit of wind power generator and government carbon tax revenues is also investigated in the simulated electricity market. Below a concise summary and implications are provided.

(i) Joint CO_2 emission reduction options can substantially reduce total CO_2 emissions.

It is shown that CO_2 emissions are decrease by 6.17% under 17.7% of wind penetration rate and \$20/tCO$_2$ of carbon tax imposition relative to base case.

(ii) The effects of CO_2 reduction options on CO_2 emissions can differ by fuel type

CO_2 emissions from coal, gas, and oil generation are decreased under wind power penetration relative to base case. CO_2 emissions from coal and oil generation are decreased under carbon tax imposition but CO_2 emissions from gas generation are increased under carbon tax imposition relative to base case. On the other hand, CO_2 emissions from

nuclear generation are not changed under these two CO_2 reduction options because it does not emit CO_2 at all.

(iii) CO_2 reduction options can affect net load and its volatility

Net load decreases but its volatility increases as wind penetration rate increases relative to base case.

(iv) CO_2 reduction options can affect average LMP and its volatility

Average LMP decreases but its volatility increases as wind penetration rate increases relative to base case. On the other hand, average LMP increases but its volatility decreases as carbon tax rate increases relative to base case.

(v) The effects of CO_2 reduction options on generation dispatch can differ by fuel type

Generation dispatch of coal, gas, and oil generation is decreased but generation dispatch of nuclear generation is increased under wind power penetration relative to base case. Generation dispatch of coal and oil generation is decreased but generation dispatch of nuclear and gas generation is increased under carbon tax imposition relative to base case.

(vi) CO_2 reduction options can affect total profit of thermal generator

Total profit of thermal generator is decreased under wind power penetration or carbon tax imposition relative to base case.

(vii) The effects of CO_2 reduction options on profit can differ by fuel type

Profit of nuclear, coal, and oil generator is decreased under wind power penetration relative to base case. Profit of gas generator is decreased under 9.66% of wind power penetration rate but it is increased under 17.7% of wind power penetration rate relative to base case. Profit of coal and oil generation is decreased but profit of nuclear and gas generation is increased under the carbon tax imposition relative to base case.

Thus governments need to investigate the effects of the decrease in profit of thermal generator by fuel type for implementing CO_2 emission reduction options. Guarantee-

ing appropriate profit is important to attain resource adequacy by providing proper incentives for generator to invest in electric power utilities. Thus appropriate profit is inevitable factor to obtain electric power market reliability and security.

Under this circumstance, governments should consider plans to attain appropriate profit when they introduce CO_2 emission reduction options. For example, guaranteeing appropriate coal generator profit is important because coal generator faces the decrease in profit under any simulated scenarios. If not, coal generator retires or do not invest on its infrastructure. This will reduce capacity of coal generation which plays an important role as base generation and electricity markets can suffer from insufficient capacity.

(viii) The effects of CO_2 reduction options on profit of wind power generator and carbon tax revenue

The profit of wind power generator increases as wind power penetration rate decreases and carbon tax rate increases. The carbon tax revenue increases as wind power penetration rate decreases and carbon tax imposition rate increases.

Although wind power generator faces loss in the simulation results, carbon tax revenue is greater than the loss of wind power generator whenever the wind penetration and the carbon tax imposition coexist in electricity markets. Thus carbon tax revenue can be sufficient source of subsidies for the loss of wind power generator when these two options.

In addition to this study, we can consider investment decisions for wind power generation. The decision making process for wind power generation investment can be incorporated into the test bed for future work. Also, future work will permit learning capabilities for electric power traders to analyze strategic behaviors and their effects on CO_2 emissions and other market key outcomes given CO_2 reduction options. Moreover, price-responsive demands can be included, which is an important aspect of the envisioned future smart grid. Future work can also consider incorporation of electricity market models into Macroeconomic models to investigate the effects of CO_2 emission reduction options on national and/or global economies.

CHAPTER 6.   GENERAL CONCLUSION

This thesis investigates the implication of empirical grounded electric power market facts using multiple methodologies, including market and contract design, analytic method, statistical method, and agent-based simulation method. Basically, this thesis focuses on centrally-managed electric power markets.

European and U.S. electricity sectors have undergone substantial restructuring over the past twenty years. They have devolved from highly regulated systems operated by vertically integrated utilities to relatively decentralized systems based more fully on market valuation and allocation mechanisms.

As part of this restructuring, oversight agencies have been established at several different levels to encourage cooperation and coordination. The European Network of Transmission System Operators for Electricity (ENTSO-E), founded in 2008, currently consists of forty-one Transmission System Operators (TSOs) from thirty-four European countries; its primary task is to promote the coordinated management of the European power grid. The U.S. Federal Energy Regulatory Commission (FERC) oversees the activities of seven Independent System Operators (ISOs), established since the mid-1990s, that are tasked with managing power system operations in seven U.S. electric energy regions comprising over 60% of U.S. generating capacity: namely, CAISO, ERCOT, ISO-NE, MISO, NYISO, PJM, and SPP.

These restructuring efforts have been driven by a desire to ensure efficient energy production and utilization, reliable energy supplies, affordable energy prices, and effective rules and regulations for environmental protection. In keeping with the latter goal, a

dramatic change is taking place in energy mixes: namely, a rapid penetration of variable energy resources combined with a movement away from traditional thermal generation.

Variable energy resources (VERs) are renewable energy resources, such as wind and solar power, whose generation cannot be closely controlled to match changes in load or to meet other system requirements. Consequently, the integration of VERs tends to increase the volatility of net load (ie, load minus as-available generation) as well as the frequency of strong ramp events. Flexibility in service provision by other types of resources then becomes increasingly important to maintain the reliability and efficiency of power system operations.

To accommodate increased VER penetration, TSOs and ISOs have introduced major changes in their market rules and operational procedures. These changes have included new product definitions to enhance load-following capability (eg, ramping products), revised market eligibility requirements to encourage greater VER participation, and the introduction of capacity markets in an attempt to ensure sufficient thermal generation as a backstop for the intermittency of VER generation.

Also, CO_2 emission issues are increasing important in electric power markets. In the U.S., the largest source of CO_2 emissions is the electricity sector, which was responsible for 32% of total emissions in 2012. The Obama Administration proposed a Clean Power Plan in June 2014; nationwide, by 2030, this plan would achieve approximately 30 percent of CO_2 emission reduction relative to 2005 CO_2 emission levels in the power sector. There are several important issues arising from carbon mitigation options such as a carbon tax imposition and increase penetration of VERs need to be resolved.

First, current electric power markets need appropriate compensation for flexibility in service provision. TSO/ISO product definitions are specified in broad rigid terms (eg, capacity, energy, ramp-rate, regulation, non-spinning reserve) that do not permit resources to be further differentiated and compensated on the basis of additional valuable flexibility in service provision, such as an ability to ramp up and down between minimum

and maximum values over very short time intervals. Second, VERs increase volatility and uncertainty in electric power markets because VERs are non-dispatchable. When the penetration of renewable energy reaches relatively high levels, characteristics and operations of the current power system will be significantly changed and additional costs will be incurred in order to ensure sufficient resources for system reliability. Third, carbon tax imposition can change relative generation costs of generators based on carbon intensities implied by fuel type. This can lead fuel mix changes in current power markets and affects market participants' profits. Thus a thorough studies are necessary to resolve these key issues in electric power markets.

Chapter 2 introduces standardized energy and reserve contracts with swing (flexibility) in their contractual terms to resolve key issues that have arisen for centrally-managed wholesale electric power markets with increased penetration of renewable energy resources. Key policy implications of our proposed market-supported trading of standardized contracts (SCs) permitting swing (flexibility) in their contractual terms are as follows:

- The SC system permits separate full market-based compensation for service availability and service performance

- The SC system facilitates a level playing field for market participation

- The SC system facilitates co-optimization of energy and reserve markets

- The SC system supports forward-market trading of energy and reserve

- The SC system permits resources to offer flexible service availability

- The SC system gives system operators flexibility in their real-time use of offered services

- The SC system encourages accurate load forecasting and the accurate following of real-time dispatch instructions

- The SC system permits resources to internally manage unit commitment and generation-capacity constraints

- The SC system permits robust-control management of uncertain net load

- The SC system eliminates need for out-of-market payment adjustments

- The SC system reduces the complexity of market rules

Chapter 3 develops an extended system pattern method for short-term forecasting of power market performance. Chapter 3 demonstrates that the penetration of renewable energy resources can change the realization of system patterns. Also, uncertainties embedded in the non-dispatchable renewable energy can change the system pattern given fixed load. The transition probabilities governing the system pattern changes depend on the probability density function of the non-dispatchable renewable power generation. Also, Chapter 3 introduces the concept of empirically-based system pattern transition matrix which can be constructed from historical system pattern data. This transition matrix can be applicable to the prediction of system patterns (or status of system variables). In addition, the system pattern method can be applicable to a load scenario reduction method, because i) each system pattern corresponds to a unique combination of binding constraints in the power system; and ii) the LMP volatility is relatively lower when the net load fluctuates within the same system pattern, while the LMP volatility is relatively higher when the net load fluctuates across the system patterns.

Chapter 4 develops an empirically-based test system based on data from the Midcontinent Independent System Operator (MISO) for application in electric power market studies. This test system embeds MISO's rules of operation, physical attributes of market generation technology and capacity, transmission constraints, and capacity proportion by fuel type. The performance test of the test system reports that this test system can well demonstrate the actual MISO situations.

Chapter 5 systematically analyzes the effects of a carbon tax and wind power penetration on electric power market key outcomes such as CO_2 emissions, generator dispatch levels, costs, revenues and profits, and carbon tax revenues using the test system developed in Chapter 4. Key findings are as follows:

- Joint CO_2 emission reduction options can substantially reduce total CO_2 emissions.

- The effects of CO_2 reduction options on CO_2 emissions can differ by fuel type

- CO_2 reduction options can affect net load and its volatility

- CO_2 reduction options can affect average LMP and its volatility

- The effects of CO_2 reduction options on generation dispatch can differ by fuel type

- CO_2 reduction options can affect total profit of thermal generator

- The effects of CO_2 reduction options on profit can differ by fuel type

- The effects of CO_2 reduction options on profit of wind power generator and carbon tax revenue

For interesting extensions of Chapter 2, we can explore more carefully the optimal design of linked forward markets for the market supported trading of standardized contracts. we can also develop a software test bed that will permit the study of these issues by means of systematic computational experiments.

For interesting extensions of Chapter 5, we can consider investment decisions for wind power generation. The decision making process for wind power generation investment can be incorporated into the test bed for future work. Future work can also permit learning capabilities for electric power traders to analyze strategic behaviors and their effects on CO_2 emissions and other market key outcomes given CO_2 reduction options. Moreover, price-responsive demands can be included, which is an important aspect of the

envisioned future smart grid. Future work can also consider incorporation of electricity market models into Macroeconomic models to investigate the effects of CO_2 emission reduction options on national and/or global economies.

APPENDIX A.   COMPARISON: PROPOSED SC SYSTEM

VS. REAL-WORLD ISO

Table A.1: Comparison between proposed SC system and real-world ISOs

ISO name	Product name	Contract form	Price determination process	Settlement	Changes under proposed SC system	Remarks on proposed SC system
CAISO	Capacity	Bilateral contracts	Bilateral contracts	Negotiated by counterparties	1. No rigid separation of capacity, reserve and energy products	1. SC system does not limit bilateral trade between market participants
	Regulation	DAM/RTM contracts	DAM/RTM co-opt process for reg., other anc. services, & energy	Capacity & performance payments (Order 755 compliance)		
	Other ancillary services	DAM/RTM contracts	DAM/RTM co-opt process for reg., other anc. services, & energy	Marginal pricing	2. SCs with swing can be used for capcity, reserve (various types), and energy	2. SC system uses discriminatory pricing for SC procurement while current centrally-managed markets use local uniform pricing for product procurement
	Energy	DAM/RTM contracts	DAM/RTM co-opt process for reg., other anc. services, & energy	LMP pricing	3. Cleared SCs are separately compensated for service availability	
ERCOT	Capacity	No capacity market	DAM/RTM scarcity pricing	LMP pricing	and for service performance under a discriminatory-price mechanism	
	Regulation	DAM/RTM contracts	DAM/RTM co-opt process for reg., other anc. services, & energy	Marginal pricing		
	Other ancillary services	DAM/RTM contracts	DAM/RTM co-opt process for reg., other anc. services, & energy	Marginal pricing	4. Service availability is compensated at time of SC procurement through SC offer prices and	3. SC system's two-part pricing attained by discriminatory price mechanism eliminates need for out-of-market
	Energy	DAM/RTM contracts	DAM/RTM co-opt process for reg., other anc. services, & energy	LMP pricing		

ISO name	Product name	Contract form	Price determination process	Settlement	Changes under proposed SC system	Remarks on proposed SC system
ISO-NE	Capacity	Forward capacity market contracts	Capacity auction	Several-steps-ahead process to determine capacity settlements	SC service performance is compensated ex post via SC performance payment methods	make-whole payments
	Regulation	RTM contracts	RTM co-opt process for reg., other anc. services, & energy	Capacity & performance payments (Order 755 compliance)		
	Other ancillary services	Forward reserve market & RTM contracts	Forward reserve market; RTM co-opt process for reg., other anc. services, & energy	Marginal pricing		
	Energy	DAM/RTM contracts	Energy opt in DAM with reserve constraint; Energy co-opt with reg. & other anc. services in RTM	LMP pricing		
MISO	Capacity	Forward capacity market contracts	Capacity auction	Several-steps-ahead process to determine capacity settlements		
	Regulation	DAM/RTM contracts	DAM/RTM co-opt process for reg., other anc. services, & energy	Capacity & performance payments (Order 755 compliance)		
	Other ancillary services	DAM/RTM contracts	DAM/RTM co-opt process for reg., other anc. services, & energy	Marginal pricing		
	Energy	DAM/RTM contracts	DAM/RTM co-opt process for reg., other anc. services, & energy	LMP pricing		
NYISO	Capacity	Forward capacity market contracts	Capacity auction	Several steps ahead process to determine capacity settlements		
	Regulation	DAM/RTM contracts	DAM/RTM co-opt process for reg., other anc. services, & energy	Capacity & performance payments (Order 755 compliance)		
	Other ancillary services	DAM/RTM contracts	DAM/RTM co-opt process for reg., other anc. services, & energy	Marginal pricing		
	Energy	DAM/RTM contracts	DAM/RTM co-opt process for reg., other anc. services, & energy	LMP pricing		

ISO name	Product name	Contract form	Price determination process	Settlement	Changes under proposed SC system	Remarks on proposed SC system
PJM	Capacity	Forward capacity market contracts	Capacity auction	Several-steps-ahead process to determine capacity settlements		
	Regulation	DAM/RTM contracts	DAM/RTM co-opt process for reg., other anc. services, & energy	Capacity & performance payments (Order 755 compliance)		
	Other ancillary services	DAM/RTM contracts	DAM/RTM co-opt process for reg., other anc. services, & energy	Marginal pricing		
	Energy	DAM/RTM contracts	DAM/RTM co-opt process for reg., other anc. services, & energy	LMP pricing		
SPP	Capacity	Bilateral contracts scheduled in DAM	Load shares adjusted by self-provision	Invoiced by SPP		
	Regulation	DAM/RTM contracts	DAM/RTM co-opt process for reg., other anc. services, & energy	Capacity & performance payments (Order 755 compliance)		
	Other ancillary services	DAM/RTM contracts	DAM/RTM co-opt process for reg., other anc. services, & energy	Marginal pricing		
	Energy	DAM/RTM contracts	DAM/RTM co-opt process for reg., other anc. services, & energy	LMP pricing		

APPENDIX B.   PROOF OF PROPOSITION 2

The proof of **Proposition 2** follows the proof presented in Zhou et al. [97]. The Lagrangian function for the extended DC-OPF problem (3.19) can be written as follows:

$$
\begin{aligned}
\mathcal{L} = &\sum_{k=1}^{K}[a_k P_k + b_k P_k^2] + \lambda \sum_{k=1}^{K}[P_k - L_k^{NET}] \\
&+ \sum_{k'=1}^{2K} \psi_{k'}(\sum_{k=1}^{K} \alpha_{kk'} P_k - C_{k'}) \\
&+ \sum_{\tau=1}^{2T} \mu_\tau (\sum_{k=1}^{K} \beta_{k\tau}[P_k - L_k^{NET}] - F_\tau)
\end{aligned}
\tag{B.1}
$$

The first order necessary Karush-Kuhn-Tucker (KKT) conditions for this problem are expressed as follows:

$$
a_k + 2b_k P_k + \lambda + \sum_{k'=1}^{2K} \psi_{k'} \alpha_{kk'}
$$
$$
+ \sum_{\tau=1}^{2T} \mu_\tau \beta_{k\tau} = 0, \quad k = 1, ..., K
$$

$$
\sum_{k=1}^{K}[P_k - L_k^{NET}] = 0,
$$

$$
\psi_{k'}(\sum_{k=1}^{K} \alpha_{kk'} P_k - C_{k'}) = 0,
$$

$$
\psi_{k'} \geq 0, \quad \sum_{k=1}^{K} \alpha_{kk'} P_k - C_{k'} \leq 0, \quad k' = 1, .., 2K
$$

$$\mu_\tau(\sum_{i=k}^{K} \beta_{k\tau}[P_k - L_k^{NET}] - F_\tau = 0,$$

$$\mu_\tau \geq 0, \quad \sum_{k=1}^{K} \beta_{k\tau}[P_k - L_k^{NET}] - F_\tau = 0, \quad \tau = 1, .., 2T$$

Table B.1 describes the number of binding and non-binding constraints for generation capacities and transmission lines and corresponding slack variables for non-binding constraints.

Table B.1: Number of binding and non-binding constraints

Constraint category	Binding constraints	Non-Binding constraints	Slack variables
Capacity	First $\mathcal{B}$	$2K - \mathcal{B}$	$\mathcal{S}_{k'}$
Line limit	First $\mathcal{M}$	$2T - \mathcal{M}$	$\mathcal{V}_\tau$

By using slack-variables introduced in Table B.1, the KKT first order conditions can be rewritten as follows:

$$a_k + 2b_k P_k + \lambda + \sum_{k'=1}^{2K} \psi_{k'} \alpha_{kk'}$$

$$+ \sum_{\tau=1}^{2T} \mu_\tau \beta_{k\tau} = 0, \quad k = 1, ..., K$$

$$\sum_{k=1}^{K} [P_k - L_k^{NET}] = 0,$$

$$\sum_{k=1}^{K} \alpha_{kk'} P_k - C_k' = 0,$$

$$\psi_{k'} \geq 0, \quad k' = 1, ..., \mathcal{B}$$

$$\sum_{k=1}^{K} \alpha_{kk'} P_k - C_{k'} = -\mathcal{S}_{k'},$$

$$\psi_{k'} = 0, \quad k' = \mathcal{B} + 1, ..., 2K$$

$$\sum_{k=1}^{K} \beta_{k\tau} P_k - \sum_{k=1}^{K} \beta_{k\tau} L_k^{NET} - F_\tau = 0,$$

$$\mu_\tau \geq 0, \quad \tau = 1, ..., \mathcal{M}$$

$$\sum_{k=1}^{K} \beta_{k\tau} P_k - \sum_{k=1}^{K} \beta_{k\tau} L_k^{NET} - F_\tau = -\mathcal{V}_\tau,$$

$$\mu_\tau = 0, \quad \tau = \mathcal{M} + 1, ..., 2T$$

By total differentiation of these KKT first order conditions, the sensitivity relations between variables can be expressed as follows:

$$2b_k dP_k + d\lambda + \sum_{k'=1}^{\mathcal{B}} \alpha_{kk'} d\psi_{k'}$$
$$+ \sum_{\tau=1}^{\mathcal{M}} \beta_{k\tau} d\mu_\tau = 0, \quad k = 1, ..., K \tag{B.2}$$

$$\sum_{k=1}^{K} [dP_k - dL_k^{NET}] = 0, \tag{B.3}$$

$$\sum_{k=1}^{K} \alpha_{kk'} dP_k = 0, \quad k' = 1, ..., \mathcal{B} \tag{B.4}$$

$$\sum_{k=1}^{K} \beta_{k\tau} dP_k = \sum_{k=1}^{K} \beta_{k\tau} dL_k^{NET},$$

$$\tau = 1, ..., \mathcal{M} \tag{B.5}$$

$$\sum_{k=1}^{K} \alpha_{kk'} dP_k = -dS_{k'}, \quad k' = \mathcal{B}+1, ..., 2K \tag{B.6}$$

$$\sum_{k=1}^{K} \beta_{k\tau} dP_k = \sum_{k=1}^{K} \beta_{k\tau} dL_k^{NET} - dV_\tau,$$

$$\tau = \mathcal{M}+1, ..., 2T \tag{B.7}$$

Let only L_k^{NET} be varied while all other net loads are held fixed, i.e., $dL_k^{NET} \neq 0$ and $dL_{k'}^{NET} = 0$ for $k' = 1, ..., k-1, k+1, ..., K$. Dividing the sensitivity relations by dL_k^{NET}, the resulting relations can be expressed in matrix form as follows:

$$
\left[
\begin{array}{cccc|cccccccc}
2b_1 & 0 & \cdots & 0 & 1 & \alpha_{11} & \alpha_{12} & \cdots & \alpha_{1\mathcal{B}} & \beta_{11} & \beta_{12} & \cdots & \beta_{1\mathcal{M}} \\
0 & 2b_2 & \cdots & 0 & 1 & \alpha_{21} & \alpha_{22} & \cdots & \alpha_{2\mathcal{B}} & \beta_{21} & \beta_{22} & \cdots & \beta_{2\mathcal{M}} \\
\vdots & \vdots & \ddots & \vdots & \vdots & \vdots & \vdots & \ddots & \vdots & \vdots & \vdots & \ddots & \vdots \\
0 & 0 & \cdots & 2b_K & 1 & \alpha_{K1} & \alpha_{K2} & \cdots & \alpha_{K\mathcal{B}} & \beta_{K1} & \beta_{K2} & \cdots & \beta_{K\mathcal{M}} \\
\hline
1 & 1 & \cdots & 1 & 0 & 0 & 0 & \cdots & 0 & 0 & 0 & \cdots & 0 \\
\alpha_{11} & \alpha_{21} & \cdots & \alpha_{K1} & 0 & 0 & 0 & \cdots & 0 & 0 & 0 & \cdots & 0 \\
\alpha_{12} & \alpha_{22} & \cdots & \alpha_{K2} & 0 & 0 & 0 & \cdots & 0 & 0 & 0 & \cdots & 0 \\
\vdots & \vdots & \ddots & \vdots & \vdots & \vdots & \vdots & \ddots & \vdots & \vdots & \vdots & \ddots & \vdots \\
\alpha_{1\mathcal{B}} & \alpha_{2\mathcal{B}} & \cdots & \alpha_{K\mathcal{B}} & 0 & 0 & 0 & \cdots & 0 & 0 & 0 & \cdots & 0 \\
\beta_{11} & \beta_{21} & \cdots & \beta_{K1} & 0 & 0 & 0 & \cdots & 0 & 0 & 0 & \cdots & 0 \\
\beta_{12} & \beta_{22} & \cdots & \beta_{K2} & 0 & 0 & 0 & \cdots & 0 & 0 & 0 & \cdots & 0 \\
\vdots & \vdots & \ddots & \vdots & \vdots & \vdots & \vdots & \ddots & \vdots & \vdots & \vdots & \ddots & \vdots \\
\beta_{1\mathcal{M}} & \beta_{2\mathcal{M}} & \cdots & \beta_{K\mathcal{M}} & 0 & 0 & 0 & \cdots & 0 & 0 & 0 & \cdots & 0
\end{array}
\right]
\left[
\begin{array}{c}
dP_1/dL_k^{NET} \\
dP_2/dL_k^{NET} \\
\vdots \\
dP_K/dL_k^{NET} \\
\hline
d\lambda/dL_k^{NET} \\
d\psi_1/dL_k^{NET} \\
d\psi_2/dL_k^{NET} \\
\vdots \\
d\psi_{\mathcal{B}}/dL_k^{NET} \\
d\mu_1/dL_k^{NET} \\
d\mu_2/dL_k^{NET} \\
\vdots \\
d\mu_{\mathcal{M}}/dL_k^{NET}
\end{array}
\right]
=
\left[
\begin{array}{c}
0 \\
0 \\
\vdots \\
0 \\
1 \\
0 \\
0 \\
\vdots \\
0 \\
\beta_{k1} \\
\beta_{k2} \\
\vdots \\
\beta_{k\mathcal{M}}
\end{array}
\right]
\tag{B.8}
$$

158

$$
\begin{bmatrix}
\alpha_{1(\mathcal{B}+1)} & \alpha_{2(\mathcal{B}+1)} & \cdots & \alpha_{K(\mathcal{B}+1)} \\
\alpha_{1(\mathcal{B}+2)} & \alpha_{2(\mathcal{B}+2)} & \cdots & \alpha_{K(\mathcal{B}+2)} \\
\vdots & \vdots & \ddots & \vdots \\
\alpha_{1(2K)} & \alpha_{2(2K)} & \cdots & \alpha_{K(2K)} \\
\beta_{1(\mathcal{M}+1)} & \beta_{2(\mathcal{M}+1)} & \cdots & \beta_{K(\mathcal{M}+1)} \\
\beta_{1(\mathcal{M}+2)} & \beta_{2(\mathcal{M}+2)} & \cdots & \beta_{K(\mathcal{M}+2)} \\
\vdots & \vdots & \ddots & \vdots \\
\beta_{1(2T)} & \beta_{2(2T)} & \cdots & \beta_{K(2T)}
\end{bmatrix}
\begin{bmatrix}
dP_1/dL_k \\
dP_2/dL_k \\
\vdots \\
dP_K/dL_k
\end{bmatrix}
=
\begin{bmatrix}
-d\mathcal{S}_{\mathcal{B}+1}/dL_k^{NET} \\
-d\mathcal{S}_{\mathcal{B}+2}/dL_k^{NET} \\
\vdots \\
-d\mathcal{S}_{2K}/dL_k^{NET} \\
\beta_{i(\mathcal{M}+1)} - d\mathcal{V}_{\mathcal{M}+1}/dL_k^{NET} \\
\beta_{k(\mathcal{M}+2)} - d\mathcal{V}_{\mathcal{M}+2}/dL_k^{NET} \\
\vdots \\
\beta_{k(2T)} - d\mathcal{V}_{2T}/dL_k^{NET}
\end{bmatrix}
\tag{B.9}
$$

Zhou et al. [98] prove that the following regularity condition automatically satisfied by DC OPF solutions suffices to guarantee the invertibility of the coefficient matrix (B.8):

$$
\mathcal{B} + \mathcal{M} + 1 \leq K \tag{B.10}
$$

Consequently the indicated system variable variations have a unique solution and this solution is a linear function of the net load variation given specific system pattern $j \in J$. By substituting this solution into (B.9), the slack variables can also be solved for as linear-affine functions of the net load variation and have a unique solution. The solution can be expressed as a reduced form with $J_{k\eta}^{SV,j}$, where SV denotes a relevant sub-vector of the system variables such as power generation level, P, power flows in transmission line, F, and LMPs; j denotes the underlying system pattern; η denotes the ηth element in the sub-vector of the specific system variable; and k denotes the index of bus for the net load variation. Following equation (B.11) and equation (B.12) show particular relations for power generation level, P, and power flows in transmission line, F.

$$
\begin{bmatrix}
dP_1/dL_k^{NET} \\
dP_2/dL_k^{NET} \\
\vdots \\
dP_K/dL_k^{NET}
\end{bmatrix}
=
\begin{bmatrix}
J_{1k}^{P,j} \\
J_{2k}^{P,j} \\
\vdots \\
J_{Kk}^{P,j}
\end{bmatrix}
\tag{B.11}
$$

$$
\begin{bmatrix}
d\mathcal{V}_{\mathcal{M}+1}/dL_k^{NET} \\
d\mathcal{V}_{\mathcal{M}+2}/dL_k^{NET} \\
\vdots \\
d\mathcal{V}_{2T}/dL_k^{NET}
\end{bmatrix}
\begin{bmatrix}
J_{(\mathcal{M}+1)k}^{F,j} \\
J_{(\mathcal{M}+2)k}^{F,j} \\
\vdots \\
J_{(2T)k}^{F,j}
\end{bmatrix}
\tag{B.12}
$$

Assume that every value in a net load interval between L_k^{NET0} and L_k^{NET} is associated with the same system pattern j. Let $P_{k'}$ and $P_{k'}^0$ denote the power generation solutions at bus k' for given net loads L_k^{NET0} and L_k^{NET} respectively. By integrating (B.11) with respect to dL_k^{NET}, a linear-affine relation between power generation and net load can be derived as follows:

$$
\int_{L_k^{NET0}}^{L_k^{NET}} \frac{dP_{k'}}{dL_k^{NET}} dL_k^{NET} = \int_{L_k^{NET0}}^{L_k^{NET}} J_{k'k}^{P,j} dL_k^{NET}
\tag{B.13}
$$

$$
P_{k'} - P_{k'}^0 = J_{k'k}^{P,j}[L_k^{NET} - L_k^{NET0}]
\tag{B.14}
$$

$$
P_{k'} = J_{k'k}^{P,j} L_k^{NET} + [P_{k'}^0 - J_{k'k}^{P,j} L_k^{NET0}]
\tag{B.15}
$$

By expressing this equation in vector form, the relation between power generation and net load can be expressed as a linear-affine function for each system pattern j taking the general form.

$$
\mathbf{P}^j = \mathbf{J}^{P,j} \mathbf{L}^{NET} + \mathbf{O}^{P,j}
\tag{B.16}
$$

where $\mathbf{P}^j = [P_1^j, ..., P_K^j]'$, $\mathbf{L}^{NET,j} = [L_1^{NET,j}, ..., L_K^{NET,j}]'$, $\mathbf{J}^{P,j}$ (sensitivity matrix) is a $K \times K$ matrix with k'th row and kth column element $J_{k'k}^{P,j}$ and $\mathbf{O}^{P,j}$ (ordinate vector) is a $K \times 1$ vector.

Similarly, this linear-affine relation can also be derived for other system variables. Particularly, the linear-affine function between power flows in transmission lines and net loads conditional on a system pattern j is as follows:

$$
\mathbf{F}^j = \mathbf{J}^{F,j} \mathbf{L}^{NET} + \mathbf{O}^{F,j}
\tag{B.17}
$$

where $\mathbf{F}^j = [F_1^j, ..., F_T^j]'$ is a $T \times 1$ vector of power flows in transmission lines, $\mathbf{J}^{F,j}$ is a $T \times K$ sensitivity matrix of power flows in transmission lines, and $\mathbf{O}^{F,j}$ is a $T \times 1$ ordinate vector of power flows in transmission lines.

Also, the linear-affine relation between LMPs and net load conditional on system pattern j is as follows:

$$\mathbf{LMP}^j = \mathbf{J}^{LMP,j}\mathbf{L}^{NET} + \mathbf{O}^{LMP,j} \tag{B.18}$$

where $\mathbf{LMP}^j = [LMP_1^j, ..., LMP_N^j]'$ is a $K \times 1$ LMP vector , $\mathbf{J}^{LMP,j}$ is a $K \times K$ LMP sensitivity matrix, and $\mathbf{O}^{LMP,j}$ is a $K \times 1$ LMP ordinate vector.

Moreover, the fuel types of the generating units located at each bus k are known in practice or can be assigned in simulation models. Table 5.1 in Section 3.3.1.1 already describes the coefficient of CO_2 emission per KWh (or MWh) by fuel type. Therefore, the linear-affine relation between power generation level and net load conditional on the system pattern j in equation (62) can be applied to obtain a linear-affine relation between CO_2 emissions and net load in electricity markets by the multiplying $K \times K$ CO_2 emission coefficient matrix $\mathbf{E}^{CO_2}$ on both sides of equation (62).[1]

$$\mathbf{E}^{CO_2} = \begin{bmatrix} e_{11}^{CO_2} & 0 & \cdots & 0 \\ 0 & e_{22}^{CO_2} & \cdots & 0 \\ \vdots & \vdots & \ddots & \vdots \\ 0 & 0 & \cdots & e_{KK}^{CO_2} \end{bmatrix} \tag{B.19}$$

$$\mathbf{E}^{CO2}\mathbf{P}^j = \mathbf{E}^{CO2}\mathbf{J}^{P,j}\mathbf{L}^{NET} + \mathbf{E}^{CO2}\mathbf{O}^{P,j}$$

$$\Rightarrow \mathbf{CO2}^j = \mathbf{J}^{CO2,j}\mathbf{L}^{NET} + \mathbf{O}^{CO2,j} \tag{B.20}$$

---

[1]By substituting other pollution emission coefficient matrices (for example, $SO_\times$, $NO_\times$,...) corresponding to generation fuel type in place of the CO_2 emission coefficient matrix, the linear-affine relation between CO_2 emissions and net load can be easily converted into a linear-affine relation between other types of pollution emissions and net load.

where e_{kk}^{CO2} is a CO_2 emission coefficient for the generating unit corresponding to its fuel type at bus k, $\mathbf{CO2}^j$ is a $K \times 1$ CO_2 emission vector, $\mathbf{J}^{CO2,j}$ is a $K \times K$ CO_2 emission sensitivity matrix, and $\mathbf{O}^{CO2,j}$ is a $K \times 1$ CO_2 emission ordinate vector.

APPENDIX C.   SIMULATED OUTCOMES FOR ALL CO_2 REDUCTION SCENARIOS

- CO_2-N: Average daily CO_2 emissions from nuclear generators (tCO_2)

- CO_2-C: Average daily CO_2 emissions from coal generators (tCO_2)

- CO_2-G: Average daily CO_2 emissions from gas generators (tCO_2)

- CO_2-O: Average daily CO_2 emissions from oil generators (tCO_2)

- CO_2-AG: Average daily CO_2 emissions from all generators (tCO_2)

- N-L: Average daily net load (MW)

- N-L CV: Average daily coefficient of variation of net load

- LMP: Average daily LMPs ($)

- LMP CV: Average daily coefficient of variation of LMPs

- Disp-N: Average daily dispatch level of nuclear generators (MW)

- Disp-C: Average daily dispatch level of coal generators (MW)

- Disp-G: Average daily dispatch level of gas generators (MW)

- Disp-O: Average daily dispatch level of oil generators (MW)

- Disp-W: Average daily dispatch level of wind power generators (MW)

- Disp-AG: Average daily dispatch level of all generators (MW)

- Rev-N: Average daily revenues of nuclear generators ($)

- Rev-C: Average daily revenues of coal generators ($)

- Rev-G: Average daily revenues of gas generators ($)

- Rev-O: Average daily revenues of oil generators ($)

- Rev-Tm: Average daily revenues of thermal generators ($)

- Rev-W: Average daily revenues of wind power generators ($)

- Rev-AG: Average daily revenues of all generators ($)

- Cost-N: Average daily costs of nuclear generators ($)

- Cost-C: Average daily costs of coal generators ($)

- Cost-G: Average daily costs of gas generators ($)

- Cost-O: Average daily costs of oil generators ($)

- Cost-Tm: Average daily costs of thermal generators ($)

- Cost-W: Average daily costs of wind power generators ($)

- Cost-AG: Average daily costs of all generators ($)

- Prof-N: Average daily profits of nuclear generators ($)

- Prof-C: Average daily profits of coal generators ($)

- Prof-G: Average daily profits of gas generators ($)

- Prof-O: Average daily profits of oil generators ($)

- Prof-O: Average daily profits of thermal generators ($)

- Prof-W: Average daily profits of wind power generators ($)

- Prof-AG: Average daily profits of all generators ($)

- Tax-N: Average daily carbon tax revenues from nuclear generators ($)

- Tax-C: Average daily carbon tax revenues from coal generators ($)

- Tax-G: Average daily carbon tax revenues from nuclear generators (\$)

- Tax-O: Average daily carbon tax revenues from nuclear generators (\$)

- Tax-AG: Average daily carbon tax revenues from nuclear generators (\$)

- Numbers in parenthesis denote standard deviations

Table C.1: All simulated outcomes for CO_2 reduction scenarios

	BC	SC1	SC2	SC3	SC4	SC5	SC6	SC7	SC8
CO_2-N	0	0	0	0	0	0	0	0	0
	(0)	(0)	(0)	(0)	(0)	(0)	(0)	(0)	(0)
CO_2-C	137648	135821	133617	137294	137291	135120	132768	135125	132763
	(5003)	(4744)	(4382)	(5327)	(5328)	(5015)	(4554)	(5017)	(4554)
CO_2-G	11130	8856	7599	11133	11137	8952	7606	8956	7616
	(5493)	(3950)	(3173)	(5493)	(5495)	(3960)	(3176)	(3960)	(3178)
CO_2-O	3789	3271	2785	3789	3784	3317	2789	3307	2779
	(1232)	(1064)	(897)	(1234)	(1230)	(1074)	(899)	(1070)	(895)
CO_2-AG	152567	147948	144001	152215	152213	147389	143163	147388	143158
	(11203)	(9379)	(8202)	(11493)	(11492)	(9680)	(8283)	(9680)	(8283)
N-L	184752	178486	172972	184752	184752	178486	172972	178486	172972
	(15586)	(13148)	(11067)	(15586)	(15586)	(13148)	(11067)	(13148)	(11067)
N-L CV	0.70	0.74	0.77	0.70	0.70	0.74	0.77	0.74	0.77
LMP	57	51	47	61	71	56	52	67	63
	(12)	(10)	(8)	(11)	(10)	(9)	(8)	(8)	(7)
LMP CV	0.41	0.47	0.51	0.36	0.27	0.40	0.44	0.30	0.32
Disp-N	18255	18621	18257	18615	18615	19113	19113	19113	19113
	(1956)	(425)	(555)	(1994)	(1994)	(1)	(1)	(0)	(0)
Disp-C	141671	139791	137523	141307	141305	139070	136649	139074	136643
	(5149)	(4883)	(4510)	(5483)	(5484)	(5161)	(4687)	(5164)	(4687)
Disp-G	20094	15989	13719	20099	20107	16161	13732	16168	13750
	(9916)	(7132)	(5728)	(9917)	(9921)	(7149)	(5734)	(7149)	(5738)
Disp-O	4783	4129	3515	4782	4777	4187	3520	4175	3508
	(1555)	(1343)	(1132)	(1558)	(1553)	(1356)	(1135)	(1351)	(1130)
Disp-W	N/A	6266	11780	N/A	N/A	6266	11780	6266	11780
		(2607)	(4901)			(2607)	(4901)	(2607)	(4901)
Disp-AG	184803	184796	184794	184803	184803	184796	184794	184797	184795
	(18576)	(16390)	(16827)	(18952)	(18951)	(16275)	(16459)	(16272)	(16457)

	BC	SC1	SC2	SC3	SC4	SC5	SC6	SC7	SC8
Rev-N	1018381	945446	850781	1114164	1295107	1050827	960528	1251218	1167731
	(232861)	(199578)	(160611)	(222723)	(216426)	(184619)	(150747)	(163936)	(134855)
Rev-C	8291083	7558994	6951668	8928690	10256180	8202116	7575903	9606191	8985272
	(1829975)	(1580845)	(1348935)	(1791801)	(1714240)	(1552064)	(1328801)	(1464984)	(1262784)
Rev-G	1567585	1247738	1093622	1640240	1791294	1319674	1143114	1441128	1245760
	(786604)	(565147)	(488022)	(822304)	(896776)	(592163)	(507114)	(645626)	(547030)
Rev-O	350463	296778	244503	369611	406262	315955	258086	349456	286597
	(117310)	(101865)	(82011)	(123476)	(135406)	(107298)	(86495)	(117112)	(95085)
Rev-Tm	11227513	10048956	9140574	12052705	13748843	10888573	9937631	12647993	11685361
	(2865172)	(2409948)	(2021547)	(2845786)	(2826452)	(2396485)	(2017178)	(2343697)	(1980477)
Rev-W	N/A	314075	510192	N/A	N/A	345635	569013	410616	697999
		(168616)	(240260)			(179049)	(262786)	(200280)	(311793)
Rev-AG	11227513	10048956	9140574	12052705	13748843	10888573	9937631	12647993	11685361
	(2865172)	(2409948)	(2021547)	(2845786)	(2826452)	(2396485)	(2017178)	(2343697)	(1980477)
Cost-N	283063	288862	283290	288441	288441	296208	296210	296217	296217
	(30630)	(6492)	(8577)	(31202)	(31202)	(24)	(22)	(0)	(0)
Cost-C	2547017	2508787	2465534	3432192	5285130	3373510	3311946	5197535	5103172
	(109897)	(103837)	(96901)	(151065)	(222989)	(142171)	(130164)	(209910)	(191580)
Cost-G	1536253	1223280	1052285	1608882	1759772	1294645	1102653	1415976	1206834
	(761964)	(548806)	(442822)	(797724)	(872151)	(575811)	(463845)	(629252)	(507114)
Cost-O	171907	148378	126214	196522	247386	172054	144531	216224	181563
	(55821)	(48261)	(40623)	(63951)	(80357)	(55702)	(46595)	(69987)	(58452)
Cost-Tm	4538240	4169306	3927324	5526037	7580729	5136417	4855340	7125952	6787786
	(896427)	(687770)	(566793)	(970653)	(1123036)	(752185)	(619993)	(880520)	(729731)
Cost-W	N/A	505039	949473	N/A	N/A	505039	949473	505039	949473
		(210133)	(395050)			(210133)	(395050)	(210133)	(395050)
Cost-AG	4538240	4169306	3927324	5526037	7580729	5136417	4855340	7125952	6787786
	(896427)	(687770)	(566793)	(970653)	(1123036)	(752185)	(619993)	(880520)	(729731)
Prof-N	735318	656584	567490	825722	1006666	754619	664318	955002	871514
	(221387)	(194378)	(158148)	(213417)	(203243)	(184627)	(150750)	(163936)	(134855)
Prof-C	5744065	5050207	4486134	5496499	4971050	4828607	4263956	4408656	3882100
	(1722353)	(1479568)	(1253352)	(1644108)	(1496168)	(1412805)	(1201613)	(1258406)	(1074960)
Prof-G	31332	24458	41337	31358	31522	25029	40462	25152	38926
	(27547)	(16902)	(75824)	(27509)	(27555)	(16897)	(72152)	(16914)	(65788)
Prof-O	177224	147526	118308	171750	157644	142881	113574	132302	105054
	(61449)	(53369)	(41704)	(59569)	(55180)	(51355)	(40192)	(46892)	(36948)
Prof-Tm	6687940	5878775	5213269	6525330	6166882	5751135	5082310	5521111	4897594
	(2003296)	(1740399)	(1474780)	(1909952)	(1735726)	(1661963)	(1414202)	(1482162)	(1266648)
Prof-W	N/A	-190964	-439281	N/A	N/A	-159404	-380460	-94423	-251475
		(44621)	(165098)			(33663)	(142272)	(13788)	(94894)
Prof-AG	6687940	5878775	5213269	6525330	6166882	5751135	5082310	5521111	4897594
	(2003296)	(1740399)	(1474780)	(1909952)	(1735726)	(1661963)	(1414202)	(1482162)	(1266648)
Tax-N	N/A	N/A	N/A	0	0	0	0	0	0
				(0)	(0)	(0)	(0)	(0)	(0)
Tax-C	N/A	N/A	N/A	892412	2745829	878280	862995	2702494	2655253
				(34626)	(106562)	(32596)	(29603)	(100347)	(91085)
Tax-G	N/A	N/A	N/A	72362	222749	58186	49440	179112	152324
				(35706)	(109906)	(25739)	(20643)	(79200)	(63569)
Tax-O	N/A	N/A	N/A	24626	75679	21559	18128	66147	55585
				(8022)	(24600)	(6980)	(5846)	(21408)	(17897)
Tax-AG	N/A	N/A	N/A	989400	3044257	958025	930562	2947753	2863163
				(74703)	(229841)	(62919)	(53843)	(193599)	(165653)

BIBLIOGRAPHY

[1] ACER, 2014. Commission implementing regulation (EU). Agency for the Cooperation of Energy Regulators (ACER), No. 1348/2014. *Official Journal of the European Union*, L363/121-L363/142.

[2] Aggarwal, S.K., Saini, L.M., Kumar, A., 2009. Electricity price forecasting in deregulated markets: A review and evaluation. *Electrical Power and Energy Systems 31*, 13-22.

[3] Äid, R., 2015. *Electricity Derivatives*. SpringerBriefs in Quantitative Finance. Springer International Publishing, ISSN 2192-7014 (electronic).

[4] AMES Wholesale Power Market Test Bed Homepage. Available at: http://www.econ.iastate.edu/tesfatsi/AMESMarketHome.htm

[5] Barber, C.B., Dobkin, D.P., Huhdanpaa, H., 1996. The quickhull algorithm for convex hulls. *ACM Transaction on Mathematical Software 22(4)*, 469-483.

[6] Bastian, J., Zhu, J., Banunarayanan, V., Mukerji, R., 1999. Forecasting energy Prices in a competitive market. *IEEE Computer Applications in Power 12(3)*, 40-45.

[7] Beacon Power, LLC., 2014. Overview of FERC Order 755 and pay-for-performance regulation. Available at:
http://www.ercot.com/content/meetings/fast/keydocs/2014/0321/Regulation%20Pay-for-Performance-032114.pdf

[8] Bidwell, M., 2005. Reliability options: A market-oriented approach to long-term adequacy. *The Electricity Journal 18(5)*, 11-25.

[9] Binh Dam, Q., Meliopoulos, A.P.S., Heydt, G., Bose, A., 2010. A breaker-oriented, three-phase IEEE 24-substation test system. *IEEE Transactions on Power Systems 25(1)*, 59-67.

[10] Bo, R., Li, F., 2009. Probabilistic LMP forecasting considering load uncertainty. *IEEE Transactions on Power Systems 24(3)*, 1279-1289.

[11] Bovenberg, A.L., Goulder, L.H., 1995. Costs of environmentally motivated taxes in the presence of other taxes: general equilibrium analyses. NBER Working Paper Series No. 5117, Cambridge, MA.

[12] Bull, N., Hassett, K., Metcalf, G., 1994. Who pays broad-based energy taxes? computing lifetime and regional incidence. The Energy Journal 15, 145-164.

[13] Bunn, D., 2004. Structural and behavioural foundations of competitive electricity prices, in: Bunn, D. (Eds.). *Modelling Prices in Competitive Electricity Markets.* John Wiley & Sons, 1-17.

[14] Bushnell, J.B., 2013. JP Morgan and market complexity. Energy Economics Exchange Blog. Available at: energyathaas.wordpress.com/2013/08/12/jp-morgan-and-market-complexity.

[15] CAISO, 2011. Technical Bulletin. Available at: http://www.caiso.com/Documents/TechnicalBulletin-MarketOptimizationDetails.pdf

[16] Casler, S.D., Rafiqui, A., 1993. Evaluating fuel tax equity: Direct and indirect distributional effects. National Tax Journal 56, 197-205.

[17] CBO (U.S. Congressional Budget Office), 2008. Policy Options for Reducing CO_2 Emissions. Available at: https://www.cbo.gov/publication/41663

[18] Chao, H.P., Wilson, R. 2002. Multi-dimensional procurement auctions for power reserves: Robust-incentive compatible scoring and settlement rules. *Journal of Regulatory Economics 22(2)*, 161-183.

[19] Chappin, E.J.L., Dijkema, G.P.J, 2009. On the impact of CO_2 emission-trading on power generation emissions. Technological Forecasting and Social Change 76, 358-370.

[20] Cong, R.G., Wei, Y.M., 2010. Potential impact of carbon emissions trading on China's power sector: A perspective from different allowance allocation options. *Energy 35*, 3921-3931.

[21] Contreras, J., Espinola, R., Nogales, F.J., Conejo, A.J., 2003. ARIMA models to predict next-day electricity prices. *IEEE Transactions on Power Systems 18(3)*, 1014-1020.

[22] Cramton, P., Ockenfels, A., 2012. Economics and design of capacity markets for the power Sector. *Zeitschrift für Energiewirtschaft 36(2)*, 113-134.

[23] Deb, R., Albert, R., Hsue, L.L., Brown, N., 2000. How to incorporate volatility and risk in electricity price forecasting.*Electricity Journal 13(4)*, 65-75.

[24] Delmas, M.A., Montes-Sancho, M.J., 2011. U.S. state policies for renewable energy: Context and effectiveness. Energy Policy 39, 2273-2288.

[25] Deng, S.J., Oren, S.S., 2006. Electricity derivatives and risk management. *Energy 31*, 940-953.

[26] EEI, 2014. Edison Electric Institute (EEI) Master Contract. Available at: http://www.eei.org/resourcesandmedia/mastercontract/Pages/default. aspx

[27] EEX, 2015. European Energy Exchange (EEX) Group Homepage.
Available at: https://www.eex.com/en/

[28] EIA, 2015. Energy Information Administration (EIA) Homepage. Available at: www.eia.gov/electricity/

[29] Ela, E., Milligan, M., Kirby, B., 2011. Operating reserves and variable generation, National Renewable Energy Laboratory, Technical Report NREL/TP-5500-51976, April.

[30] Ellison, J.F., Tesfatsion, L.S., Loose, V.W., Byrne, R.H., 2012. A survey of operating reserve markets in U.S. ISO/RTO-managed electric energy regions. Sandia National Laboratories Report (SAND2012-1000).

[31] ENTSO-E, 2014. Power system vision action paper, European Network Transmission System Operators for Electricity (ENTSO-E) Policy Paper. Available at: https://www.entsoe.eu/Documents/Publications/RDC%20publications/140822_Power_System_Vision_and_Action_Paper.pdf

[32] ENTSO-E, 2015. European Network Transmission System Operators for Electricity (ENTSO-E) Homepage. Available at: https://www.entsoe.eu/

[33] EPA, 2014. Inventory of U.S. Greenhouse Gas Emissions and Sinks: 1990 - 2012, EPA 430-R-14-003.

[34] EPA, 2015. Environmental Protection Agency (EPA) Homepage. Available at: http://www.epa.gov/

[35] EPEX, 2015. EPEX spot operational rules 20/03/2015. European Power Exchange (EPEX), March 20.

[36] EPRI, 2011. Impacts of Wind Generation Integration, EPRI White Paper. Available at: http://www.epri.com/abstracts/pages/productabstract.aspx?ProductID=000000000001023166

[37] FERC (U.S. Federal Energy Regulatory Commission), 2003. Notice of White Paper.

[38] FERC, 2011. Frequency regulation compensation in the organized wholesale power markets. Order No. 755: Final Rule.

[39] FERC, 2011. Recent ISO Software Enhancements and Future Software and Modeling Plans. Available at: http://www.ferc.gov/industries/electric/indus-act/rto/rto-iso-soft-2011.pdf

[40] Garcia, R.C., Contreras, J., Akkeren, M., Garcia, J.B.C., 2005. A GARCH forecasting model to predict day-ahead electricity prices. *IEEE Transactions on Power Systems 20(2)*, 867-874.

[41] Goulder, L.H., 1995. Effects of carbon taxes in an economy with prior tax distortions: an inter temporal general equilibrium analysis. *Journal of Environmental Economics and Management 29*, 271-297.

[42] Goulder, L.H., Schein, A., 2013. Carbon taxes vs. cap and trade: a critical review. NBER Working Paper 19338.

[43] Grant, B., Schuerger, M., 2013. Minnesota renewable energy integration and transmission study. MN Laws 2013 Conference.

[44] Gröwe-Kuska, N., Heitsch, Ho., Römisch, W., 2003. Scenario reduction and scenario tree construction for power management problems. 2003 IEEE Bologna Power Tech Conference. Bologan, Italy.

[45] Hassett, K.A., Mathur, A., Metcalf, G.E., 2009. The consumer burden of a carbon tax on gasoline. AEI Working Paper 147.

[46] Helmut, L., 2006. New Introduction to Multiple Time Series Analysis, Berlin, Germany: Springer.

[47] Henry, S., Panciatici, P., Parisot, A., 2014. Going green: Transmission grids as enablers of the transition to a low-carbon European economy. *IEEE Power and Energy Magazine 12(2)*, 27-35.

[48] IER (Institute for Energy Research), 2013. Estimating the State-Level Impact of Federal Wind Energy Subsidies. Available at: http://instituteforenergyresearch.org/wp-content/uploads/2013/12/State-Level-Impact-of-Federal-Wind-Subsidies.pdf

[49] Jorgenson, D.W., Wilcoxen, P.J., 1993. Reducing U.S. carbon emissions: an econometric general equilibrium assessment. *Resource and Energy Economics 15*, 7-25.

[50] Juban, J., Fugon, L., Kariniotakis, G., 2007. Probabilistic short-term wind power forecasting based on kernel density estimators. European Wind Energy Conference and exhibition, Milan, Italy.

[51] Krishnamurthy, D., Li, W., Tesfatsion, L., 2015. An 8-zone test system based on ISO New England data: Development and application. *IEEE Transactions on Power Systems*, to appear.

[52] Krishnan, V., Das, T., Ibanez, E., Lopez, C., McCalley, J., 2013. Modeling operational effects of wind generation within national long-term infrastructure planning software. *IEEE Transactions on Power Systems 28 (2)*, 1308-1317.

[53] Lemming, J., 2004. Price modelling for profit at risk management. In Bunn, D. W. ed. *Modeling Prices in Competitive Electricity Markets*. John Wiley & Sons, 287-306.

[54] Lew, D., Milligan, M., Jordan, G., Piwko, R., 2011. The value of wind power forecasting. American Meteorological Society Annual Meeting, the Second Conference on Weather, Climate, and the New Energy Economy. Washington DC, USA.

[55] Li, F., Bo, R., 2009. Congestion and price prediction under load variation. *IEEE Transactions on Power Systems 24(2)*, 911-922.

[56] Li, G., Liu, C-C., Salazar, H., 2006. Forecasting transmission congestion using day-ahead shadow prices. IEEE Power Systems Conference and Exposition, 1705-1709.

[57] Li, H., Tesfatsion, L., 2011. ISO net surplus collection and allocation in wholesale power markets under locational marginal pricing. *IEEE Transactions on Power Systems 26(2)*, 627-641.

[58] Løland, A., Ferkingstad, E., Wilhelmsen, M., 2012. Forecasting transmission congestion. *The Journal of Energy Markets 5(3)*, 65-83.

[59] Ma, T., Nakamori, Y., 2009. Modeling technological change in energy systems - from optimization to agent-based modeling. *Energy 34*, 873-879.

[60] Menz, F.C., 2005. Green electricity policies in the United States: case study. *Energy Policy 33*, 2398-2410.

[61] Metcalf, G.E., 1994. A distributional analysis of green tax reforms. *National Tax Journal 52 (4)*, 655-682.

[62] Metcalf, G.E., 2007. A proposal for a U.S. carbon tax swap. The Hamilton Project Discussion Paper. Available at: http://www.hamiltonproject.org/files/downloads_and_links/An_Equitable_Tax_Reform_to_Address_Global_Climate_Change.pdf

[63] Min, L., Lee, S.T., Zhang, P., Rose, V., Cole, J., 2008. Short-term probabilistic transmission congestion forecasting. IEEE 3rd International Conference on Electric Utility Deregulation and Restructuring and Power Technologies, 764-770. Nanjing, China.

[64] MISO, 2011. Dispatchable Intermittent Resource Workshop II. Available at: https://www.misoenergy.org/Library/Repository/Meeting%20Material/ Stakeholder/Workshops%20and%20Special%20Meetings/2011/DIR% 20Workshops/20111017%20DIR%20Workshop%202%20Presentation.pdf

[65] MISO, 2012. 2012 Binding Constraint Report : Day-Ahead Market.

[66] MISO, 2012. MISO Corporate Fact Sheet. Available at: https://www.misoenergy. org/Library/Repository/Communication%20Material/Corporate/Corporate% 20Fact%20Sheet.pdf

[67] MISO, 2013. July 2013 Monthly Market Assessment Report.

[68] MISO Homepage, 2015. Available at: https://www.misoenergy.org/

[69] Morales, J.M., Conejo, A., Pérez-Ruiz, J., 2009. Economic valuation of reserves in power systems with high penetration of wind power. *IEEE Transactions on Power Systems 24(2)*, 900-910.

[70] Morales, J.M., Pineda, S., Conejo, A.J., Carrión, M., 2009. Scenario reduction for futures market trading in electricity markets. *IEEE Transactions on Power Systems 24(2)*, 878-888.

[71] Moriarty, J., Palczewski, J., 2014. American call options for power system balancing. Working Paper. School of Mathematics, University of Manchester, UK. Available at SSRN: http://papers.ssrn.com/sol3/papers.cfm?abstract_id=2508258

[72] Navid, N., Rosenwald G., 2013. Ramp capability product design for MISO markets, Midcontinent ISO. Available at:
https://www.misoenergy.org/Library/Repository/Communication%
20Material/Key%20Presentations%20and%20Whitepapers/Ramp%20Product%
20Conceptual%20Design%20Whitepaper.pdf

[73] Nogales, F., Contreras, J., Conejo, A., Espinola, R., 2002. Forecasting next-day electricity prices by time series models. *IEEE Transactions on Power Systems 17(2)*, 342-348.

[74] NREL, 2012. Hand, M.M., Baldwin, S., DeMeo, E., Reilly, J.M., Mai, T., Arent, D., Porro, G., Meshek, M., Sandor, D. eds. *Renewable Electricity Futures Study* (4 vols.). National Renewable Energy Laboratory (NREL), NREL/TP-6A20-52409. Available at: http://www.nrel.gov/analysis/re_futures/

[75] NYMEX, 2015. New York Mercantile Exchange Homepage. Available at: http://www.cmegroup.com/company/nymex.html

[76] Oren, S.S., 2005. Generation adequacy via call options obligations: Safe passage to the promised land. *The Electricity Journal 18(9)*, 28-42.

[77] Papavasiliou, A., Oren, S., O'Neill, R., 2011. Reserve requirements for wind power integration: A scenario-based stochastic programming framework. *IEEE Transactions on Power Systems 26(4)*, 2197-2206.

[78] Power Market Subcommittee, 1979. IEEE reliability test system. *IEEE Transactions on Power Apparatus and Systems PAS-98(6)*, 469-483.

[79] Schweppe, F.C., Caramanis, M.C., Tabors, R.D., Bohn, R.E., 1988. *Spot Pricing of Electricity*. Kluwer Academic Publishers.

[80] Seliga, K., George, S., DePillis, M., 2014. Energy market offer flexibility. ISO New England Webex Broadcast: Customer Training Webinar. Available at: www.iso-ne.com/support/training/courses/energy_mkt_ancil_serv_top/energy_market_offer_flexibility_06_2014.pdf

[81] Sensfuß, F., Genoese, M., Ragwitz, M., 2008. Analysis of the impact of renewable electricity generation on CO_2 emissions and power plant operation in Germany. Symposium Energieinnovation, February 13 - 15, Graz, Austria.

[82] Sensfuß, F., Ragwitz, M., Genoese, M., 2008. The merit-order effect: A detailed analysis of the price effect of renewable electricity generation on spot market prices in Germany. *Energy Policy 36(8)*, 3086-3094.

[83] Stern, N., 2007. The economics of climate change - the Stern review, Cambridge University Press.

[84] Stoft, S., 2002. *Power System Economics: Designing Markets for Electricity.* Wiley-Interscience.

[85] Tesfatsion, L., 2009. Auction basics for wholesale power markets: Objectives and pricing rules, *Proceedings of the IEEE Power and Energy Society General Meeting*, Calgary, Alberta, CA, July 26-30 (electronic). Available at: http://www.econ.iastate.edu/tesfatsi/AuctionBasics.IEEEPES2009.LT.pdf

[86] Tesfatsion, L.S., Silva-Monroy, C.S., Loose, V.W., Ellison, J.F., Elliott, R.T., Byrne, R.H., Guttromson, R.T., 2013. New wholesale power market design using linked forward markets. Sandia National Laboratories Report (SAND2013-2789). Available at: www.econ.iastate.edu/tesfatsi/MarketDesignSAND2013-2789.LTEtAl.pdf

[87] UNFCCC (United Nation Framework Convention on Climate Change), 1998. Kyoto Protocol to the United Nations framework convention on climate change. Available at: `https://treaties.un.org/pages/ViewDetails.aspx?src=TREATY&mtdsg_no=XXVII-7-a&chapter=27&lang=en`

[88] UNFCCC, 2013. Status of ratification of the Kyoto Protocol. Available at: `http://unfccc.int/kyoto_protocol/status_of_ratification/items/2613.php`

[89] USCAN (U.S. Climate Action Network), 2009. Copenhagen Climate Negotiations - the briefing book. Available at: `http://www.usclimatenetwork.org/policy/copenhagen-climate-negotiations-briefing-book`

[90] Vrakopoulou, M., Margellos, K., Lygeros, J., Andersson, G., 2013. A probabilistic framework for reserve scheduling and N-1 security assessment of systems high wind power penetration. *IEEE Transactions on Power Systems 28(4)*, 3885-3896.

[91] Wang, J., Koritarov, V., Kim, J.H., 2009. An agent-based approach to modeling interactions between emission market and electricity market. 2009 IEEE Power and Energy Society General Meeting, Calgary in Alberta, Canada, 26-30 July, (electronic).

[92] Weidlich, A., Sensfuß, F., Genoese, M., Veit, D., 2008. Studying the effects of CO_2 emissions trading on the electricity market: a multi-agent-based approach (Editor: R. Antes, B. Hansjürgens, P. Letmathe). Emissions Trading, 91-101, Springer.

[93] Wild, P., Bell, P., Foster, J., 2012. The impact of carbon pricing on wholesale electricity prices, carbon pass-through rates and retail electricity tariffs in Australia. Energy Economics and Management Group Working Papers, No. 5-2012, School of Economics, University of Queensland, Australia.

[94] Wong, P., Albrecht, P., Allan, R., Billinton, R., Chen, Q., Fong, C., Haddad, S., Li, W., Mukerji, R., Patton, D., Schneider, A., Shahidehpour, M., Singh, C., 1999. The IEEE reliability test system-1996: A report prepared by the reliability test system task force of the application of probability methods subcommittee. *IEEE Transactions on Power Systems 14(3)*, 1010-1020.

[95] WSPP, 2014. Western Systems Power Pool (WSPP) Agreement Description. Available at: http://www.wspp.org/documents_agreement.php

[96] Xu, L., Tretheway, D., 2014. Flexible ramping products incorporating FMM and EIM, California ISO. Available at: www.caiso.com/Documents/RevisedStrawProposal_FlexibleRampingProduct_includingFMM-EIM.pdf

[97] Zhou, Q., Tesfatsion, L., Liu, C-C., 2010. Global sensitivity analysis for the short-term prediction of system variable. 2010 IEEE Power and Energy Society General Meeting. Minneapolis, MN, USA.

[98] Zhou, Q., Tesfatsion, L., Liu, C-C., 2011. Short-term congestion forecasting in wholesale power markets. *IEEE Transactions on Power Systems 26(4)*, 2185-2196.